SCHOOL OF CIVIL ENGINEERING

INDIANA DEPARTMENT OF HIGHWAYS

JOINT HIGHWAY RESEARCH PROJECT

Volume II Final Report

FHWA/IN/JHRP-88/6 -1

STRUCTURAL BEHAVIOR OF HIGH STRENGTH CONCRETE PRESTRESSED I-BEAMS

M.K. Kaufman and J.A. Ramirez

PURDUE UNIVERSITY

JOINT HIGHWAY RESEARCH PROJECT

Volume II Final Report

FHWA/IN/JHRP-88/6 -1

STRUCTURAL BEHAVIOR OF HIGH STRENGTH CONCRETE PRESTRESSED I-BEAMS

M.K. Kaufman and J.A. Ramirez

Final Report

RE-EVALUATION OF THE ULTIMATE STRENGTH AND BEHAVIOR OF HIGH STRENGTH CONCRETE PRESTRESSED I-BEAM SECTIONS

August 10, 1988

TO: H. L. Michael, Director
Joint Highway Research Program

FROM: J. A. Ramirez

PROJECT: C-36-56W

FILE: 7-4-23

Attached is a copy of the second and final volume of the Final Report of the HPR Part II study "Re-Evaluation of the Ultimate Strength and Behavior of High Strength Concrete Prestressed I-Beam Sections". I have served as the Principal Investigator on this study, directed the project and have co-authored the report.

The research results reported in this second volume include recommendations to allow the use of concrete compressive strengths up to 6500 psi in the design of precast prestressed I-Beams in the State of Indiana. No modifications of the current design equations to evaluate flexural capacity of the precast composite I bridge section are needed. The use of current IDOH Shear Design Specifications for continuous bridges with pretensioned I-beams is adequate. At simple supports of typical bridge structures the support centerlines is usually between six and twelve inches from the end of the beam, and as a result, the transfer length of the strand extends into the shear span. Three tests conducted during this study, using this standard detailing, resulted in a premature strand anchorage failure as a web-shear crack penetrated into the transfer length of the strand. Although the specimens tested in thsi study had minimum amounts of shear reinforcement at the end regions, it is felt that the use of higher strength concrete in pretensioned beams requires an evaluation of the efficiency of the shear reinforcement in preventing this mode of failure. The effect of strand debonding in pretensioned members which was not part of the study, also needs further study.

The current AASHTO and the Zia and Mostafa methods to predict transfer length of the strand were also evaluated. The results of this study showed that the Zia and Mostafa method predicted better the transfer length of the strand.

The results of this study have been recommended for implementation in the State of Indiana. The use of high strength concrete in the design of

prestressed I-Beams offers substantial benefits. The increased tensile strength of higher strength concretes is helpful in the service load design. Also, the increase in the modulus of elasticity results in better deflection control. The inherent relationship between higher strength concrete and better quality control makes high strength concrete attractive because of its improved long-term service performance. The qualities of high strength concrete are also proving themselves economically attractive in long span bridges. High strength concrete's comparatively greater compressive strength per unit weight and unit volume results in a reduction in dead load allowing lighter more slender bridges. This study also indicated the increased importance of adequate detailing in higher strength concrete members to insure proper ultimate load behavior and strength.

The results of this study and other findings should provide the necessary information so that designers can use higher concrete strengths to improve the economics and structural safety of bridges.

Sincerely,

Julio A. Ramirez

cc:

A.G. Altschaeffl	R.A. Howden	B.K. Partridge
J.M. Bell	M.K. Hunter	G.T. Satterly
M.E. Cantrall	J.P. Isenbarger	C.F. Scholer
W.F. Chen	J.F. McLaughlin	K.C. Sinha
W.L. Dolch	K.M. Mellinger	C.A. Venable
R.L. Eskew	R.D. Miles	T.D. White
J.D. Fricker	P.L. Owens	L.E. Wood

TECHNICAL REPORT STANDARD TITLE PAGE

1. Report No.	2. Government Accession No.	3. Recipient's Catalog No.
FHWA, IN JHRP-88/6		

4. Title and Subtitle	5. Report Date / 6. Performing Organization Code
Title: Re-evaluation of the Ultimate Strength and Behavior of High Strength Concrete Prestressed I-Beams Sub: Structural Behavior of High Strength Concrete	5. August 10, 1988 6.

7. Author(s)	8. Performing Organization Report No.
M. K. Kaufman and J. A. Ramirez	JHRP - 88/6

9. Performing Organization Name and Address	10. Work Unit No. / 11. Contract or Grant No.
Joint Highway Research Project Civil Engineering Building Purdue University West Lafayette, IN 47907	10. 11. HPR - Part II

12. Sponsoring Agency Name and Address	13. Type of Report and Period Covered / 14. Sponsoring Agency Code
Indiana Department of Highways State Office Building 100 North Senate Avenue Indianapolis, IN 46204	13. Final Report 14.

15. Supplementary Notes

Conducted in Cooperation with the U.S. Department of Transportation, Federal Highway Administration

16. Abstract

The research results presented in this report include recommendations to allow the use of concrete strengths up to 6500 psi in the design of prestressed I-beams in the state of Indiana. No modifications of the current design equations to evaluate flexural and shear capacity are necessary. At simple supports of typical bridge structures the support centerline is usually between six and twelve inches from the end of the beam, and as a result, the transfer length of the strand extends into the shear span. Three tests conducted during this study, using this standard detailing, resulted in a premature strand anchorage failure as a web-shear crack penetrated into the transfer length of the strand. Although the specimens tested in this study had minimum amounts of shear reinforcement at the end regions, it is felt that the use of higher strength concrete in pretensioned beams requires an evaluation of the efficiency of the shear reinforcement in preventing this mode of failure. The effect of strand debonding in pretensioned beams also needs study. The current AASHTO and the Zia and Mostafa methods to predict transfer length of the strand were also evaluated. The results of this study showed that the Zia and Mostafa method predicted better the transfer length of the strand.

17. Key Words	18. Distribution Statement
High Strength Concrete, Compressive Strength, Detailing, I-Beams, Flexural Strength, Shear Strength, Web Reinforcement, Trusses.	No restrictions. This document is available to the public through the National Technical Information Service, Springfield, VA 22161

19. Security Classif. (of this report)	20. Security Classif. (of this page)	21. No. of Pages	22. Price
Unclassified	Unclassified	157	

Form DOT F 1700.7 (8-69)

Final Report

RE-EVALUATION OF THE ULTIMATE STRENGTH AND BEHAVIOR OF HIGH STRENGTH CONCRETE PRESTRESSED I-BEAM SECTIONS

Volume II
STRUCTURAL BEHAVIOR OF HIGH STRENGTH CONCRETE PRESTRESSED I-BEAMS

by

M. K. Kaufman
Graduate Research Assistant
and
J. A. Ramirez
Assistant Professor
Civil Engineering
Purdue University

Project No. C-36-56W
File No. 7-4-23

Prepared as Part of an Investigation
conducted by the
Joint Highway Research Project
Engineering Experiment Station
Purdue University
in cooperation with the
Indiana Department of Highways
and the
U.S. Department of Transportation
Federal Highway Administration

Purdue University
West Lafayette, Indiana
August 10, 1988

PREFACE

This is the second and final volume on the research project, "Re-Evaluation of the Ultimate Strength and Behavior of High Strength Concrete Prestressed I-Beam Sections." An evaluation of the adequacy of current design procedures for higher strength concrete AASHTO I-girders is presented in this volume. Where necessary, new recommendations are given for the design of these members. This study includes an experimental program consisting of nine tests on six full scale Type I and Type II AASHTO I-Girders with concrete strengths ranging from 8000 to 9000 psi. An evaluation of the recommendations of this research study is illustrated with the example of an existing structure containing prestressed I-girders and a cast-in-place slab.

This work was conducted as Joint Highway Research Project No. C-36-56W. The experimental study was carried out at the Purdue University Civil Engineering Structural Laboratory. The specimens were fabricated at Hydro-Conduit, Lafayette, Indiana.

TABLE OF CONTENTS

LIST OF TABLES

LIST OF FIGURES

Figure | Page

Figure Page

LIST OF NOMENCLATURE AND ABBREVIATIONS

a = shear span, distance between concentrated load and centerline of support

A_b = area of beam cross section

A_c = area of composite cross section

A_{ps} = area of prestressed reinforcement in tension zone

A_s' = area of compression reinforcement

A_v = area of shear reinforcement within a spacing s

b = width of compression face of member

b_w = web width

b_f = effective flange width

c_1 = distance from centroid of section to compression face

c_2 = distance from centroid of section to tension face

d = distance from extreme compression fiber to centroid of tension reinforcement

d' = distance from extreme compression fiber to centroid compression reinforcement

d_b = nominal diameter of prestressing strand

d_p = distance from extreme compression fiber to centroid of prestressed reinforcement in the tension flange

d_p' = distance from extreme compression fiber to centroid of bottom prestressed reinforcement in the compression flange

e_1 = distance from centroid of prestressed reinforcement in compression flange to centroid of the section

e_2 = distance from centroid of prestressed reinforcement in tension flange to centroid of the section

E_c = modulus of elasticity of concrete

E_s = modulus of elasticity of reinforcement

E_{ps} = modulus of elasticity of prestressed reinforcement

f'_c = compressive strength of concrete

$\sqrt{f'_c}$ = square root of compressive strength of concrete

f'_{ci} = compressive strength of concrete at time of initial prestress

f_d = stress due to unfactored dead load, at extreme fiber of section where tensile stress is caused by externally applied loads

f_{pc} = compressive stress in concrete (after allowance for all prestress losses) at centroid of cross section resisting externally applied loads or at junction of web and flange when the centroid lies within the flange. In a composite member, f_{pc} is resultant compressive stress at centroid of composite section, or at junction of web and flange when the centroid lies with in the flange, due to both prestress and moments resisted by precast member acting alone.

f_{pe} = compressive stress in concrete due to effective prestress forces only (after allowance for all prestress losses) at extreme fiber of section where tensile stress is caused by externally applied loads

f_{ps} = stress in prestressed reinforcement at nominal strength

f_{pu} = tensile strength of prestressing tendons

f_{py} = specified yield strength of prestressing tendons

f'_r = modulus of rupture of concrete

f_{se} = effective stress in prestressed reinforcement, (after allowance for all prestress losses)

f_{si} = initial stress in prestressed reinforcement, (after allowance for initial prestress losses)

f_{sj} = jacking stress in prestressed reinforcement

f_{sp} = concrete splitting tensile strength

f'_t = concrete tensile strength

f_y = yield strength of nonprestressed reinforcement

h = overall height of member

I = moment of inertia of section resisting externally factored applied loads

I_b = moment of inertia of beam section

I_c = moment of inertia of composite section

I_y = moment of inertia of beam section about the weak axis

l = span length of beam

L_b = flexure development length of prestressing strand

L_d = development length of prestressing strand

L_t = transfer development length of prestressing strand

M_{cr} = moment causing flexural cracking at section due to externally applied loads

M_d = moment at section due to unfactored dead load

M_{max} = maximum factored moment at section due to externally applied loads

M_n = nominal moment strength at section

M_u = factored moment at section

P_{e1} = effective force in prestress reinforcement in compression flange

P_{e2} = effective force in prestress reinforcement in tension flange

Q_b = area moment of beam cross section about centroid of composite section

Q_c = area moment of composite cross section about centroid of composite section

r = web reinforcement index, $\dfrac{A_v}{b_w\, s}$ or $\dfrac{\text{total } A_v \text{ in shear span}}{b_w a}$

s = spacing of shear reinforcement in direction parallel to longitudinal reinforcement,

S_1 = Section modulus with respect to the extreme compression fiber

S_2 = Section modulus with respect to the extreme tension fiber

V_c = nominal shear strength provided by concrete

V_{ci} = nominal shear strength provided by concrete when diagonal cracking results from combined shear and moment

V_{cw} = nominal shear strength provided by concrete when diagonal cracking results from excessive principal tensile stress in the web

V_d = shear force at section due to unfactored dead load

V_l = shear force at section due to unfactored live load

V_{DL} = shear force at section due to unfactored dead load

V_{LL+I} = shear force at section due to unfactored live load plus impact

V_i = factored shear force at section due to externally applied loads occurring simultaneously with M_{max}

V_n = nominal shear strength

V_p = vertical component of effective prestress force at section

V_s = nominal shear strength provided by shear reinforcement

V_u = factored shear force at section

w_c = unit weight of concrete

w_o = self weight of member

y_t = distance from centroidal axis of gross section to extreme fiber in tension

z = internal moment lever arm

Δ_u = deflection of the beam at ultimate strength

Δ_y = deflection of the beam when the strain in the prestressing strand = 1%

μ = deflection ductility index, $\dfrac{\Delta_u}{\Delta_y}$

ρ_p = ratio of prestressed reinforcement, $\dfrac{A_{ps}}{b\ d_p}$

ϕ = strength reduction factor

ω_{max} = maximum prestressed reinforcement index

ω_p = prestressed reinforcement index, $\rho_p \dfrac{f_{ps}}{f'_c}$

ABSTRACT

This report deals with the evaluation of the ultimate behavior of AASHTO I-beams with concrete strengths up to 9000 psi. The relevant AASHTO and IDOH design specifications are thoroughly evaluated based on the results of this research. The findings of this study remark the many beneficial implications of the use of higher strength concrete in precast prestressed AASHTO I-beams. Higher strength concrete's with comparatively greater compressive strength per unit weight and unit volume would result in reductions in dead load allowing lighter more slender bridges. The increased stiffness of higher strength concrete is advantageous in the stability and control of deflections in these longer more slender structures. The larger tensile and compressive strength is also helpful in the service load design of these members. Furthermore, the inherent relationship between higher strength concrete and higher quality concrete should result in an improved long-term preformance under service loads. This study also points out the increased importance of adequate detailing of higher strength concrete members to insure ductile behavior under ultimate load. At simple supports of typical bridge structures the support centerline is usually between six and twelve inches from the end of the beam, and as a result, the transfer length of the strand extends into the shear span. Three tests conducted during this study, using this standard detailing, resulted in a premature strand anchorage failure as a web-shear crack penetrated into the transfer length of the strand. Although the specimens tested in this study had minimum amounts of shear reinforcement at the end regions, it is felt that the use of higher strength

concrete in pretensioned beams requires an evaluation of the efficiency of the shear reinforcement in preventing this mode of failure. The effect of strand debonding in pretensioned beams also needs further study. The current AASHTO and the Zia and Mostafa methods to predict transfer length of the strand were also evaluated. The results of this study showed that the Zia and Mostafa method predicted better the transfer length of the strand.

CHAPTER 1

INTRODUCTION

1.1 General

Higher strength concrete is being produced by precast plants manufacturing precast I-girders for the state of Indiana. In Volume I[1] of the final report it was suggested that 28 day concrete compressive design strength for these members could be increased to 6500 psi without substantial changes or additional cost to the product. Also, the study conducted on the engineering material properties for compressive strengths up to 9000 psi indicated that current empirically derived expressions could be used to determine modulus of elasticity and tensile strength. Volume II will focus on the structural behavior and current design procedures of prestressed AASHTO I-beams fabricated with the higher strength concrete.

1.2 Problem Statement

Many of the current design equations for pretensioned I-beams were empirically derived for concrete compressive strengths less than 6000 psi. As indicated in the state of the art report by ACI Committee 363[2], extrapolation of these design procedures to higher strength concrete members is unjustified and may be dangerous. Thus, before the multiple advantages of higher strength concrete can be utilized, it is necessary to investigate the ultimate strength and behavior of such members with careful control on the actual concrete strength.

1.3 Objectives of the Study

The structural behavior of prestressed AASHTO I-beams containing higher strength concrete and the evaluation of current flexure and shear design procedures for these members are the main objective of this study. The main emphasis is focused on their shear behavior. The use of higher strength concrete in the fabrication of the precast I-sections will generally not effect the ultimate flexural strength of the composite section since the compressive force of the internal moment typically remains with the cast-in-place slab which has compressive strengths ranging from 3000 to 4000 psi. Also, the adequate transportation of these type of members will be discussed along with other relating topics effected by the use of higher strength concrete in the fabrication of precast prestressed I-beams.

CHAPTER 2

THE STRUCTURAL BEHAVIOR AND DESIGN OF PRESTRESSED I-BEAMS WITH HIGHER STRENGTH CONCRETE

2.1 General

The use of higher strength concrete in the fabrication of I-beams in the State of Indiana is a common practice. The use of this higher strength concrete would result in a more efficient and economic structure. However, due to the empirical nature of some of the current design specifications developed using tests of beams with concrete compressive strengths less than 6000 psi, it is necessary to re-evaluate such specifications before they can be extrapolated to higher strength materials.

This chapter reviews and evaluates current specifications from the Indiana Department of Highways[3] (IDOH) and American Association of State and Highway Transportation Officials[4] (AASHTO) and available literature dealing with the structural behavior of prestressed AASHTO I-girders. The flexure and shear behavior of these members is discussed in detail. In addition, the effects of higher strength concrete on the behavior are presented. The topics of horizontal shear strength for composite action, development length of prestressing strand, lateral stability, and use of trusses as behavioral models are also discussed.

2.2 Behavior of Prestressed I-Beams

The behavior of a bridge superstructure consisting of a continuous cast-in-place slab and prestressed concrete AASHTO I-girders is quite complex. Several loading conditions must be evaluated, beginning with the transfer of the prestress force to the I-beam and continuing with the composite superstructure under all loading conditions. Once erected into position, the girders act as simply supported. In this stage, the beams must support their own weight, transverse diaphragms, formwork for the placement of the slab, and the weight of the cast-in-place slab. This type analysis assumes unshored construction. Future loads are resisted by the continuous composite section.

The use of the higher strength concrete in the fabrication of prestressed I-beams can result in many beneficial effects to the overall structure. Longer spans, wider lateral spacing of I-girders, increased tensile and compressive strength of the concrete, and control of deflections are some of the benefits provided by the increase in the compressive concrete strength.[5–8]

Flexural and shear behavior of the composite structure are the main topics discussed in this section.

2.2.1 Flexure

Moments produced by service and factored loads are evaluated at critical stages. Stresses produced by service loads and prestressing must be kept under allowable limits. Under the assumption of elastic behavior, stresses are calculated using gross section properties of the I-beam and of the transformed composite section at or below service load levels. Under ultimate load conditions the flexural strength of the composite section must be greater than the moments produced by factored service loads.

Stresses at transfer of the prestress force to the I-girders is the first critical stage. Two methods are used to control stresses at the ends of the

members due to the transfer of the prestress force, draped strand or debonding of a percentage of the total number of strands. Debonding of the strand is usually achieved by the strand encapsulation with plastic tubing. Both methods are used in the fabrication of prestressed I-beams for the State of Indiana. Stresses in the prestressed beam due to handling and storage must also be checked. Once the design strength is obtained, the members are shipped to the bridge site. The simply supported I-girder must withstand the construction loads including diaphragms and the cast-in-place slab for unshored type construction. The composite section resists future live loads.

The ultimate flexural strength of the composite section must be greater than the moments produced by factored service loads. The ultimate flexural strength of the composite section is given by AASHTO Specification (9.17.2),

$$\phi\, M_n = \phi\, A_{ps}\, f_{ps}\, d_p\, (1 - 0.6\, \rho_p\, \frac{f_{ps}}{f_c'}) \tag{1}$$

where, ϕ = strength reduction factor, 1.0 for flexure

M_n = nominal moment strength at section

A_{ps} = area of prestressed reinforcement in tension zone

f_{ps} = stress in prestressed reinforcement at nominal strength

d_p = distance from extreme compression fiber to centroid of prestressed reinforcement in the tension flange

ρ_p = ratio of prestressed reinforcement, $\frac{A_{ps}}{b\, d_p}$

f_c' = compressive strength of concrete in the cast in place slab

The following assumptions are made in Equation (1): the section is under-reinforced and the depth of the Whitney[9] stress distribution remains within the depth of the cast-in-place slab. Provided the effective prestress is greater

than 0.5 f_{pu}, the stress in the strand at ultimate strength is given in AASHTO Specification (9.17.4) as:

$$f_{ps} = f_{pu} \left(1 - 0.5\, \rho_p \frac{f_{pu}}{f'_c}\right) \tag{2}$$

where, f_{ps} = stress in prestressed reinforcement at nominal strength

f_{pu} = tensile strength of prestressing tendons

f'_c = compressive strength of concrete in the cast in place slab

ρ_p = ratio of prestressed reinforcement, $\dfrac{A_{ps}}{b\, d_p}$

Strain compatibility type analysis can be used as an alternative to determine the stress in the strand at ultimate strength.

Higher strength concrete can produce beneficial effects when evaluating stresses produced by service loads, and on the ultimate strength. Figures 2.1 and 2.2 show a typical internal distribution of stresses at different stages and resulting forces on the prestressed I-beam acting alone, and on the composite section under positive and negative bending moments, respectively. The negative moment shown in Figure 2.2 simulates the typical behavior of a section near a continuous interior support.

The increased concrete compressive and tensile properties strengthen midspan regions where moments will be larger and at the lower flange of the prestressed I-beam near interior continuous supports where compressive stresses produced by negative moments could exceed allowable limits.

Figure 2.1 shows that at ultimate strength, the compression block remains within the slab which typically has compressive concrete strength in the range of 3000 to 4000 psi. At the negative moment region shown in Figure

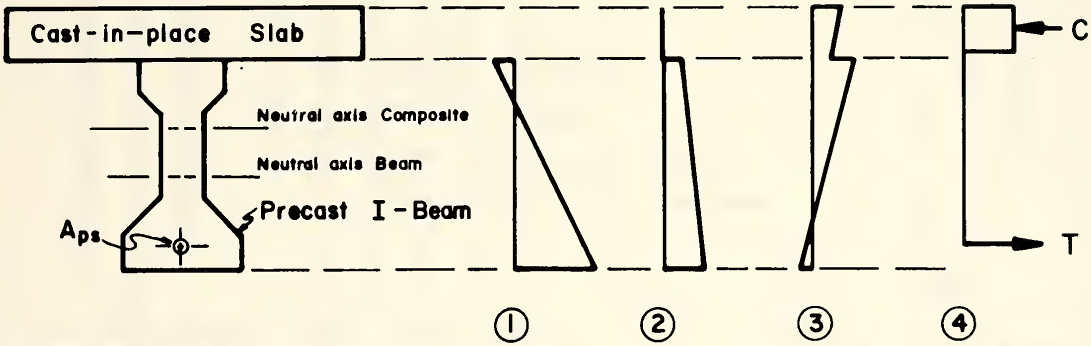

1. After Transfer of Prestress
2. After Casting of the Slab
3. Service Loading
4. Ultimate Strength

Figure 2.1 - Stress Distribution and Internal Forces, Positive Moment

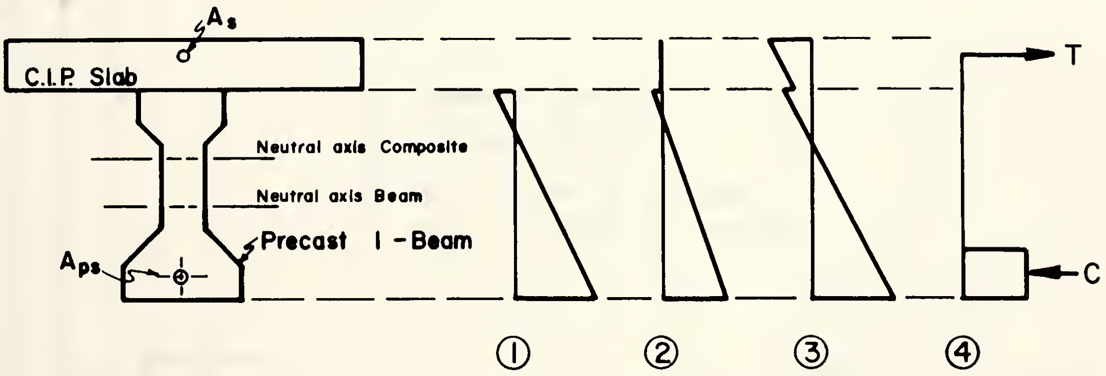

1. After Transfer of Prestress
2. After Casting of the Slab
3. Service Loading
4. Ultimate Strength

Figure 2.2 - Stress Distribution and Internal Forces, Negative Moment

2.2, the compression block is in the lower flange of the I-section. Thus, the increased concrete strength of the I-section can be utilized in the evaluation of the flexural strength resisting factored negative moments.

2.2.2 Shear Strength

The design and analysis of the shear strength for a composite section consisting of prestress I-beams and a cast-in-place slab is not as straight forward as the flexural evaluation. Three different methods are available to evaluate the shear strength. AASHTO Specifications allow two possible alternatives and IDOH allows a third one in the design of the web reinforcement. The latest provision recommended by 1983 AASHTO specifications presents the most detailed analysis procedure; however, the analysis and design become very cumbersome and unclear when dealing with continuous structures. The 1979 Interim AASHTO Specifications presents a method which is easier to apply, but it has shortcomings in the evaluation of the true behavior of the composite section. IDOH is the simplest of the three methods to apply. The IDOH specification is a modification of some of the earliest recommendations applied to prestressed concrete.

Each design procedure shall be discussed in detail along with the use of higher strength concrete.

2.2.2.1 IDOH Specifications

Indiana Department of Highways recommends that the amount of web reinforcement be determined by

$$A_v = \frac{3}{4} \frac{(V_u - V_p)\, s}{f_y\, h} \tag{3}$$

where, A_v = area of shear reinforcement within a spacing s

$$V_u = \frac{1.3}{\phi}\left[V_{DL} + \frac{5}{3}V_{LL+I}\right]$$

V_{DL} = shear force at section due to unfactored dead load

V_{LL+I} = shear force at section due to unfactored live load plus impact

ϕ = strength reduction factor, 0.9

V_p = vertical component of effective prestress force at section

f_y = yield strength of shear reinforcement

h = overall height of member

This design specification has its roots in the design procedure proposed by T.Y. Lin as early as 1956. In an opening statement to his book, "Prestressed Concrete Structures,[10]" T.Y. Lin wrote, "To engineers who, rather than blindly following the codes of practice, seek to apply the laws of nature." At that time, there was no specifications or guidelines for the shear design of prestressed members. The Building Code Requirements for Reinforced Concrete[11] (ACI-1956) were based on an elastic analysis to determine the amount of web reinforcement. When the shear at the section of interest exceeded the allowable concrete shear strength, the remainder of the shear had to be carried by web reinforcement stressed to some fraction of its yield stress. However for the stirrups to be stressed, the concrete has to be cracked; this would then invalidate the assumptions of elastic behavior. In part due to this inconsistency, Lin stated, "To ensure safety under overloads, ultimate design must be adopted." The first proposed ultimate strength design procedure can be summarized as follows:

1. Compute the total ultimate shear at the section. A load factor of 2 was chosen.

2. The web reinforcement is assumed to carry the ultimate shear less the vertical component of the draped strand.
3. Assume that the shear crack has a 45° projection. The number of stirrups crossing the crack is $\frac{h}{s}$.
4. Assuming the stirrups to be at the yield stress, equating vertical forces, and solve for the area of web reinforcement. The proposed design equation from this approach is shown below

$$A_v = \frac{(V_u - V_p)\,s}{f_y\,h} \tag{4}$$

where, A_v = area of web reinforcement within a spacing s

V_u = factored shear force at section

V_p = vertical component of effective prestress force at section

f_y = yield strength of shear reinforcement

h = overall height of member

Figure 2.3 shows the free body used to illustrate this procedure. Equation (4) assumes a 45° failure crack, the concrete provides no resistance at ultimate strength ie. no contributions from aggregate interlock across the shear crack or from the uncracked concrete at the tip of the crack, and the effect of the axial compression produced by the prestress force is neglected, all of which are conservative assumptions.

Equation (3) is similar to Equation (4), but with a constant of $\frac{3}{4}$ to obtain the required area of web reinforcement. This factor recognizes the effects of any concrete contribution and precompression due to the presence of prestress to avoid unnecessary conservatism. The concrete strength, although not directly reflected in Equation (3), is then represented in the $\frac{3}{4}$ factor.

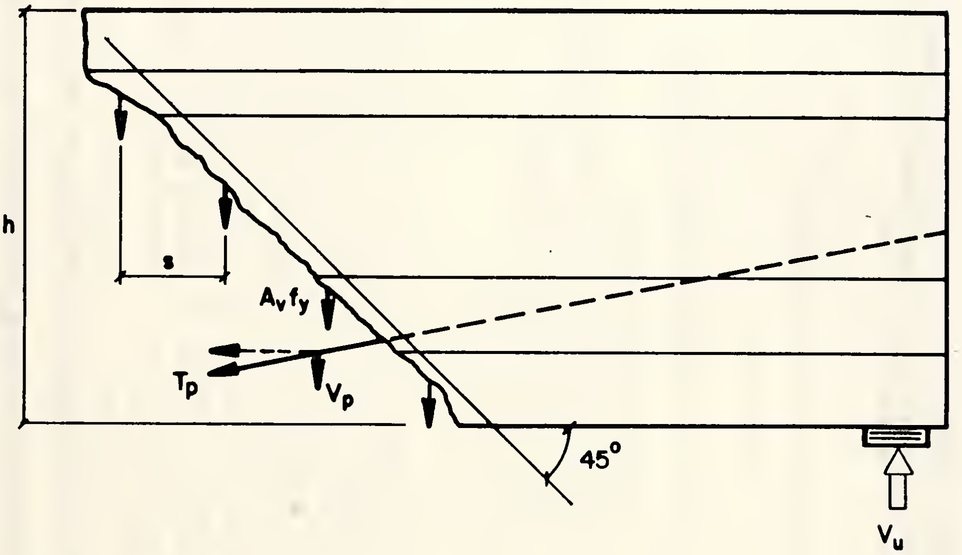

Figure 2.3 - Internal Shear Forces Free-Body-Section

2.2.2.2 AASHTO 1979 Interim Specifications

Current AASHTO Bridge Specifications permit the use of the 1979 Interim Specifications[12] as an alternate method to determine the amount of web reinforcement. The area of web reinforcement is calculated as follows:

$$A_v = \frac{1}{2} \frac{(V_u - V_c)\, s}{f_y\, jd} \tag{5}$$

where, $V_u = \dfrac{1.3}{\phi} \left[V_{DL} + \dfrac{5}{3} V_{LL+I} \right]$

V_{DL} = shear force at section due to unfactored dead load

V_{LL+I} = shear force at section due to unfactored live load plus impact

ϕ = strength reduction factor, 0.9

A_v = area of shear reinforcement within a spacing s

f_y = yield strength of shear reinforcement

jd = internal moment arm

V_c = $0.06\, f'_c\, b_w\, jd$ but not more than $180\, b_w\, jd$

with b_w being the web width of I-section

For continuous bridges, web reinforcement shall be designed for the full length of the interior spans and for the interior three-forths of the exterior spans. This provision indicates that the presence of shear in addition to flexure produces a critical inclined shear crack from a previously formed flexure crack. Hence, the locations of high moments and shears are evaluated for web reinforcement.

The 1958 ACI-ASCE Joint Committee 323[13] "Tentative Recommendations for Prestressed Concrete" serve as the basis for Equation (5). The load factors recommended by the AASHTO Committee on Bridges and Structures at

that time were 1.5 for dead Load and 2.5 for Live Load. These factors were considered adequate for spans of moderate length and simply supported. Equation (5) includes a concrete contribution; the effects of the precompression produced by the prestress force are accounted for in the $\frac{1}{2}$ factor. The $\frac{1}{2}$ factor shall be increased as the amount of prestress force is reduced and the member approaches conventionally reinforced concrete. The procedure to conduct this transfer from conventionally reinforced concrete to prestressed is not clear. Using this expression, the shear needs to be investigated only within the middle half of the span length. The web reinforcement required at these points should then be used throughout the outer quarters of the simply supported span. The design of continuous members is not addressed.

The use of higher strength concrete is not reflected in Equation (5), since for compressive strengths in excess of 3000 psi, the V_c term is equal to a constant value of 180 b_w jd.

2.2.2.3 AASHTO 1983 Specifications

AASHTO Specification 9.20 presents the third and most current method available to evaluate the shear strength of a prestressed member. Members subjected to shear must be designed to satisfy Equation (6) written as,

$$V_u \leq \phi \, (V_c + V_s) \tag{6}$$

where, V_u = factored shear force at section

V_c = nominal strength provided by concrete

V_s = nominal strength provided by shear reinforcement, $A_v \, f_y \, \frac{d}{s}$

$\phi =$ strength reduction factor, 0.90 for shear.

The shear strength provided by the concrete as specified in AASHTO (9.20.2) shall be taken as the lesser of V_{cw} or V_{ci}. Two types of shear cracks are recognized by this particular provision, web shear cracks and inclined flexural shear cracks.

The term, V_{cw} predicts the load required to produce a web shear crack; this type of cracks typically appears in regions of high shear and small flexural stresses:

$$V_{cw} = (3.5\sqrt{f'_c} + 0.3\, f_{pc})\, b_w\, d + V_p \tag{7}$$

where, $V_{cw} =$ nominal shear strength provided by concrete when diagonal cracking results from excessive principal tensile stress in the web

$f'_c =$ compressive strength of concrete

$f_{pc} =$ compressive stress in concrete (after allowance for all losses) at the centroid of cross section resisting externally applied loads or at junction of web and flange when the centroid lies within the flange. In a composite member, f_{pc} is resultant compressive stress at centroid of composite section, or at junction of web and flange when centroid lies within the flange, due to both prestress and moments resisted by precast member acting alone.

$b_w =$ web width

$d =$ distance from extreme compression fiber to centroid of tension reinforcement

$V_p =$ vertical component of effective prestress force at section

Equation (7) is an empirical approximation to the elastic solution of the problem. The shear required to produce a web shear crack is determined by calculating the principal tension stress at the centroid of the cross section and setting it equal to the tensile strength of the concrete. Shown in Figure 2.4 is a

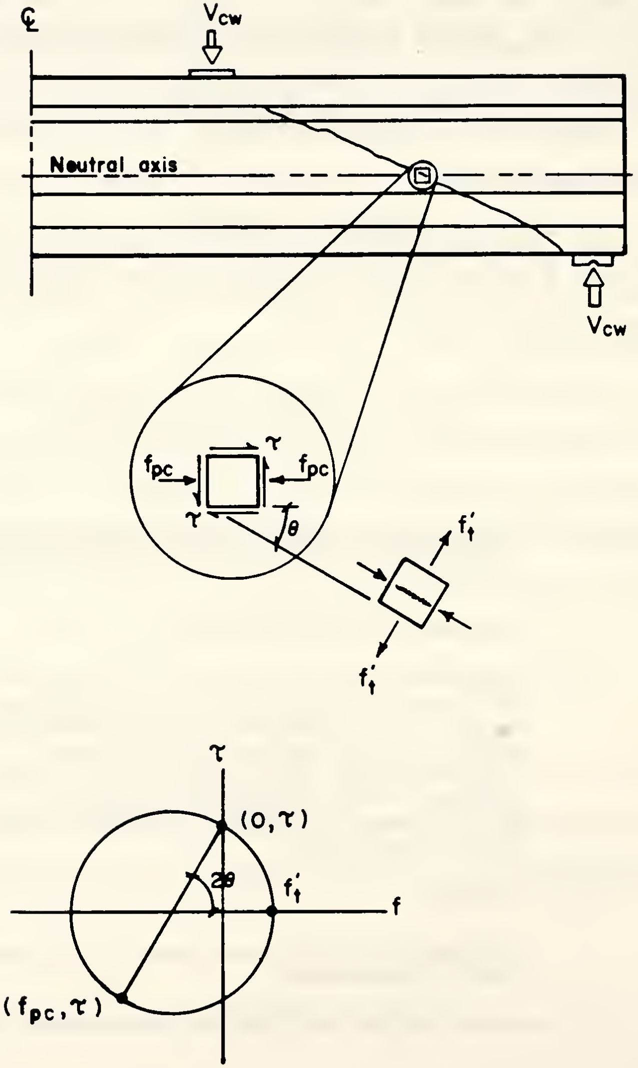

Figure 2.4 - Web Shear Crack, V_{cw} Elastic Solution for Non-Composite Section

typical web shear crack in an I-section. Mohr's circle can be used to obtain the elastic solution of the principal stresses. The presence of the axial prestress force flattens the angle of the crack with respect to a horizontal plane. Using Mohr's Circle and solving for the shear force required to produce a principal tensile stress equal to the tensile strength of the concrete, V_{cw} becomes:

for non-composite sections

$$V_{cw} = \frac{I_b\, b_w}{Q_b}\, f_t' \sqrt{1 + \frac{f_{pc}}{f_t'}} \tag{8}$$

and, for composite sections (see Appendix B for derivation)

$$V_{cw} = \frac{I_c\, b_w}{Q_c} \left[f_t' \sqrt{1 + \frac{f_{pc}}{f_t'}} - V_d \frac{Q_b}{I_b\, b_w} \right] + V_d \tag{9}$$

where, I_b = moment of inertia of beam section

I_c = moment of inertia of composite section

b_w = web width

Q_b = area moment of beam cross section about centroid of composite section

Q_c = area moment of composite cross section about centroid of composite section

f_{pc} = compressive stress in concrete (after allowance for all losses) at the centroid of cross section resisting externally applied loads. In a composite member, f_{pc} is resultant compressive stress at centroid of composite section due to both prestress and moments resisted by precast member acting alone. This assumes the centroid of the composite section remains within the web.

f_t' = concrete tensile strength

V_d = shear force at section due to unfactored dead load resisted

by the non-composite section

When the centroid of the section is in the flange, the junction of the web and flange is considered to be the critical location of a web shear crack. In this case, the calculation of the compressive stress in the concrete, f_{pc}, is a function of the external load; hence, a trial an error method must be used to determine the cracking load.

Figure 2.5 compares the elastic solution given by Equation (8), versus the AASHTO prediction, Equation (7). The two equations set the tensile strength of the concrete equal to $3.5\sqrt{f'_c}$. It should be noted that Figure 2.5 is a normalized graph comparing the shear stress to the compressive stress f_{pc} at the centroid of the section. To obtain the shear force required to produce a web shear crack in a non-composite section, the elastic solution is multiplied by the constant $\frac{I_b\, b_w}{Q_b}$, and the AASHTO prediction is multiplied by $b_w\, d$. The ACI 318-83 Building Code[14,15] allows the use of the elastic solution, with the tensile strength of the concrete equal $4\sqrt{f'_c}$, as an acceptable alternative. The 1983 AASHTO Specifications does not include the use of the elastic solution as an alternative.

Equations (8) and (9) were first proposed based on work conducted at the University of Illinois.[16] A value of $5\sqrt{f'_c}$ was suggested for the tensile strength of concrete. This value was determined from tensile strength of split cylinder tests. Figures 2.6 and 2.7 show comparisons of the AASHTO approximation, Equation (7), and the elastic solution, Equation (8), for the non-composite AASHTO Type I and Type II sections, respectively. Both figures indicate that the elastic theory, setting the tensile strength of concrete equal to $5\sqrt{f'_c}$, compares relatively well to the AASHTO prediction for the Type I and Type II beams.

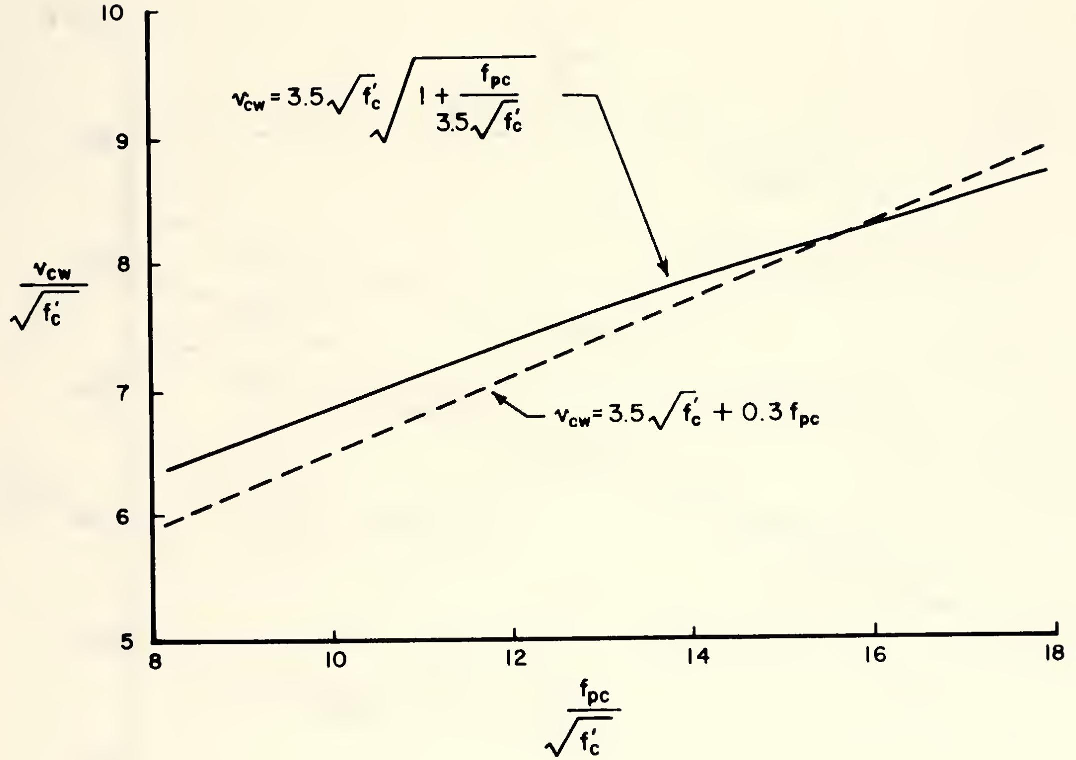

Figure 2.5 - Web Shear Crack, AASHTO and Elastic Predictions

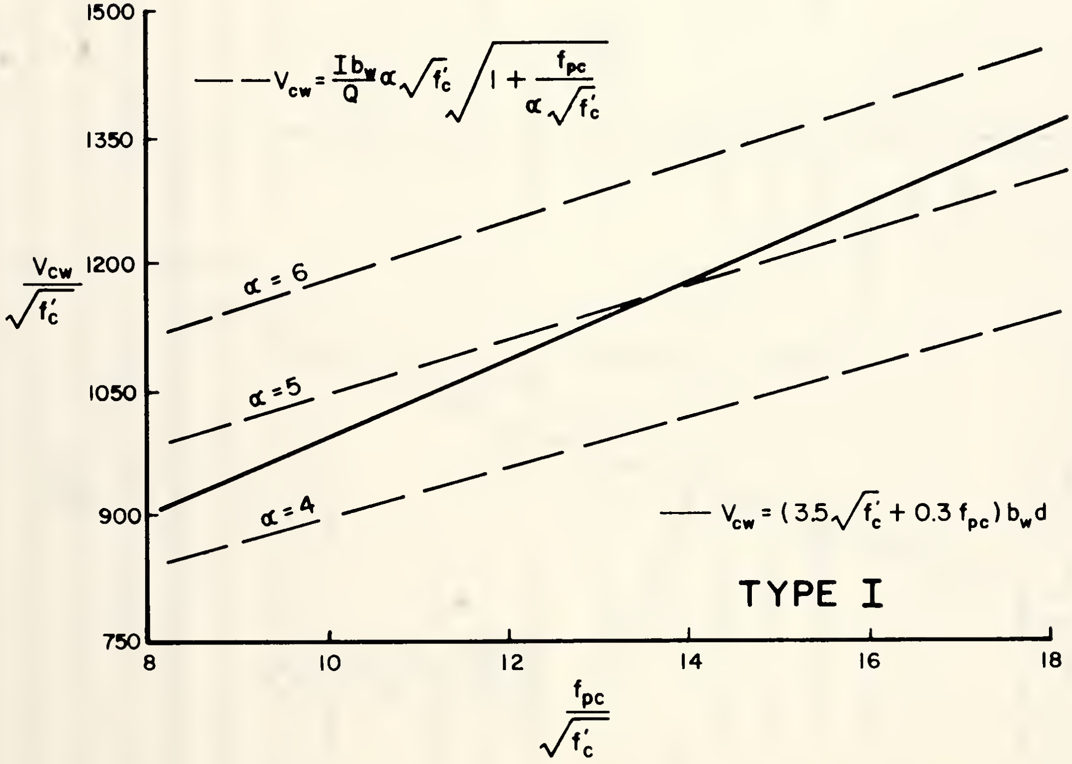

Figure 2.6 - Web Shear Crack, AASHTO and Elastic Predictions, Type I

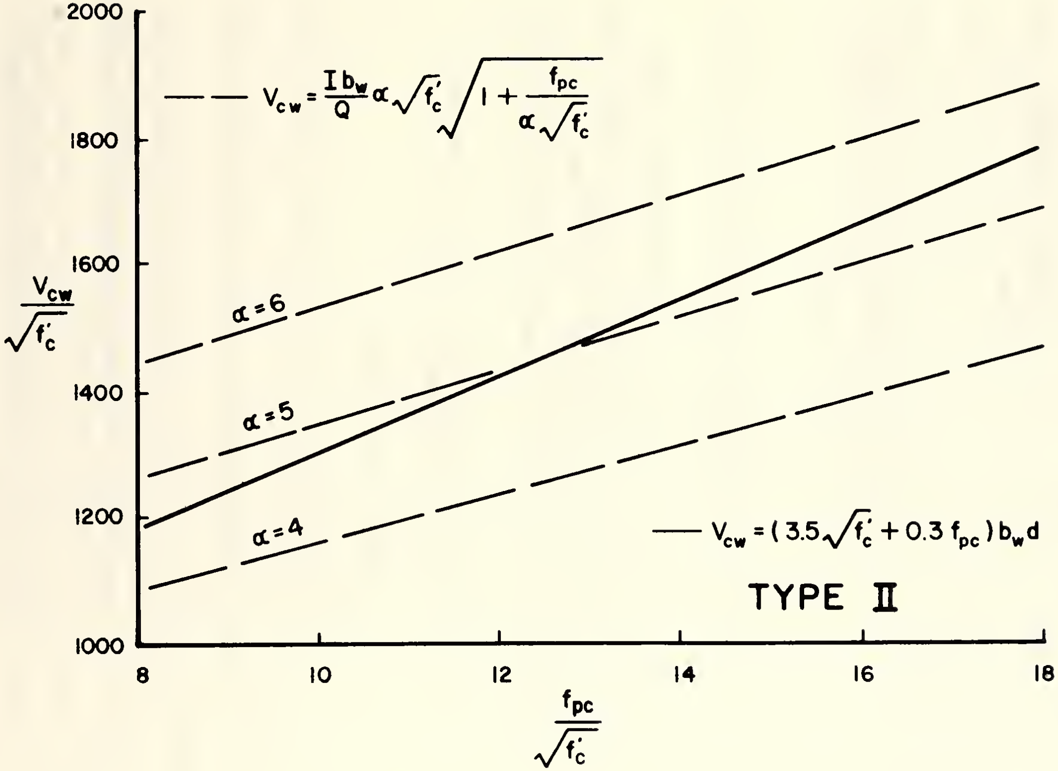

Figure 2.7 - Web Shear Crack, AASHTO and Elastic Predictions, Type II

The second cracking mechanism represented by the term V_{ci} reflects the shear required to produce a critical inclined shear crack originated from a flexure crack:

$$V_{ci} = 0.6\sqrt{f'_c}\, b_w\, d + V_d + \frac{V_i\, M_{cr}}{M_{max}} \geq 1.7\sqrt{f'_c}\, b_w\, d \tag{10}$$

where, V_{ci} = nominal shear strength provided by concrete when diagonal cracking results from combined shear and moment

f'_c = compressive strength of concrete

b_w = web width

d = distance from extreme compression fiber to centroid of tension reinforcement

V_d = shear force at section due to unfactored dead load

V_i = factored shear force at section due to externally applied loads occurring simultaneously with M_{max}

M_{max} = maximum factored moment at section due to externally applied loads

M_{cr} = moment causing flexural cracking at section due to externally applied loads

$= \frac{I}{y_t}(6\sqrt{f'_c} + f_{pe} - f_d)$

I = moment of inertia of section resisting externally factored applied loads

y_t = distance from centroidal axis of gross section to extreme fiber in tension

f_{pe} = compressive stress in concrete due to effective prestress forces only (after allowance for all prestress losses) at extreme fiber of section where tensile stress is caused by externally applied loads

f_d = stress due to unfactored dead load, at extreme fiber of section where tensile stress is caused by externally applied loads

Equation (10) is an empirical prediction of the flexure-shear cracking

mechanism. Figure 2.8 shows a typical inclined shear crack along with the corresponding shear and moment diagram. The equation to predict the shear force required to produce this type of crack was first proposed based on work conducted at the University of Illinois.[16] It is assumed that a critical inclined shear crack has a horizontal projection equal to the structural depth, d. The formation of a second flexural crack, at a distance equal to $\frac{d}{2}$ from the location of the point load, is the event that triggers actual collapse. The shear required to produce the second flexure crack is

$$V = \frac{M_{cr}}{\frac{M}{V} - \frac{d}{2}} \tag{11}$$

An additional increment of load equal to $1\sqrt{f'_c}\, b_w\, d$ was said to produce the critical inclined shear crack after the formation of the second flexural crack. Thus, the shear required to produce a critical inclined flexure shear crack is

$$V_{ci} = 1\sqrt{f'_c}\, b_w\, d + \frac{M_{cr}}{\frac{M}{V} - \frac{d}{2}} \tag{12}$$

The test load required to produce a critical inclined flexure shear crack versus the shear required to produce a flexure crack at a distance $\frac{d}{2}$ from the point load letting the flexural tensile strength of the concrete equal $6\sqrt{f'_c}$, is plotted in Figure 2.9 for the Illinois test data. Equation (12) is shown to represent the average of the test data. Equation (10), the AASHTO prediction, is Equation (12) with two conservative changes. The first term represents the incremental load required to produce the critical inclined shear crack. The factor

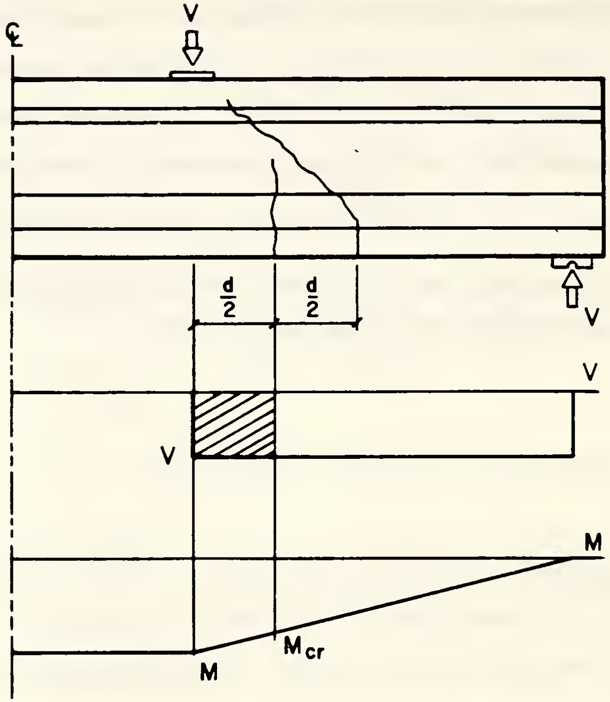

Figure 2.8 - Flexure Shear Crack, V_{ci} Derivation

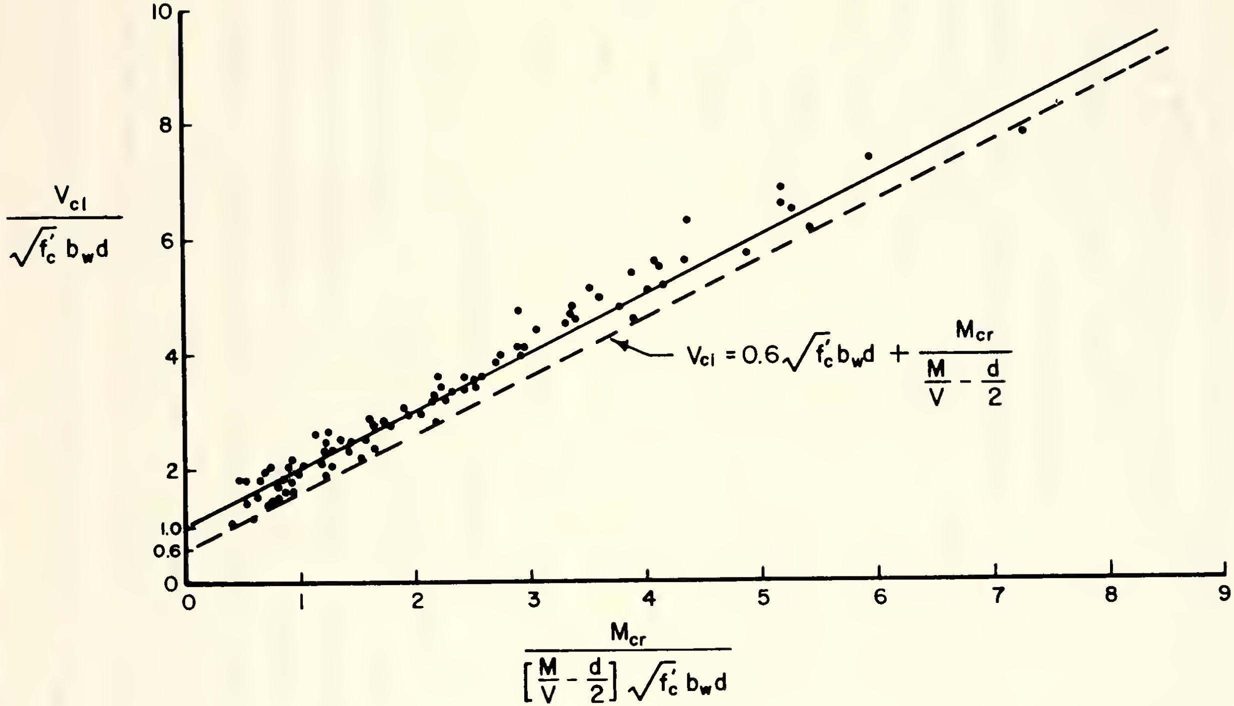

Figure 2.9 - V_{ci} versus M_{cr}, Illinois Study

of 0.6 has been applied which has the affect of producing a lower bound to the test data shown in Figure 2.9. Second, the value of $\frac{d}{2}$ has been eliminated from the third term for convenience. Also, the shear produced by dead and live load has been separated into two terms.

The 1983 AASHTO Specifications for shear were re-evaluated in a study conducted by Elzanaty et al.[17,18] at the University of Cornell for higher strength concretes. The study re-evaluated the V_{cw} and V_{ci} equations predicting a web shear and a inclined flexure shear crack, respectively. Concrete compressive strengths ranged from 6000 to 12000 psi. Two type of beams were fabricated, CW series and CI series. The section geometry and properties are shown in Figure 2.10 and Table 2.1, respectively. The beams were tested using a symmetric two point loading system. Each series consisted of 17 beams, 8 with web reinforcement and 9 without. Variables studied included; concrete strength, $\frac{a}{d}$ ratio, effective prestress force, and amounts of longitudinal and web reinforcement.

Figure 2.11 plots the test data of the 17 beams of the CW Series along with the AASHTO and elastic theory for predicting the formation of a web shear crack. The presence of web reinforcement is shown to have no effect on the behavior of the beam prior to the formation of a web shear crack. Comparing the data to the elastic theory indicates that the tensile strength of concrete is between $4\sqrt{f'_c}$ and $5\sqrt{f'_c}$ with $4\sqrt{f'_c}$ providing a safe lower bound. As the concrete strength of the beams increase and the effective prestress force remains constant, the ratio $\frac{f_{pc}}{\sqrt{f'_c}}$ decreases and the AASHTO prediction equation becomes more conservative.

Figure 2.12 plots the test data of 15 beams of the CI Series along with the AASHTO equation. However, the $\frac{d}{2}$ term is included for comparison with the

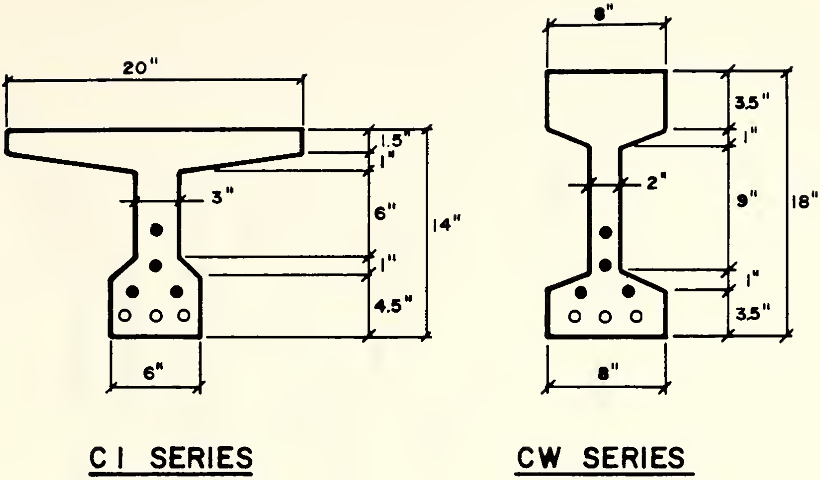

Figure 2.10 - Cross Section of CI and CW Series, Cornell Study

Table 2.1 - Section Properties, Cornell Study

	CI Series	CW Series
h (in)	14	18
b_w (in)	3	2
A_b (in^2)	91	84
Q_b (in^3)	198	249
I_b (in^4)	2046	3383
c_1 (in)	5.51	9.00
c_2 (in)	8.49	9.00
S_1 (in^3)	371	376
S_2 (in^3)	241	376
w_o (plf)	95	88

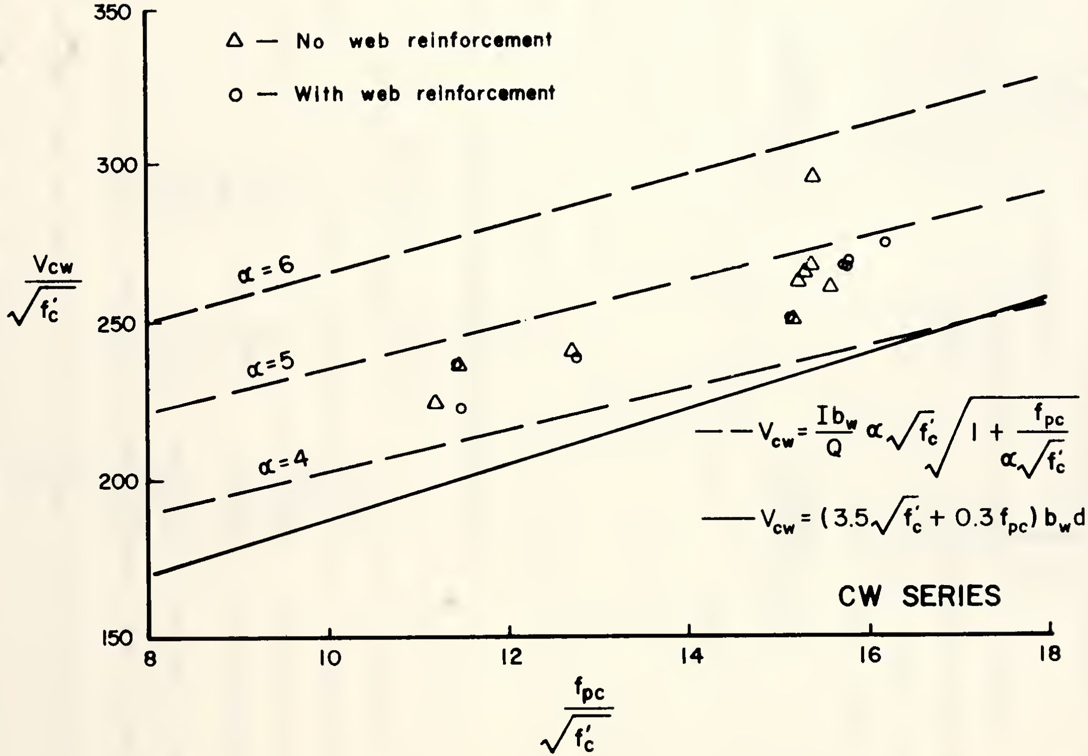

Figure 2.11 - Web Shear Crack, AASHTO and Elastic Predictions, CW Series

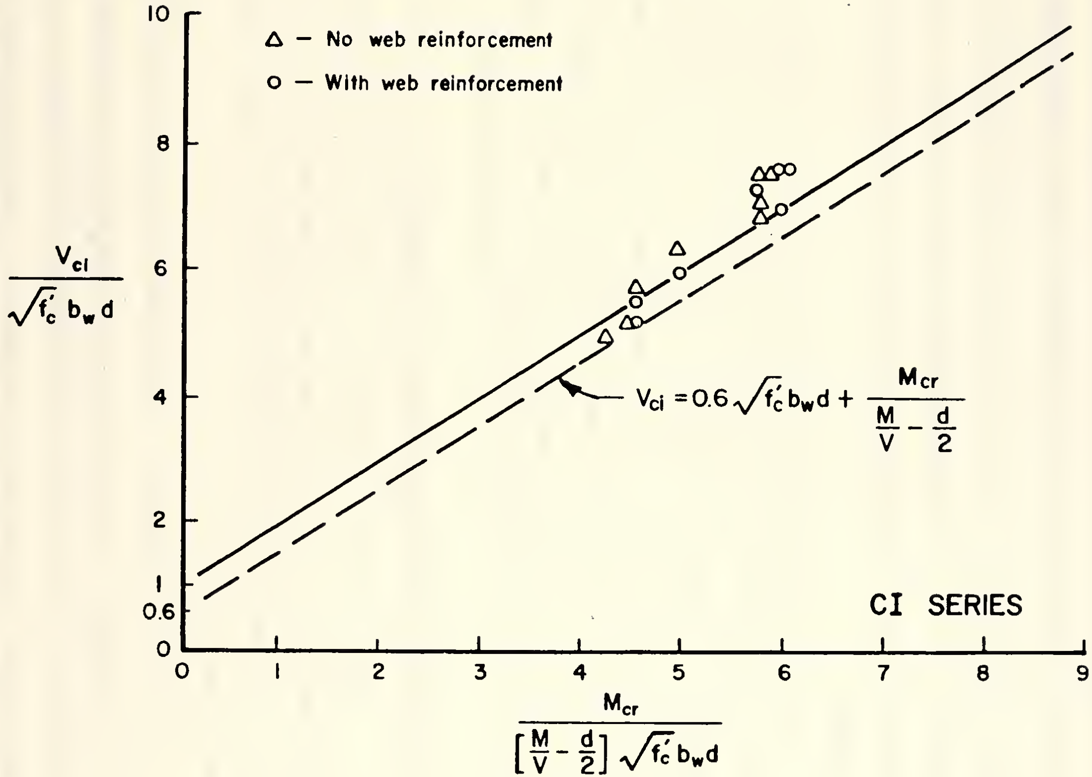

Figure 2.12 - Flexure Shear Crack, CI Series Plotted with Illinois Prediction Equation

Illinois study. The test data follows the trend of the Illinois study quite well. The AASHTO equation is shown to be a lower bound of the test data including the $\frac{d}{2}$ term. Removing the $\frac{d}{2}$ term would have the result of shifting the data to the left which would result in additional conservatism. The test data indicates that as the compressive concrete strength is increased, producing an increase in the cracking moment, the AASHTO prediction becomes more conservative.

The 1983 AASHTO specification indicates that the load required to produce a web shear crack and a inclined flexure shear crack is the concrete contribution at ultimate strength. The capacity of the web reinforcement is added as a separate term. The concrete and web reinforcement represent the nominal shear capacity of the section. The effect of higher strength concrete is reflected in the equations predicting the concrete contribution, V_{cw} and V_{ci} since both equations contain the compressive strength of the concrete.

2.2.2.4 Discussion of Current Shear Specifications

Three shear design specifications available for the design of continuous composite structures using prestressed I-beams have been discussed along with their origin. In this section a comparison between these shear specifications is conducted.

The design and analysis of a multi-span continuous structure consisting of a cast-in-place deck and prestressed I-beams can be quite difficult. Many different load cases must be evaluated throughout the fabrication and life of the structure. The evaluation of the effects of service and factored loads is conducted by developing design envelopes which represent the maximum and minimum bending moments and maximum shear force throughout the length of the structure. AASHTO specified loading conditions are used to develop

these envelopes.

In the following discussion of the three design specifications the effects of draped strand are neglected. The comparison is conducted in terms of shear strengths predicted.

IDOH Specifications

$$V_n = \frac{4}{3} \frac{A_v f_y h}{s}$$

AASHTO 1979 Interim Specifications

$$V_n = 2 \frac{A_v f_y jd}{s} + 180 b_w jd$$

AASHTO 1983 Specifications

$$V_n = (V_c + A_v f_y \frac{d}{s})$$

The concrete contribution, V_c, is taken as the lesser of the two equations, V_{cw} and V_{ci}:

$$V_{cw} = (3.5\sqrt{f'_c} + 0.3 f_{pc}) b_w d$$

and

$$V_{ci} = 0.6 \sqrt{f'_c} b_w d + V_d + \frac{V_i M_{cr}}{M_{max}} \geq 1.7 \sqrt{f'_c} b_w d$$

The IDOH specifications are by far the easiest to apply. The design engineer develops the shear envelope, reflects the type and size of web reinforcement to be used in the structure, obtains the height of the section and proceeds to design the spacing of the web reinforcement. The spacing must

also satisfy spacing limits and horizontal shear strength requirements.

The 1979 Interim Specifications are also very simple to apply. For concrete strengths in excess of 3000 psi, a constant value representing the concrete contribution is assumed. Since the critical region is located at $\frac{1}{4}$ the clear span, the formation of web shear cracks is not addressed by this equation which can result in the lack of required web reinforcement near the end region of an exterior span where shear forces are large and the web of the I-beam is relatively thin.

The 1983 Specifications recognizes two types of shear cracks. The load required to produce these shear cracks is assumed to represent the concrete contribution at ultimate strength. The specifications require a great deal of calculations and understanding. Problems arise when designing continuous structures. The equation predicting the web shear crack, V_{cw} is simplest of the two crack predictions to apply. This equation will typically control near the end regions of exterior spans for a structure consisting of prestressed I-beams. The V_{ci} equation predicting the load required to produce a critical inclined flexure crack is the most difficult to use. Problems arise in evaluating the third term in the V_{ci} equation, $\frac{V_i M_{cr}}{M_{max}}$. M_{cr} is the moment causing flexural cracking at section due to externally applied loads. M_{max} is the maximum factored moment at section due to externally applied loads, and V_i is the factored shear force at section due to externally applied loads occurring simultaneously with M_{max}. The difficulties stem from the fact that the maximum shear force envelope can not be used in this calculation since the position of the load producing maximum moment is most likely not the position producing maximum shear. In addition, if the AASHTO truck loading is used, two values of shear exist at the section of interest. To be conservative, one

would chose the algebraically lesser of the two shear values for V_i. The designer must also contend with lane loads which may control the maximum moment. Thus the evaluation of V_{ci} can present great difficulties to the design engineer and with two other design alternatives available, it is not surprising that the AASHTO 1983 Specifications are not generally used in the design of continuous structures containing prestressed I-beams and a cast-in-place deck.

The comparison of the three design equations between the quarter points of a span is conducted using the following assumptions: for the 1983 AASHTO Specifications V_{ci} controls and $V_{ci} = 1.7\sqrt{f'_c}\, b_w\, d$, $d = 0.9\, h$, $j = 0.9$, the web reinforcement contribution $V_s = A_v\, f_y\, \frac{d}{s}$, the concrete compressive strength of the prestressed I-beam is 5000 psi. Solving for the nominal shear strength, the three design equations reduce to,

IDOH Specifications

$$V_n = 1.48\, V_s$$

AASHTO 1979 Interim Specifications

$$V_n = 1.8\, V_s + 162\, b_w\, d \text{ (psi)}$$

AASHTO 1983 Specifications

$$V_n = V_s + 120\, b_w\, d \text{ (psi)}$$

The AASHTO 1979 Interim Specifications nominal shear capacity is substantially greater than the IDOH or AASHTO 1983 Specifications with the assumptions made. It appears that the IDOH and AASHTO 1983 Specifications would give very similar results.

Further comparison of the IDOH and 1979 Interim Specifications are made using the test results of the Cornell study. Table 2.2 contains the results for the beams containing web reinforcement. The CW Series were designed to evaluate the web shear capacity of prestressed beams containing high strength concrete. Both provisions underestimate the failure load. The CI Series were designed to evaluate the formation of flexure shear cracks for beams containing high strength concrete. Again, the IDOH provisions are conservative. However, the 1979 Interim Specifications is less conservative with a few exceptions.

The 1979 Interim Specifications do not recognize the formation of web shear cracks. This is shown in the comparison of the test results where the estimate was quite conservative for the CW Series and is less conservative for the CI Series. The IDOH provisions does not recognize the type of shear crack; however, the provision was conservative for both Series.

In chapter 4, the analysis of an existing bridge is conducted to further evaluate the current shear specifications.

2.3 Special Topics

A review of specific topics which are relevant in the discussion of the results of this study will be given in this section. The topics included are:

1. Horizontal Shear Strength
2. Development Length of Prestressing Strand
3. Lateral Stability
4. Truss Model

2.3.1 Horizontal Shear Strength

Adequate horizontal shear strength for composite sections must be ensured to prevent the separation of the cast-in-place slab and the I-girder. AASHTO Section (9.20.4.4) states that a minimum of two No. 3 bars on 12 inch centers must be provided across the contact surface. The equivalent to

Table 2.2 - IDOH and AASHTO 1979 Interim Specifications, Cornell Study

SERIES	h (in)	b_w (in)	jd (in)
CW	18	2	0.72 h
CI	14	3	0.72 h

$$\text{IDOH} \quad V_n = \frac{4}{3} A_v f_y \frac{h}{s}$$

$$\text{1979 Interim Specifications} \quad V_n = 2 A_v f_y \frac{jd}{s} + 180 \, b_w \, jd$$

Beam	Web reinforcement	V_n IDOH (kips)	V_n 1979 (kips)	V_u Test (kips)
CW10	#3 at 10"	16.6	22.6	39.0
CW11	#3 at 10"	16.6	22.6	35.2
CW12	#3 at 10"	16.6	22.6	31.6
CW13	#3 at 7"	16.6	22.6	41.0
CW14	#3 at 10"	23.8	30.3	42.2
CW15	#3 at 10"	16.6	22.6	33.8
CW16	#3 at 10"	16.6	22.6	42.0
CW17	#2 at 10"	6.5	11.7	32.0
CI10	#3 at 8"	16.2	22.9	24.2
CI11	#3 at 8"	16.2	22.9	23.4
CI12	#3 at 8"	16.2	22.9	22.8
CI13	#3 at 8"	16.2	22.9	28.6
CI14	#3 at 5"	25.9	33.4	33.7
CI15	#3 at 8"	16.2	22.9	23.9
CI16	#3 at 8"	16.2	22.9	28.8
CI17	#2 at 8"	6.3	12.2	24.3

the No. 3 bars at 12 inches is two No. 4 bars on 21.8 inches. This is done by extending the web reinforcement in the I-girder into the cast-in-place slab. This criteria often controls the spacing of the web reinforcement in the midspan regions where shear requirements are low. For web widths of 6 inches as in the AASHTO Type I and Type II girders, this criteria gives a value for $r\ f_y$ of 183 psi and 122 psi for Grade 60 and Grade 40 steel, respectively. The minimum area of web reinforcement as specified in Section (9.20.3.3) specifies a value of $r\ f_y$ equal to 50 psi.

2.3.2 Development Length of Prestressing Strand

In pretensioned members, generally the prestressing force is transferred to the concrete by bond. The length required to develop this force is called the transfer length. The additional length required to develop the stress in the strand at nominal strength is referred to as the flexural bond length. The development length of the strand is the summation of the transfer and flexure length.

AASHTO Specification (9.27) requires that the development length from a critical section satisfy the following equation,

$$L_d \geq \left(f_{ps} - \frac{2}{3} f_{se} \right) d_b \tag{13}$$

where, L_d = development length of prestressing strand

f_{ps} = stress in the prestressing reinforcement at nominal strength

f_{se} = effective stress in the prestressing reinforcement (after allowance for all prestress losses)

d_b = nominal diameter of prestressing strand

This equation is limited to three and seven wire strand. Equation (13) indi-

cates that the development length is a function of the nominal diameter of the strand, effective stress and the nominal stress of the strand at ultimate strength. Rearranging Equation 13 results in

$$L_d \geq \frac{f_{se}}{3} d_b + (f_{ps} - f_{se}) d_b \tag{13a}$$

In Equation (13a) the first term is the distance required to develop the transfer force and the second term is the additional length required to develop the stress in the strand at the nominal strength. The transfer length is commonly taken as 50 d_b when evaluating the web shear capacity, V_{cw}, at the ends of prestressed members. When the critical section, $\frac{h}{2}$ from the face of the support, is within the transfer length a linear transition from zero to full effective prestressed force is assumed in the transfer length. To obtain 50 d_b, the effective stress in the strand, f_{se}, is taken as 150 ksi. This assumes, Grade 270 stress relieved strand, a 70% jacking load, and approximately 20% prestress losses.

Zia and Mostafa[19] have proposed as an alternative the following equation to determine the development length

$$L_d = L_t + L_b = 1.5 \frac{f_{si}}{f'_{ci}} d_b - 4.6 + 1.25 (f_{ps} - f_{se}) d_b \tag{14}$$

where, f_{si} = initial stress in prestressing reinforcement, (after allowance for initial prestress losses)

f'_{ci} = compressive strength of concrete at time of initial prestress

The transfer length is given as,

$$L_t = 1.5 \frac{f_{si}}{f'_{ci}} d_b - 4.6 \tag{14a}$$

and the flexure length as,

$$L_b = 1.25 \, (f_{ps} - f_{se}) \, d_b \tag{14b}$$

Equation (14) is a function of, the nominal diameter of the strand, stress in the strand at transfer, effective stress after all losses, and the concrete strength at transfer. This equation includes the more significant of the identified parameters[19] affecting the development length:

a. Type of steel, wire or strand
b. Steel size, diameter
c. Stress level
d. Surface condition of the steel, oiled, clean or rusted
e. Concrete strength
f. Type of loading, static, dynamic or impact
g. Type of release, gradual, sudden
h. Confining reinforcement around steel
i. Time-dependent effects
j. Consolidation and consistency of concrete around the steel
k. Amount of concrete coverage around steel
l. Jacking stress, 75% f_{pu} for low relaxation strand.

The AASHTO specification indirectly calculates the transfer length using the effective prestress force which is a fraction of the initial prestress force at transfer. Assuming 1/2" inch strand, Grade 270, Low Relaxation, 8% initial losses, 18% total losses and a transfer concrete strength of 4000 psi, the transfer length is 27.7 and 30.3 inches for the AASHTO and the Zia and Mostafa equations, respectively. The flexure bond length is 25% greater for the Zia and Mostafa Equation as compared to the AASHTO specifications. The design concrete strength is not used as a variable in either equation; however,

a higher concrete strength at transfer will produce a smaller transfer length as indicated by the Zia and Mostafa Equation.

2.3.3 Lateral Buckling of Precast I-Sections.

The use of higher strength concrete allows the increase in bridge span lengths. Evaluation of the lateral buckling of these longer beams in the handling and transportation may become critical. The compression face of the beam if laterally unsupported could lead to lateral buckling. In this mode of failure, the beam deflects laterally, and if not restrained, could result in complete collapse.

Section 5.2.9 of the PCI Design Handbook[20] suggests a design check evaluate the lateral stability of precast sections. In this check, the factor of safety against lateral buckling is

$$F.S. = \frac{y_t}{\beta_y} \tag{15}$$

where, y_t = distance from the top to the centroid of the beam

$$\beta_y = \frac{5}{384}\,\frac{w_o\, l^4}{E_c\, I_y}$$

Equation (15) is the distance from the centroid of the member to the top fiber divided by the midspan deflection of the member due to its self weight as if the section was rotated 90° and simply supported at the pick-up points.

Five methods are suggested to improve the resistance of a member to lateral buckling.

1. Design adequate moment of inertia, I_y.

2. Specify very high-strength concrete (increase the modulus of elasticity).

3. Keep weight, w_o, low, if possible.

4. Reduce β_y by moving lifting loops away from ends of the members.

5. Attach temporary lateral bracing to compression flange or provide strongbacks, stiffening trusses or pipe frames. Sometimes two or more units can be transported together, side by side, and tied together to provide the necessary lateral strength.

2.3.4 Truss Model

Current provisions available to the engineer in the shear design of prestressed members can become very tedious and unclear in their application. The IDOH provisions are the simplest to use and tend to require an unnecessary large amount of web reinforcement. The 1979 Interim Specifications realize the formation of flexure shear cracks with no provision for the formation of web shear cracks. The 1983 AASHTO Specification attempts to model the behavior of the two types of shear cracks. However, this provision assumes that the load required to produce the formation of a web shear crack, V_{cw} or a flexure shear crack, V_{ci} represents the concrete contribution at ultimate strength. The V_{ci} equation also presents many problems when evaluating continuous structures with moving loads. A model is currently needed that actually predicts the behavior of the beam at ultimate strength and at the same time is easy to understand and apply.

Truss models are such behavioral models; they represent an overall behavioral model at ultimate strength rather than the current section by section analysis. Figure 2.13 shows the truss model for a pretensioned member under bending and shear. The bottom chord of the truss represents the tension reinforcement and is placed at the centroid of this reinforcement. The top chord is a compression chord and represents the internal compressive force. The depth of the truss is taken as the internal bending moment arm at

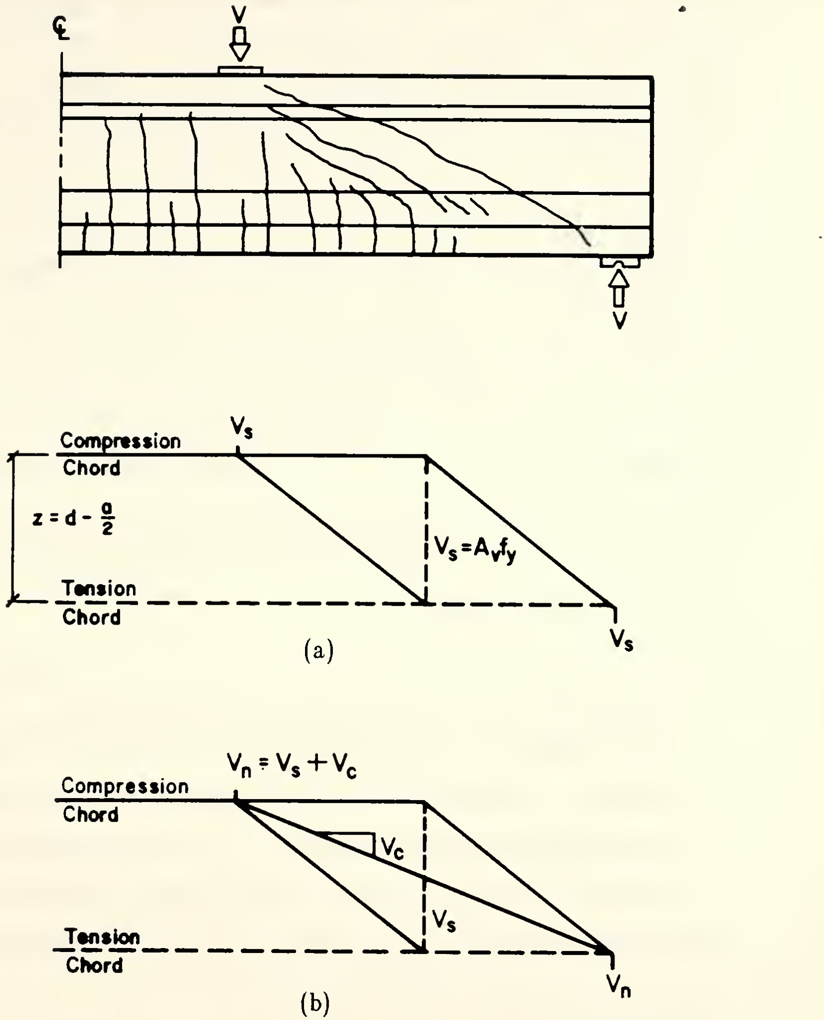

Figure 2.13 - Truss Model

ultimate strength, $z = d - \frac{a}{2}$. The vertical member represents the resultant of the web reinforcement. Diagonal members are placed to complete the static equilibrium of the truss, shown in Figure 2.13(a). The capacity of the truss at this point is that of the web reinforcement or V_s. For members with low shear span to structural depth ratios, the concrete contribution can be incorporated into the truss by placing an additional diagonal member connecting the load and support points as shown in Figure 2.13(b). The vertical component of this member represents the concrete contribution, V_c.

The use of higher strength concrete will strengthen the strut connecting the load and support point leading to a higher capacity of the truss. The use of the truss allows the engineer to design for flexure and shear. It also provides an excellent visualization of the flow of internal forces for the adequate detailing of reinforcement.

2.4 Summary

In this chapter, the structural behavior and design of composite sections consisting of prestressed I-beams and a cast-in-place slab has been reviewed. The major emphasis has been on shear. The current specifications for flexure are adequate and easy to apply. The use of higher strength concrete in the fabrication of I-beams has been shown to produce to following benefits related to flexure behavior:

1. Better control of deflections due to a higher modulus of elasticity
2. Higher allowable tensile and compressive concrete stress which will aid in the design of the structure resisting service loads.
3. Increase the ductility in negative moment regions of the beam resisting factored loads

Three shear provisions are available in the design of web reinforcement for I-beam type structures. The IDOH Specification is conservative, easiest to apply, and is the one most commonly used. The 1979 AASHTO Specifications

do not recognize the formation of web shear cracks and appear to over estimate the nominal shear strength capacity by as much as 50% compared to the IDOH and 1983 AASHTO Specifications. The 1983 AASHTO Specifications clearly account for the formation of the two types of shear cracks, web shear cracks and inclined flexure shear cracks. However, the equation used to predict the critical inclined flexure shear crack, V_{ci}, presents difficulty in continuous structures when evaluating the effects of AASHTO truck and lane loadings and is seldom used. The use of higher strength concrete is only directly accounted for in the 1983 AASHTO Specifications.

Other special topics introduced were;

a. horizontal shear strength,

b. development length of prestressing strand,

c. lateral stability, and

d. truss model used to evaluate the behavior of a beam loaded in shear and bending.

These topics will be addressed more extensively in subsequent chapters.

CHAPTER 3

EXPERIMENTAL PROGRAM

3.1 General

In Chapter 2 flexure and shear design provisions for AASHTO I-girders were reviewed. Special topics such as horizontal shear strength, development length of prestressing strand, lateral stability, and truss model were also introduced. In Chapter 3 the design, fabrication, testing, and discussion of six prestressed AASHTO I-beams will be presented.

3.2 Experimental Objective

The evaluation of the ultimate behavior of higher strength concrete prestressed I beams under flexure and shear is the main concern of this study. Special attention is directed towards the ultimate shear strength because of the highly empirical nature of the current design procedures in this area.

The study conducted at the University of Cornell[17,18] evaluated the 1983 AASHTO shear provisions for concrete strengths up to 12000 psi. The study concluded that the current provisions were adequate for the higher strength concrete. The beams in the study were fabricated and designed to produce two modes of shear cracks, web shear and flexure shear. Prestressed and non-prestressed reinforcement were used as the longitudinal reinforcement. However, the placement of the longitudinal reinforcement was not typical of prestressed members. The prestressed reinforcement extended into the web of the members.

In this study the evaluation of typical I beams used in the fabrication of continuous super-structures for bridges is conducted. Typical reinforcement schemes are used to simulate as close as possible the actual behavior of the beam in place.

External moments on the composite structure are resisted by an internal couple made out of a prestressed I beam and the composite slab. At ultimate strength in the positive moment region, the compressive force in the concrete generally remains within the slab which typically has a compressive strength between 3000 and 4000 psi. Hence, the use of high strength concrete in the fabrication of the prestressed I-girder has little effect on the ultimate flexural capacity providing the concrete strength requirements at transfer are not changed. High strength concrete does produce benefits when evaluating stresses and deflections due to service loads.

The ultimate shear carrying capacity of the composite structure is mainly carried by the precast I-beam and thus is directly affected by the increase in the concrete compressive strength. In this study, it was decided to test the prestressed I-beams without a cast-in-place slab, ie. non-composite; since the shear strength is mainly dependent on the strength of the precast member and to eliminate unwanted variables such as the concrete strength of the slab, stresses produced by the additional weight of the slab and shrinkage of the slab concrete, and additional curing time required to place a slab. Following a discussion on the behavior of these non-composite beams, the anticipated behavior of a composite structure will be examined.

3.3 Testing Program

Six AASHTO I-girders were fabricated, 4 Type I's and 2 Type II's. The beams were cast at a local plant. In this experimental program nine individual tests were conducted. Tables 3.1 and 3.2 contain the general information

Table 3.1 - Cast and Testing Dates for All Beams

Beam	Cast Date	Test Date	Curing (Days)
Type I-1	6/11/86	8/10/86	60
Type I-2	6/11/86	8/30/86	80
Type I-3	10/2/86	11/1/86	30
Type I-4	10/2/86	10/29/86	27
Type II-1	10/2/86	11/19/86	48
Type II-2	10/2/86	12/21/86	50
Type I-3A	10/2/86	4/7/87	187
Type I-4A	10/2/86	4/14/87	194
Type II-1A	10/2/86	4/24/87	204

Table 3.2 - Section Properties

	Type I-1&2	Type I-3&4	Type II-1&2
h_b (in)	28.25	28	36
b_w (in)	6	6	6
A_b (in^2)	279	276	369
Q_b (in^3)	1153	1128	1957
I_b (in^4)	23493	22750	50979
c_1 (in)	15.49	15.41	20.17
c_2 (in)	12.76	12.59	15.83
S_1 (in^3)	1517	1476	2527
S_2 (in^3)	1841	1807	3220
w_o (plf)	291	288	384

on the beam section properties. Two tests were conducted on the beam specimens Type I-3, Type I-4, and Type II-1; this is indicated by the second test designated as Type I-3A, Type I-4A and Type II-1A.

Type I-1 and 2 were cast and tested first. The transfer and 28 day concrete compressive strength was 4000 psi and 7000 psi, respectively. The design of the beams was conducted to insure that the flexural strength, M_n, exceeded the shear strength, V_n. 1983 AASHTO Specifications were used to calculate the predicted capacities. The stirrup spacing was controlled by the horizontal shear strength requirements of AASHTO Specification (9.20.4.4), two #3 bars on 12 inch spacing or equivalent.

Tables 3.3 through 3.11 contain the general information of each beam and test results. The material properties are those obtained from actual test measurements. In Appendix A the stress versus strain curves for the steel reinforcement are given. The material properties of the steel are based on the actual area of the specimen. Both failure test results and predicted capacities are shown in Table 3.3 through 3.11. The equations used to obtain the AASHTO predictions are shown below:

Shear Load Based on FLEXURE Capacity

(See Appendix C for Derivations)

$$V_{cr} = \frac{1}{a}\left[S_2\left(7.5\sqrt{f'_c} + \frac{P_{e1} + P_{e2}}{A_b}\right) - \frac{w_o\, l^2}{8} + P_{e2}e_2 - P_{e1}e_1\right]$$

$$V_n = \frac{1}{a}\left[A_{ps}\, f_{ps}\left(d_p - \frac{A_{ps}\, f_{ps}}{2\,(0.85)\, f'_c\, b_f}\right)\right]$$

Shear Load Based on SHEAR Capacity

(See Appendix C for Derivations)

$$V_{ci} = 0.6\sqrt{f'_c}\, b_w\, d_p + w_o(\frac{l}{2} - a) + \frac{M_{cr}}{a}$$

$$V_{cw} = (\ 3.5\sqrt{f'_c} + 0.3\, f_{pc}\ )\, b_w\, d_p$$

$$V_s = A_v\, f_y\, \frac{d_p}{s} = r\, f_y\, b_w\, d_p$$

$$V_n = V_{ci} + V_s$$

3.3.1 Material Properties

The mild reinforcement in the beams included Grade 40 and Grade 60 bars. The Grade 40 steel used for web reinforcement and flange reinforcement consisted of #3 bars and #4 bars from separate heats. Test samples were cut from each bar and the material properties were determined for each set of beams. The prestressing strand was supplied by the precast plant. Test specimens were obtained to evaluate the material properties of the strand.

3.3.1.1 Mild Reinforcement

Figures A.1 and A.2 in appendix A show the engineering stress versus strain curve for the Grade 40 #3 and #4 bars, respectively. Figures A.3, A.4 and A.5 show the engineering stress versus strain curve for the Grade 60 #5 bars used in beams Type I-1 and 2, Type I-3 and 4, Type II-1 and 2, respectively. Each test bar was instrumented with a electrical resistance strain (ERS) gage and a two inch extensometer to determine the axial strain. The tests were conducted on a 120,000 pound Baldwin testing machine. An automated data acquisition system was used to record the test data.

3.3.1.2 Prestressing Strand

Figure A.6 shows the engineering stress versus strain curve for the strand used in beams Type I-1 & 2. The stress versus strain curve for the strand in beams Type I-3 and 4, Type II-1 and 2 is shown in Figure A.7. The strand was instrumented with two ERS gages attached to a single wire and a 24 inch extensometer to measure the axial strain during the test. Special grips were fabricated so to prevent premature failure of the strand at the grips. The specimens were tested in a 120,000 pound Baldwin testing machine. An automated data acquisition system was used to record the test data. The area of the strand was determined by measuring the diameter of each wire and calculating the total area.

3.3.1.3 Concrete Properties

The concrete material properties were monitored from the time of transfer until the time of testing. Test cylinders were used to measure the compressive strength, split cylinder strength, and the modulus of elasticity. Two 2 inch ERS gages, placed diametrically opposite on the cylinders, were used to determine the axial strain for the cylinders representing the compressive strength of the test beam. The modulus of rupture was determined with 6x6x18 flexure beams. The flexure beams were tested at the time of the transfer of the prestress force to the I-beams and at the test date.

3.3.2 Test Setup

The test set up for the initial six tests is shown in Figure 3.1. A 600 Kip Baldwin testing machine was used in all tests. The testing machine applied a single point load to the top bearing plate of the spreader beam. The reactions of the spreader beam produced a symmetric two point loading system resulting in regions of constant moment and shear for the initial six tests. The

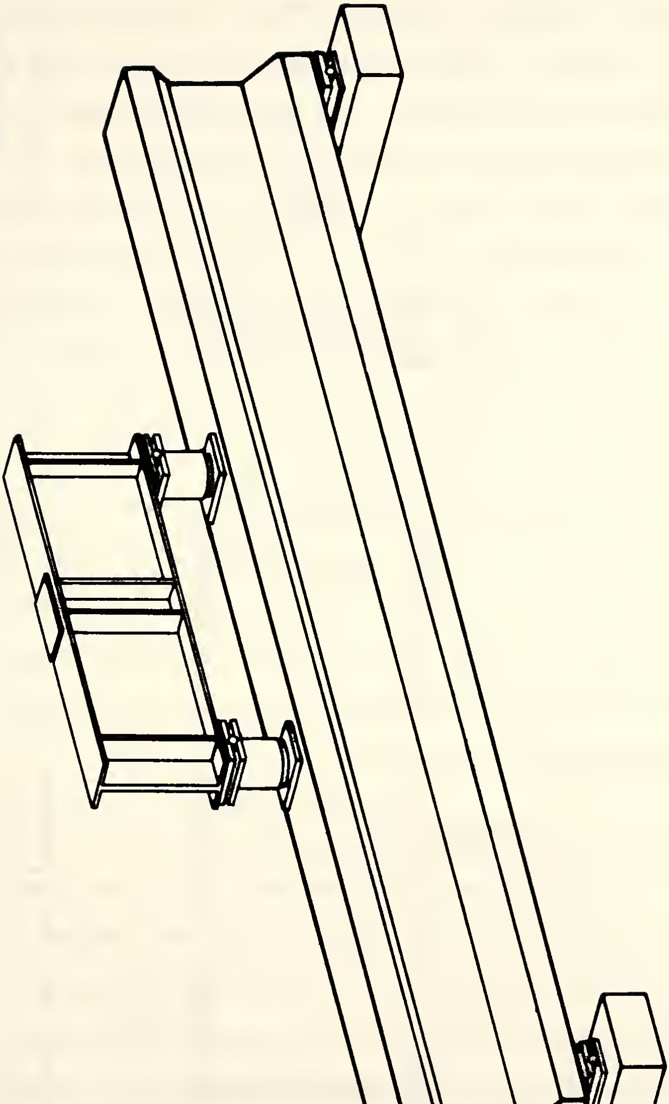

Figure 3.1 - Test Setup for Symmetric Point Load

spreader beam was a stiffened W30x132 steel section shown in Figure 3.2. Two load cells were placed under each reaction point of the spreader beam to monitor the load from the testing machine. Two concrete footings with steel bearing plates provided the supports for the reactions. The load point and reaction details are shown in Figure 3.3. A roller was used at each end to allow horizontal movements of the test beams. The length of the shear span was adjusted to produce the desired moment-shear combination. The first six beams were tested symmetrically about their centerline. The single point loading shown in Figure 3.4 was used for the beams tested a second time. Further details of each test set-up are given in following sections.

The load was applied slowly in specific increments. At each increment, cracks were outlined and the corresponding shear load was marked on the surface of the beam, test data was recorded using an automated data acquisition system as well as manual readings. As the test progressed, the loading increment decreased. The duration of a single test was between 1 and 4 hours depending on the mode of failure.

3.3.3 Instrumentation

Several different tranducers were used to record information in each test. Electric resistance Strain (ERS) gages were attached to the prestressing strand (EA-06-062D-350) and the mild reinforcement (CEA-06-125UN-350). External gages (EA-06-20CBY-120) were placed on the surface of the concrete to measure strains in the web and the compression flange. Load cells were used to monitor the load during the test. Linear variable differential transformers, potentiometers, and mechanical dial gages were used to measure deflections. Mechanical dial gages were also used to measure possible strand slip with respect to the end of the beam during each test.

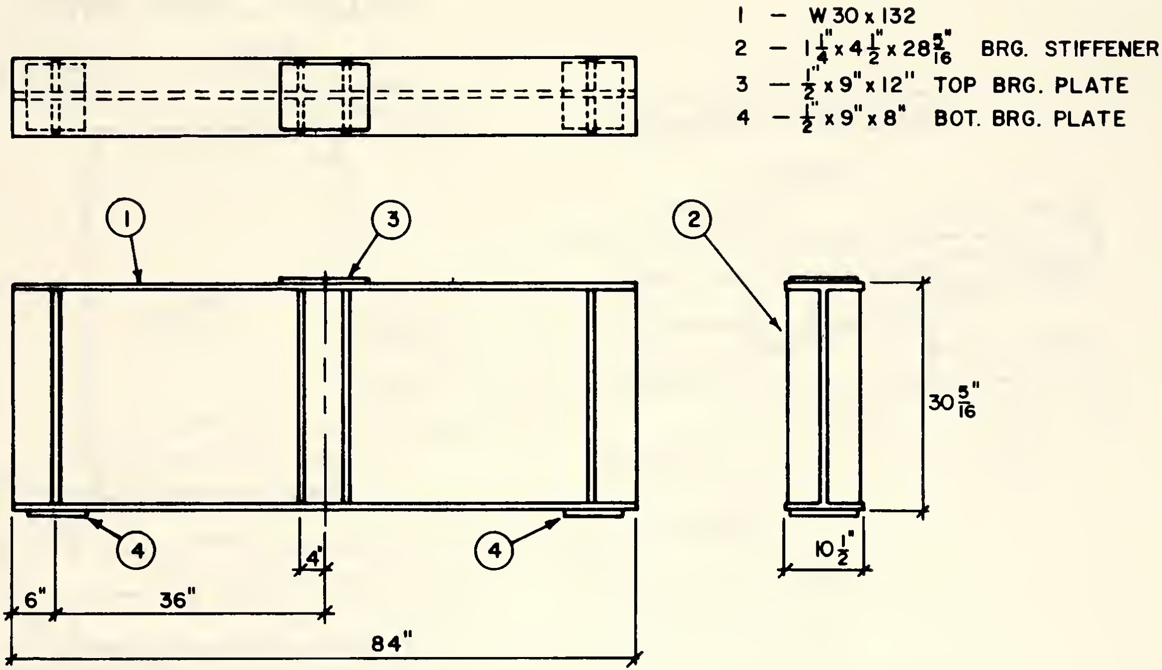

Figure 3.2 - Spreader Beam Detail

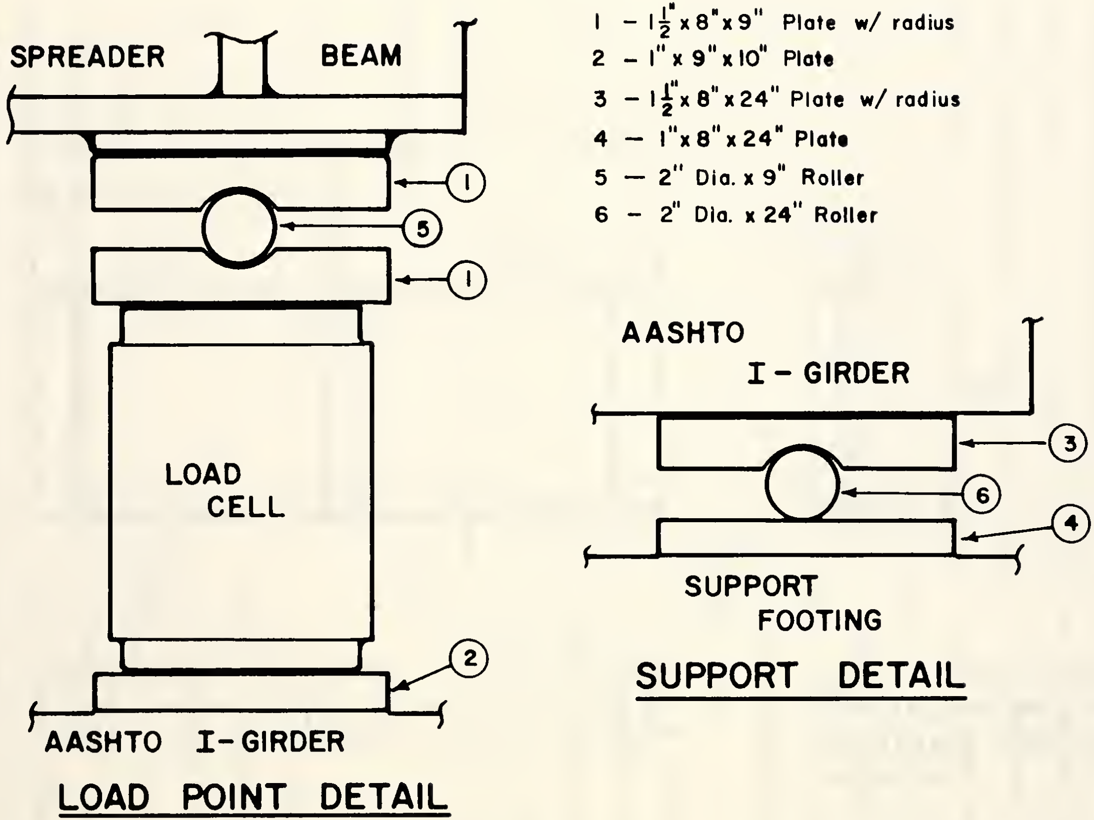

Figure 3.3 - Load Point and Support Detail

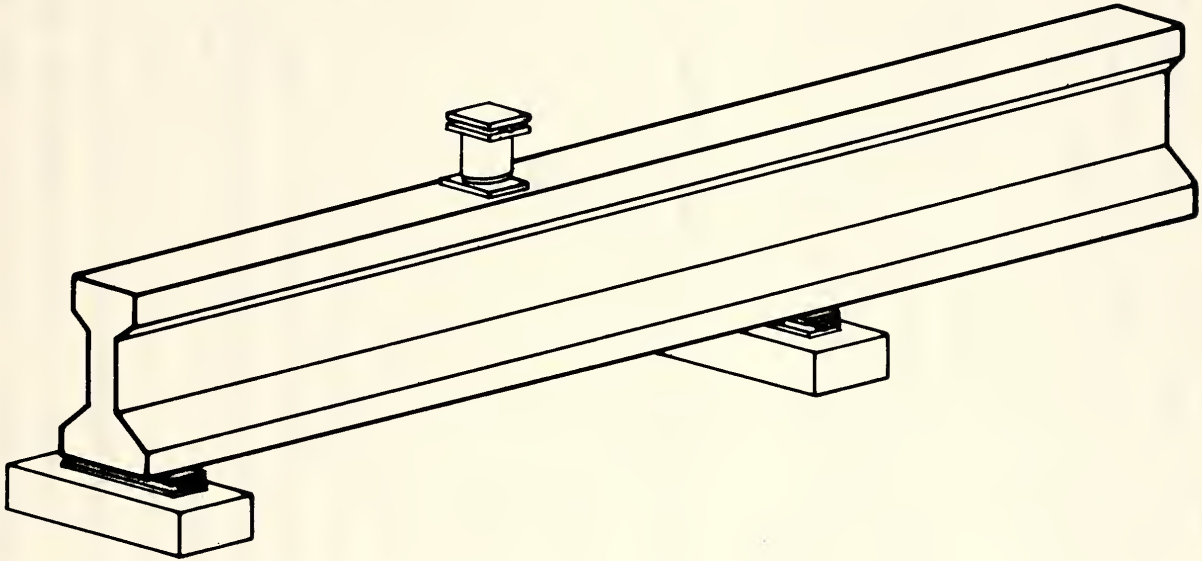

Figure 3.4 - Test Setup for Single Point Load

An ERS gage was placed on each leg of the stirrups within the shear regions of the beam. The location of the gage was selected to measure the strain of the stirrup following an expected shear crack. The two top longitudinal #5 bars were instrumented at the midspan of the beams.

Before placing the strain gages on the strand, it was pulled up to 5000 lbs. After the strain gages were attached the strand was stressed to full pull, 33818 lbs = 0.75 f_{pu} A_{ps}. Strain readings, elongation of the strand, and the gage pressure of the jacking apparatus was recorded. The locations of the gages were chosen to measure the strain in the strand throughout the span length.

3.3.4 Fabrication and Preparation for Testing

The specimens were cast at a local plant. In the fabrication sequence, the strands were first instrumented and loaded to the specified full pull. The rest of the reinforcement cage was then placed in the forms and the beam was prepared for the cast. The concrete was placed after meeting IDOH slump and air content requirements. After the compressive concrete strength requirement at transfer was satisfied the prestress force was applied to the beam. The beam was then removed and stored at the plant until the 28 day compressive strength requirement was obtained. The specimens were later shipped to the Purdue Civil Engineering Structural Laboratory and prepared for testing.

3.4 Tests Results

The results are discussed following the sequence of testing for the different specimens. However, the test results are grouped for analysis in accordance to the mode of failure.

3.4.1 Type I-1 and Type I-2

The first two beams tested were AASHTO Type I. Both beams had identical reinforcing and instrumentation schemes. The beam cross section is shown in Figure 3.5. The section properties based on the as-built geometry are given in Table 3.2.

3.4.1.1 Test Results of Type I-1

The test setup, instrumentation, and failure crack pattern of Type I-1 is shown in Figure 3.6. Also shown, is the crack pattern at ultimate strength. Table 3.3 gives the overall information of Type I-1. The shear span, measured from the centerline of the load application to the centerline of support, was 72 inches. A 24 inch overhang was provided at each end of the beam. The purpose of the overhang was to remove the transfer length of the strand, taken as $50d_b$, out of the shear span. Also, sufficient anchorage was required to develop the strand in flexure.

Flexure cracks were first to appear. They were followed by a web shear crack on the south shear span followed by a second in the north shear span. Each crack produced yielding in the web reinforcement as indicated by strain readings. Figure 3.7 shows the load versus the centerline deflection for this specimen. The two load drops in the beginning of the nonlinear portion of the curve represent the formation of the two web shear cracks. Failure of the beam was a typical flexure failure of an under-reinforced beam, yielding of the prestressing strand leading to a substantial increase in deflection followed by crushing of the concrete in the extreme compression fiber.

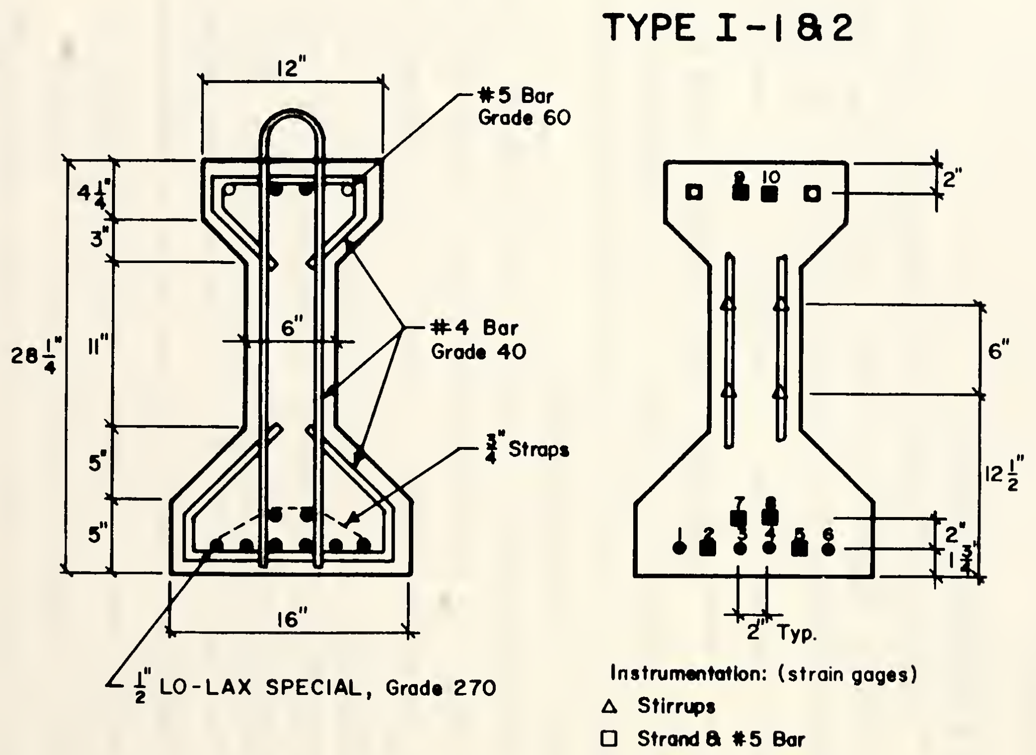

Figure 3.5 - Cross Section of Type I-1 & 2

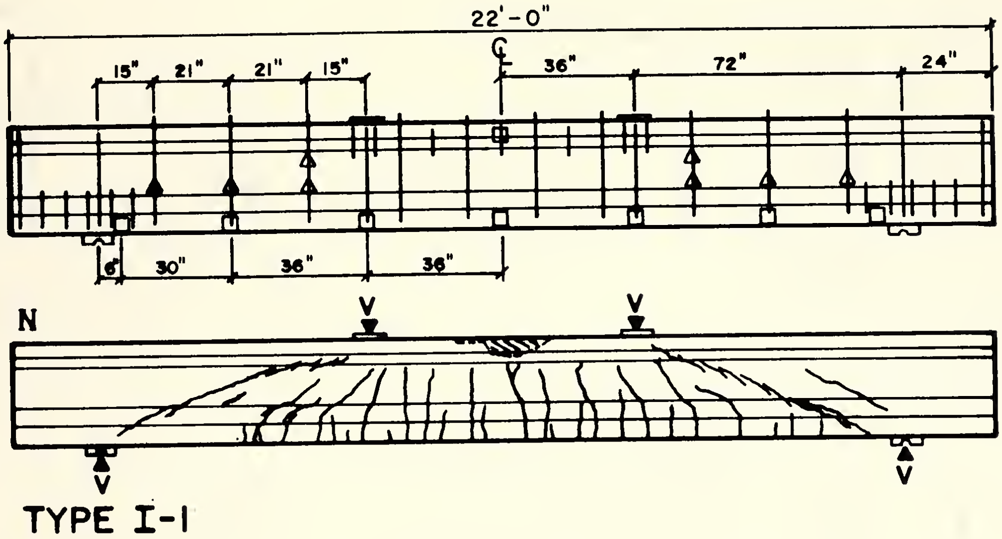

Figure 3.6 - Type I-1 Detail, Instrumentation and Failure Crack Pattern

Table 3.3 - TYPE I-1 Information

TYPE I - 1

Geometry:

Beam Length (ft)	22
Test Span (ft)	18
Shear Span,a (ft)	6
$\frac{a}{d_p}$	2.77

Concrete:

	Transfer	Test
f'_c (psi)	5450	8340
E_c (ksi)	4520	5680
f'_r (psi)	800	820
f_{sp} (psi)	-	550

Prestressing Strand:

	Top	Bottom
Grade	270	270
A_{ps} (in^2)	0.1620	0.1620
d'_p, d_p (in)	2.00	26.00
E_{ps} (ksi)	28240	28240
f_{pu} (ksi)	280.0	280.0
f_{sj} (ksi)	208.8	208.8
f_{si} (ksi)	206.8	196.4
f_{se} (ksi)	198.8	180.4
P_{e1}, P_{e2} (kips)	64.4	233.8

Mild Reinforcement:

	#5 Bar	#4 Bar
Grade	60	40
A'_s, A_v (in^2)	0.31	0.19
d', r f_y (in, psi)	2.00	137
E_s (ksi)	29180	29500
f_y (ksi)	72	52

Test Results:

FLEXURE (kips)

	ACI & AASHTO	Measured
V_{cr}	64.9	75
V_n	111.9	123

SHEAR (kips)

	ACI & AASHTO	Measured
V_{ci}	71.1	-
V_{cw}	99.9	103
		109
V_s	21.4	-
V_n	92.5	-

Mode of Failure: Flexure, 123 kips.

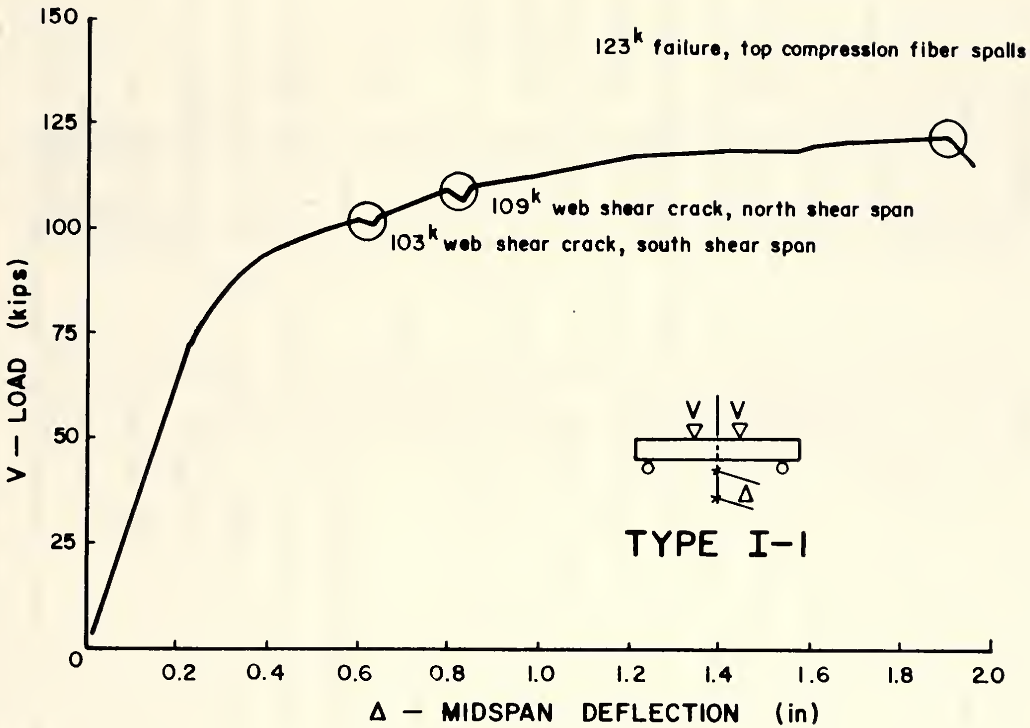

Figure 3.7 - Type I-1 Load vs. Midspan Deflection

3.4.1.2 Test Results of Type I-2

The shear spans of Type I-2 were reduced 12 inches producing a shear span of 60 inches. The purpose was to reduce the moment to shear ratio compared to Type I-1 to obtain a shear type failure. Figure 3.8 shows the instrumentation detail and failure crack pattern of Type I-2. Table 3.4 contains the overall information of Type I-2. Flexural cracks appeared first in the constant moment region. Subsequent web shear cracks formed in the north and south shear spans. Yielding of the web reinforcement was observed upon the formation of each web shear crack. The centerline load vs deflection curve is shown in Figure 3.9. The overall load versus deflection curve is similar to that of Type I-1; however, prior to reaching the predicted flexural capacity, the web on the south shear span exploded. The failure was brittle as in a test of a high strength concrete cylinder. Strain gages, located on the surface of the concrete at the location of the failure, showed strains exceeding 0.002. Also, strains exceeding 1 percent were recorded in the strand near the south support.

3.4.2 Type I-3 and Type I-4

Type I-1 and Type I-2 had overhangs of 2 and 3 feet, respectively. The overhangs provided sufficient anchorage to the strand which, in the case of Type I-2, showed strains in excess of 0.01. Figure 3.10 shows a typical end detail of a super-structure containing prestressed I-girders and a composite slab. The centerline of the support is typically between 6 and 18 inches from the end of the beam depending on the bearing system used. It was felt after the testing of the first two beams, that this type of detail might present problems since the transfer region of the strand would be within the shear span and any increase in the stress in the strand near the support could lead to a premature failure due to the slippage of the strand.

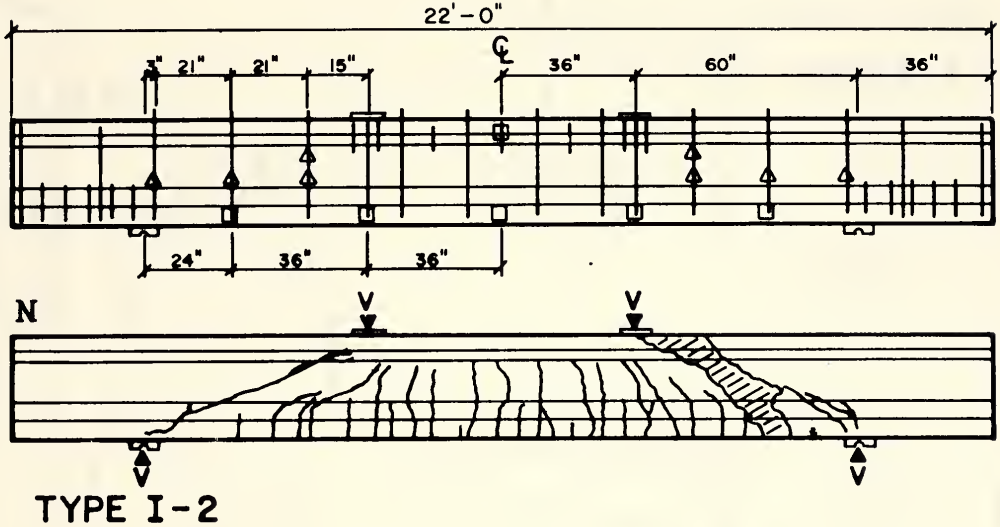

Figure 3.8 - Type I-2 Detail, Instrumentation and Failure Crack Pattern

Table 3.4 - TYPE I-2 Information

TYPE I - 2

Geometry:

Beam Length (ft)	22
Test Span (ft)	16
Shear Span,a (ft)	5
$\frac{a}{d_p}$	2.31

Concrete:

	Transfer	Test
f'_c (psi)	5450	8340
E_c (ksi)	4520	5680
f'_r (psi)	800	820
f_{sp} (psi)	-	550

Prestressing Strand:

	Top	Bottom
Grade	270	270
A_{ps} (in^2)	0.1620	0.1620
d'_p, d_p (in)	2.00	26.00
E_{ps} (ksi)	28240	28240
f_{pu} (ksi)	280.0	280.0
f_{sj} (ksi)	208.8	208.8
f_{si} (ksi)	206.8	196.4
f_{se} (ksi)	197.5	180.5
P_{e1}, P_{e2} (kips)	64.0	233.9

Mild Reinforcement:

	#5 Bar	#4 Bar
Grade	60	40
A'_s, A_v (in^2)	0.31	0.19
d', r f_y (in, psi)	2.00	110
E_s (ksi)	29180	29500
f_y (ksi)	72	52

Test Results:

FLEXURE (kips)

	ACI & AASHTO	Measured
V_{cr}	78.5	95
V_n	134.1	-

SHEAR (kips)

	ACI & AASHTO	Measured
V_{ci}	84.0	-
V_{cw}	99.8	116
		118
V_s	17.1	-
V_n	101.1	148

Mode of Failure: Shear, 148 kips - Web Crushing.

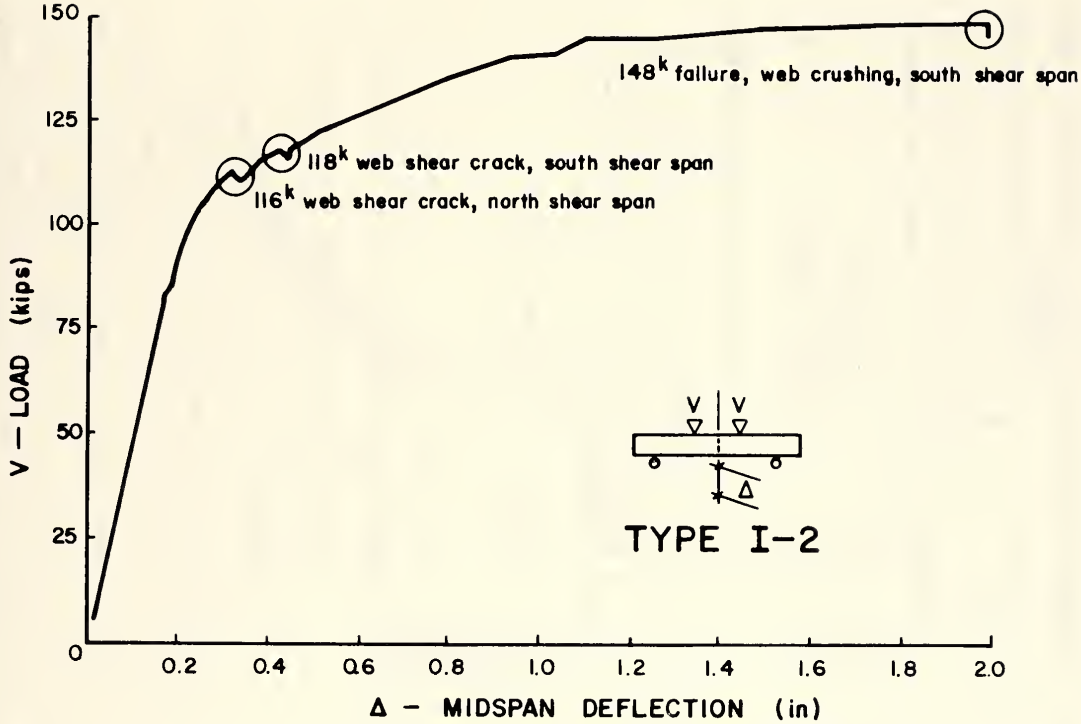

Figure 3.9 - Type I-2 Load vs. Midspan Deflection

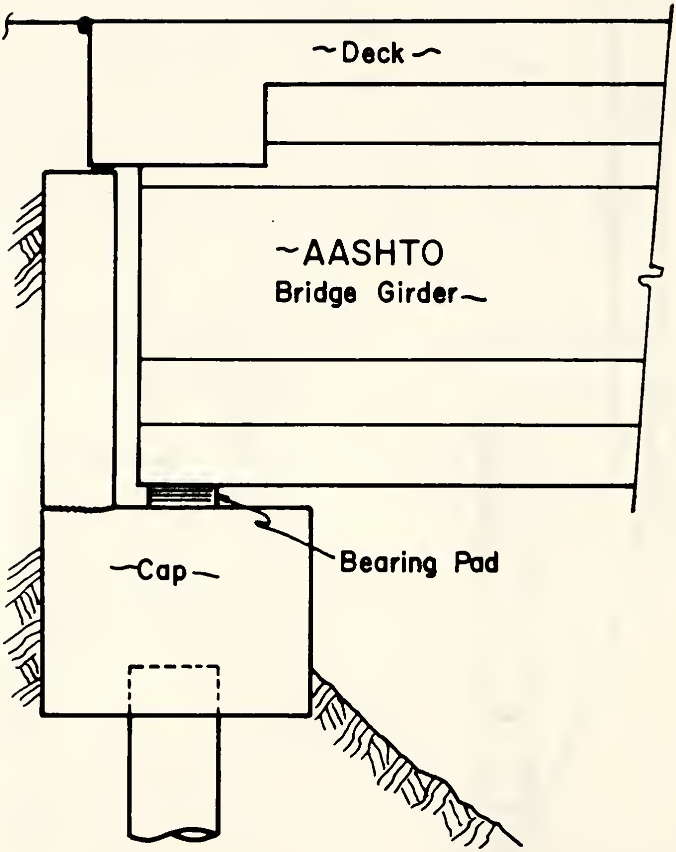

Figure 3.10 - Typical End Support Detail of AASHTO I-Girder and Cast-in-place Slab

Figure 3.11 shows the cross section of beams Type I-3 and Type I-4. Each beam had a test span length of 17 feet and the centerline of the support was placed 6 inches from the end of the beam. The instrumentation and longitudinal reinforcement was identical in these two beams except for the type of the web reinforcement. Type I-3 had #3 bars on 12 inch centers while Type I-4 had #4 bars placed on 21 inch centers. The lower flange reinforcement consisted of 3/4 inch straps and deformed reinforcement. The spacing of this reinforcement was on 6 inch centers from the end of the beam.

3.4.2.1 Test Results of Type I-3

Figure 3.12 shows the instrumentation of Type I-3 along with the failure crack pattern. The overall information of Type I-3 is given in Table 3.5. Flexural cracks appeared first in the constant moment region followed by a web shear crack opening in the south shear span after a small increase of load. Instant strand slip was recorded on the south end and a substantial load drop was observed as shown in Figure 3.13. An attempt to increase the load resulted in additional slip of the strand until the concrete spalled at the top of the beam just south of the south load point.

3.4.2.2 Test Results of Type I-4

Figure 3.14 shows the instrumentation detail of Type I-4 along with the failure crack pattern. The overall information of Type I-4 is given in Table 3.6. The load versus deflection behavior shown in Figure 3.15 was similar to that of Type I-3. A higher load was required to produced the web shear crack, but again strand slippage occurred. Any attempt to increase the load was followed by additional strand slip which led to eventual crushing of the concrete around the hinge point.

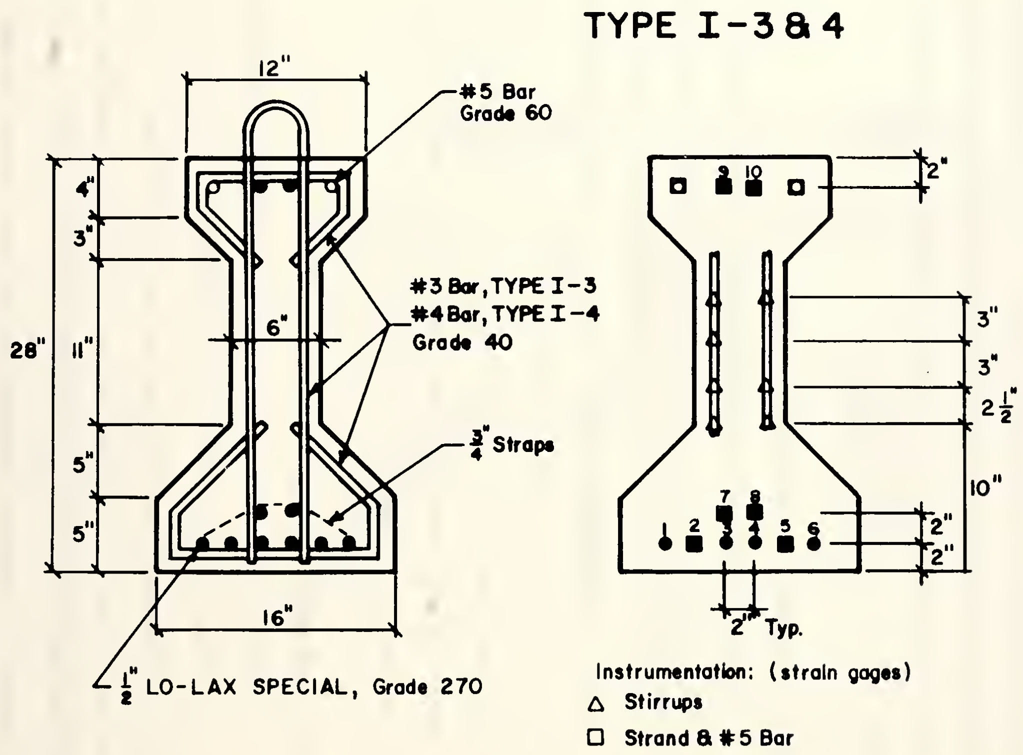

Figure 3.11 - Cross Section of Type I-3 & 4

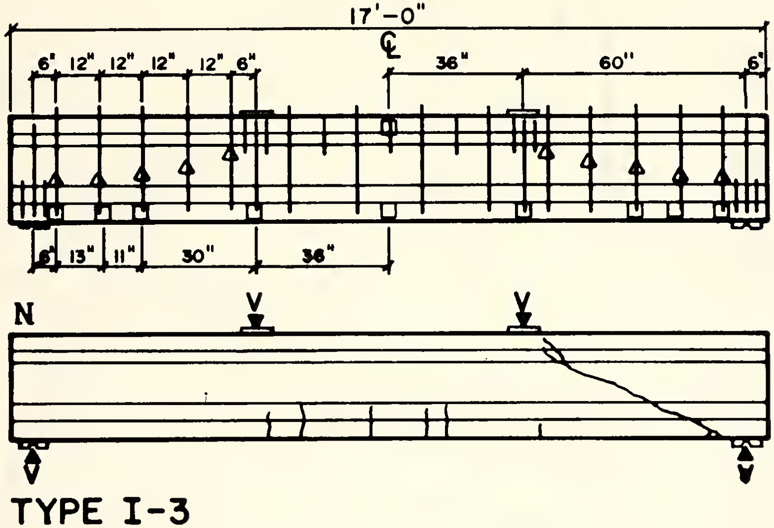

Figure 3.12 - Type I-3 Detail, Instrumentation and Failure Crack Pattern

Table 3.5 - TYPE I-3 Information

TYPE I-3

Geometry:

Beam Length (ft)	17
Test Span (ft)	16
Shear Span,a (ft)	5
$\frac{a}{d_p}$	2.35

Concrete:

	Transfer	Test
f'_c (psi)	5840	8370
E_c (ksi)	5620	5930
f'_r (psi)	920	705
f_{sp} (psi)	-	-

Prestressing Strand:

	Top	Bottom
Grade	270	270
A_{ps} (in^2)	0.1633	0.1633
d'_p, d_p (in)	2.00	25.50
E_{ps} (ksi)	27920	27920
f_{pu} (ksi)	282.0	282.0
f_{sj} (ksi)	207.1	207.1
f_{si} (ksi)	207.6	193.3
f_{se} (ksi)	200.9	184.6
P_{e1}, P_{e2} (kips)	65.6	241.2

Mild Reinforcement:

	#5 Bar	#3 Bar
Grade	60	40
A'_s, A_v (in^2)	0.31	0.104
d', r f_y (in, psi)	2.00	133
E_s (ksi)	29020	29150
f_y (ksi)	64	46

Test Results:

FLEXURE (kips)

	ACI & AASHTO	Measured
V_{cr}	78.2	95
V_n	134.6	-

SHEAR (kips)

	ACI & AASHTO	Measured
V_{ci}	83.6	-
V_{cw}	100.0	101
V_s	20.3	-
V_n	103.9	101

Mode of Failure: Shear, 101 kips - Shear Tension.

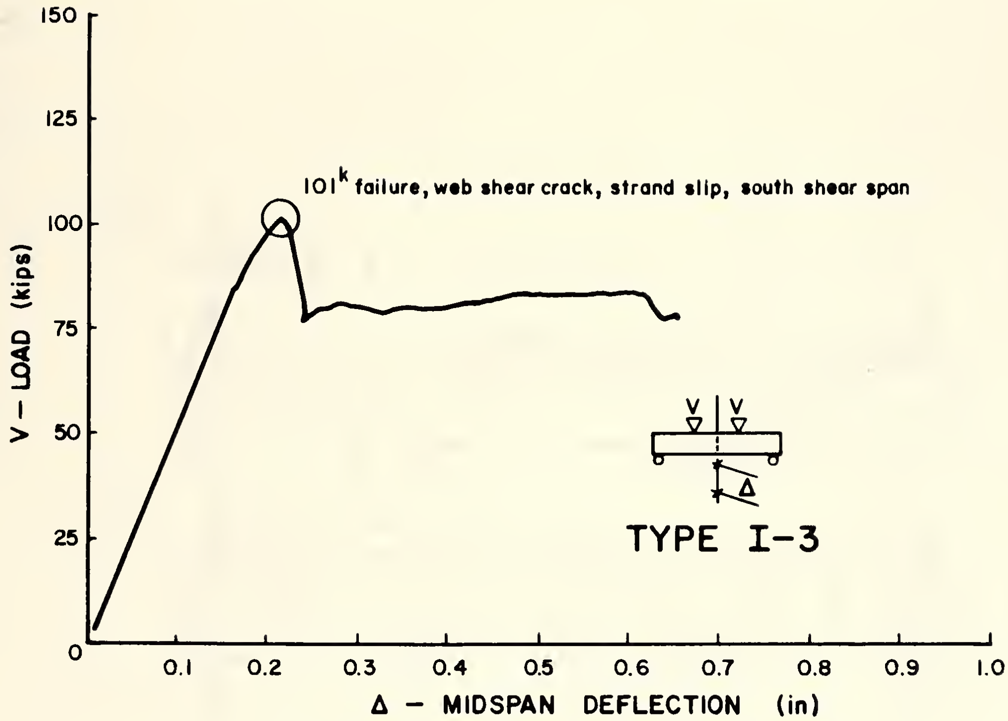

Figure 3.13 - Type I-3 Load vs. Midspan Deflection

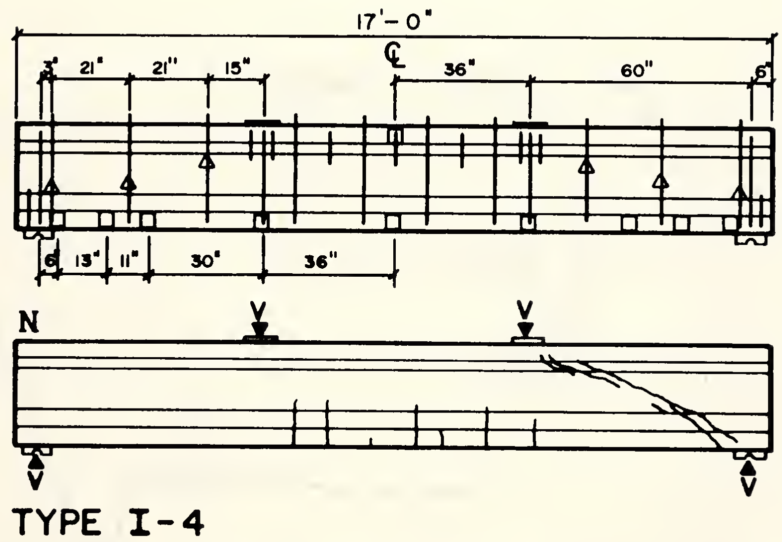

Figure 3.14 - Type I-4 Detail, Instrumentation and Failure Crack Pattern

Table 3.6 - TYPE I-4 Information

TYPE I - 4

Geometry:

Beam Length (ft)	17
Test Span (ft)	16
Shear Span,a (ft)	5.
$\frac{a}{d_p}$	2.35

Concrete:

	Transfer	Test
f'_c (psi)	5840	8370
E_c (ksi)	5620	5930
f'_r (psi)	920	705
f_{sp} (psi)	-	-

Prestressing Strand:

	Top	Bottom
Grade	270	270
A_{ps} (in^2)	0.1633	0.1633
d'_p, d_p (in)	2.00	25.50
E_{ps} (ksi)	27920	27920
f_{pu} (ksi)	282.0	282.0
f_{sj} (ksi)	207.1	207.1
f_{si} (ksi)	207.6	193.3
f_{se} (ksi)	199.9	187.8
P_{e1}, P_{e2} (kips)	65.3	245.4

Mild Reinforcement:

	#5 Bar	#4 Bar
Grade	60	40
A'_s, A_v (in^2)	0.31	0.19
d', r f_y (in, psi)	2.00	110
E_s (ksi)	29020	29500
f_y (ksi)	64	52

Test Results:

FLEXURE (kips)

	ACI & AASHTO	Measured
V_{cr}	79.4	90
V_n	134.6	-

SHEAR (kips)

	ACI & AASHTO	Measured
V_{ci}	84.8	-
V_{cw}	100.7	110
V_s	16.8	-
V_n	101.6	110

Mode of Failure: Shear, 110 kips - Shear Tension.

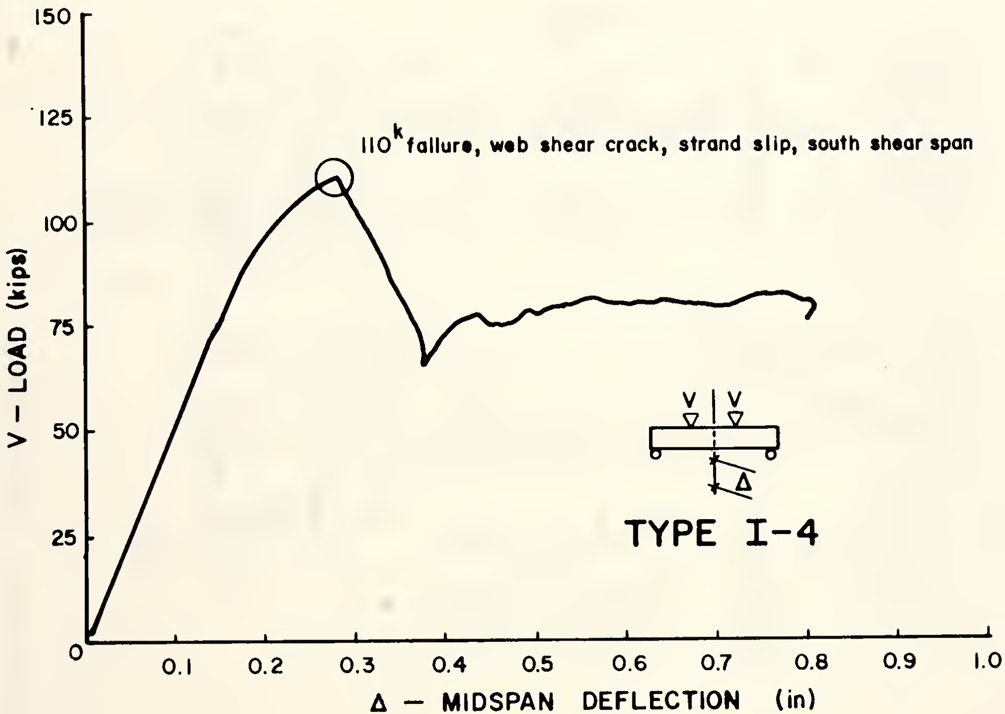

Figure 3.15 - Type I-4 Load vs. Midspan Deflection

3.4.3 Type II-1 and Type II-2

Both AASHTO Type II beams and Type I-3 and I-4 were cast at the same time. Two overhang lengths were used in these two specimens. Type II-1 had the centerline of the support 6 inches from the end of the beam, similar to Type I-3 & 4. Type II-2 had a 24 inch overhang measured from the centerline of the support to the end of the beam. Figure 3.16 shows a cross section detail of the Type II beams.

3.4.3.1 Test Results of Type II-1

A detail of Type II-1 along with the failure pattern is shown in Figure 3.17. Table 3.7 contains the overall information of Type II-1. The behavior of this beam was identical to Type I-3 & 4. Flexure cracks first appeared in the constant moment region with a subsequent web shear crack forming in the south shear span. Upon formation of the web shear crack, slippage of the prestressing strand with respect to the end of the beam was observed. An effort to increase the load led to additional slippage of the strand. The centerline load versus deflection curve for this specimen is shown in Figure 3.18.

3.4.3.2 Test Results of Type II-2

Figure 3.19 shows the instrumentation along with the failure crack pattern for beam Type II-2. Table 3.8 gives the overall information of Type II-2. Flexural cracks appeared first in the constant moment region. Three web shear cracks occurred in this beam. The first opened in the south shear span with the second opening in the north. A third crack formed approximately 6 inches below and parallel to the previously formed web shear crack in the south shear span as shown in Figure 3.19. Type II-2 had a 24 inch overhang which provided sufficient anchorage to the strand as no slip was

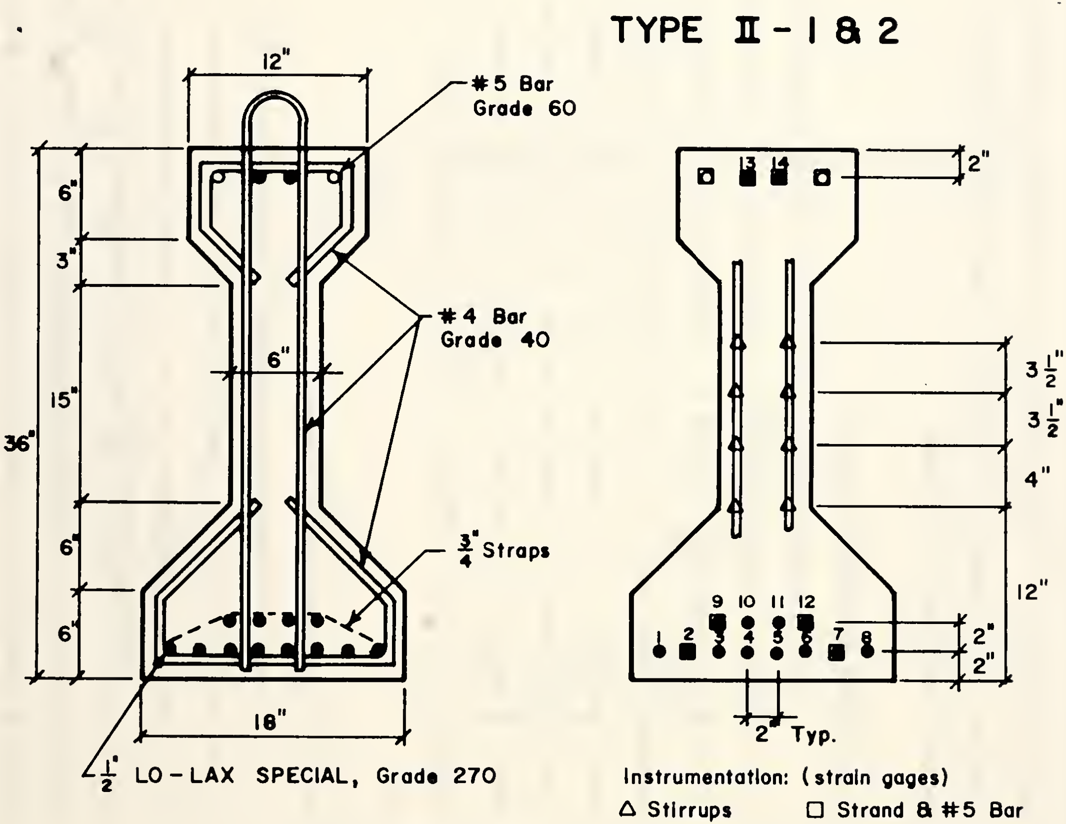

Figure 3.16 - Cross Section of Type II-1 & 2

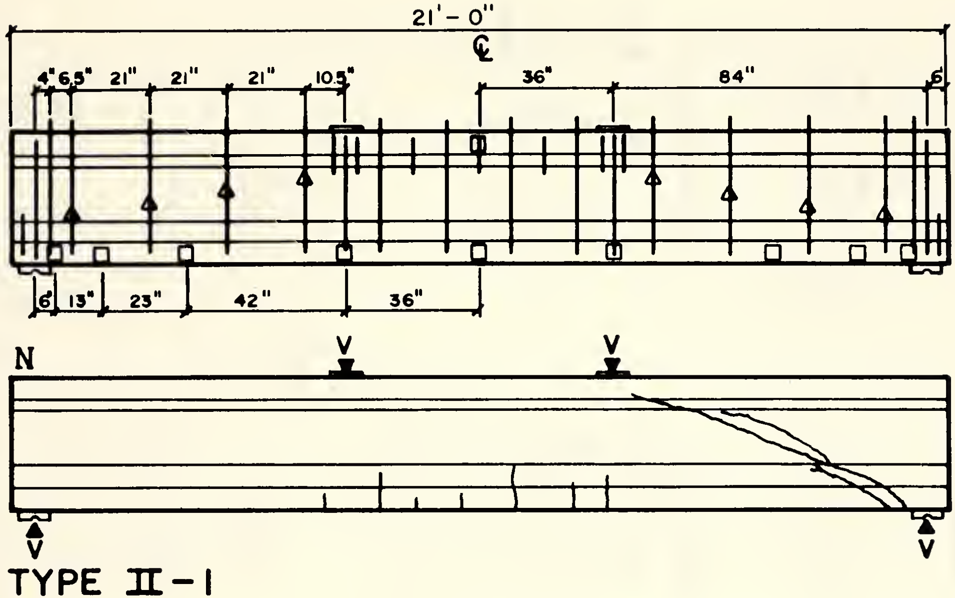

Figure 3.17 - Type II-1 Detail, Instrumentation and Failure Crack Pattern

Table 3.7 - TYPE II-1 Information

TYPE II - 1

Geometry:

Beam Length (ft)	21
Test Span (ft)	20
Shear Span,a (ft)	7
$\frac{a}{d_p}$	2.52

Concrete:

	Transfer	Test
f'_c (psi)	5980	9090
E_c (ksi)	5580	6010
f'_r (psi)	920	650
f_{sp} (psi)	-	570

Prestressing Strand:

	Top	Bottom
Grade	270	270
A_{ps} (in^2)	0.1633	0.1633
d'_p, d_p (in)	2.00	33.33
E_{ps} (ksi)	27920	27920
f_{pu} (ksi)	282.0	282.0
f_{sj} (ksi)	207.1	207.1
f_{si} (ksi)	207.4	193.5
f_{se} (ksi)	200.9	183.5
P_{e1}, P_{e2} (kips)	65.6	359.5

Mild Reinforcement:

	#5 Bar	#4 Bar
Grade	60	40
A'_s, A_v (in^2)	0.29	0.19
d', r f_y (in, psi)	2.00	157
E_s (ksi)	28570	29500
f_y (ksi)	62	52

Test Results:

FLEXURE (kips)

	ACI & AASHTO	Measured
V_{cr}	111.0	130
V_n	186.9	-

SHEAR (kips)

	ACI & AASHTO	Measured
V_{ci}	118.3	-
V_{cw}	135.8	140
V_s	31.4	-
V_n	149.7	140

Mode of Failure: Shear, 140 kips - Shear Tension.

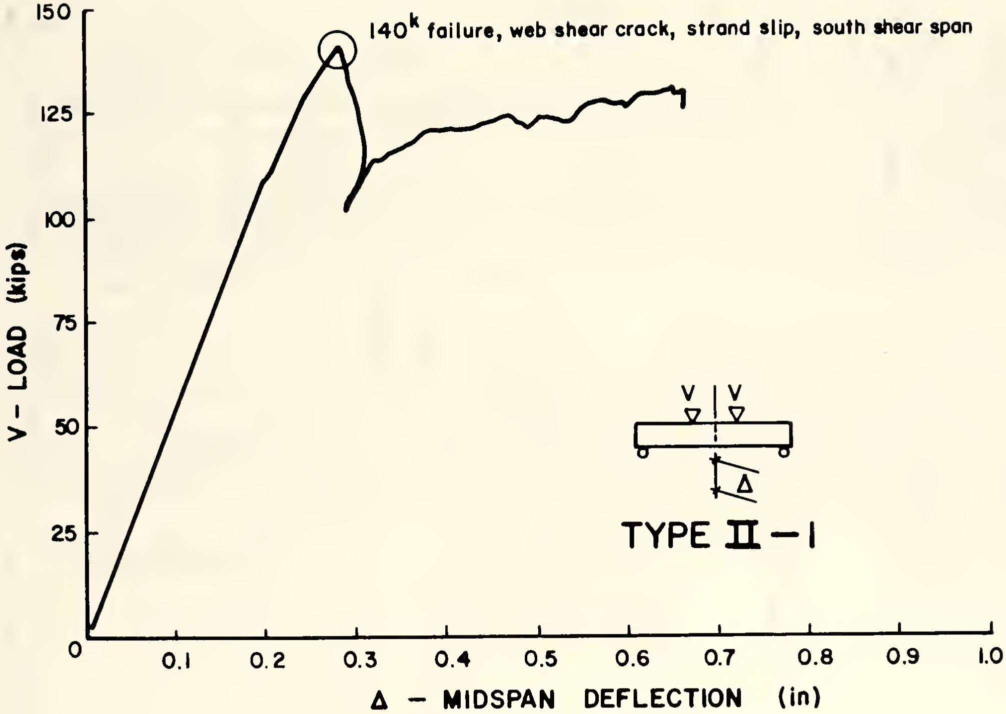

Figure 3.18 - Type II-1 Load vs. Midspan Deflection

Table 3.8 - TYPE II-2 Information

TYPE II - 2

Geometry:

Beam Length (ft)	24
Test Span (ft)	20
Shear Span,a (ft)	7
$\frac{a}{d_p}$	2.52

Concrete:

	Transfer	Test
f'_c (psi)	5980	9090
E_c (ksi)	5580	6010
f'_r (psi)	920	650
f_{sp} (psi)	-	570

Prestressing Strand:

	Top	Bottom
Grade	270	270
A_{ps} (in^2)	0.1633	0.1633
d'_p, d_p (in)	2.00	33.33
E_{ps} (ksi)	27920	27920
f_{pu} (ksi)	282.0	282.0
f_{sj} (ksi)	207.1	207.1
f_{si} (ksi)	207.2	193.6
f_{se} (ksi)	198.4	179.6
P_{e1}, P_{e2} (kips)	64.8	351.9

Mild Reinforcement:

	#5 Bar	#4 Bar
Grade	60	40
A'_s, A_v (in^2)	0.29	0.19
d', r f_y (in, psi)	2.00	157
E_s (ksi)	28570	29500
f_y (ksi)	62	52

Test Results:

FLEXURE (kips)

	ACI & AASHTO	Measured
V_{cr}	109.1	120
V_n	186.9	201

SHEAR (kips)

	ACI & AASHTO	Measured
V_{ci}	116.4	-
V_{cw}	134.5	141 152
V_s	31.4	-
V_n	147.8	-

Mode of Failure: Flexure, 201 kips.

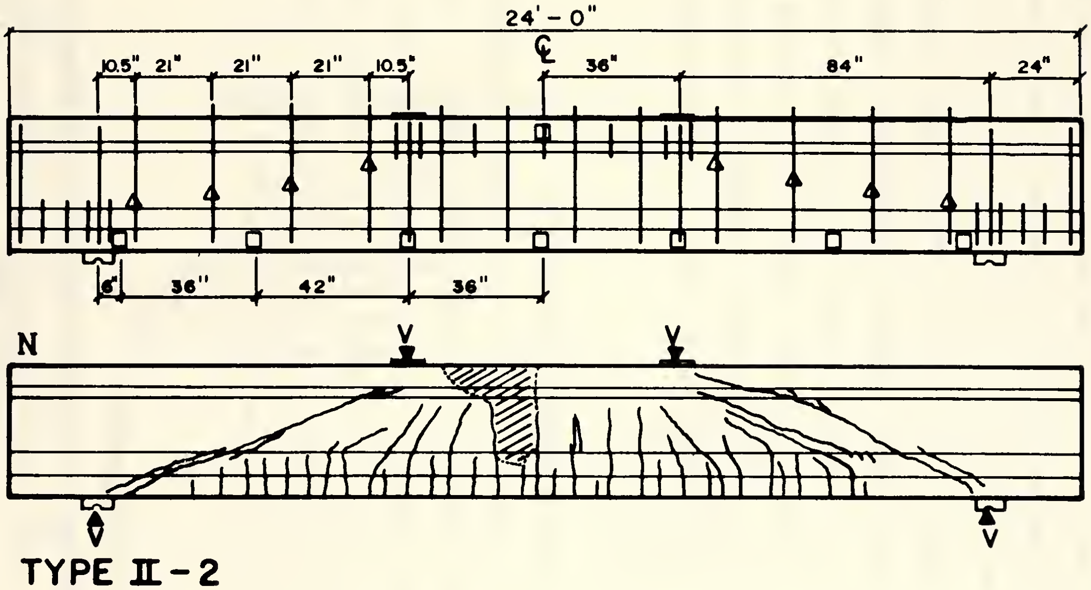

Figure 3.19 - Type II-2 Detail, Instrumentation and Failure Crack Pattern

recorded during the test. The load versus centerline deflection curve is shown in Figure 3.20. The failure of the beam was very explosive. After yielding of the strand, deflections increased up to initial spalling of the top fiber which is shown as the initial load drop off at about a two inch deflection as shown in the load versus deflection behavior. A large fraction of the load remained after the initial spalling. Top flange reinforcement spaced on 9 inch centers along with the top longitudinal reinforcement provided some confinement to the compression block. As the load was applied to the beam, spalling of the concrete around the confined concrete continued. Failure occurred as the compression block moved into the web region leading to a very sudden and explosive failure. The failure removed the section of concrete shown by the dashed area in Figure 3.19.

3.4.4 Type I-3A, Type I-4A and Type II-1A

The north shear spans of the three beams that failed in the shear tension mode remained uncracked and basically remained elastic up to failure in the initial test. Hence, it was decided to conduct a second test on these beams using a single point load. The purpose was to find out what length of overhang would provide adequate anchorage to the strand. Also, additional information could be obtained on the flexural and shear behavior of these beams.

3.4.4.1 Test Results of Type I-3A

The instrumentation detailing and the failure crack pattern for beam I-3A are shown in Figure 3.21. Table 3.9 gives the overall information for Type I-3A. An 18 inch overhang was provided in the north shear span. The extent of cracking produced in the initial test is indicated by a dot placed at the tip of the crack shown in Figure 3.21. Initially a slight increase in the

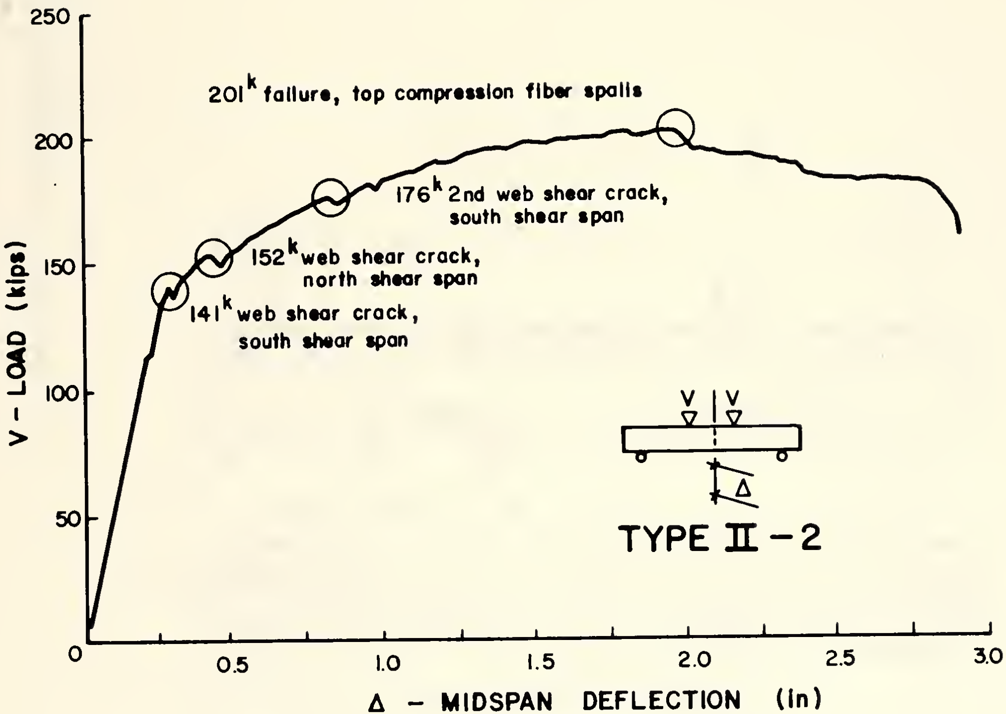

Figure 3.20 - Type II-2 Load vs. Midspan Deflection

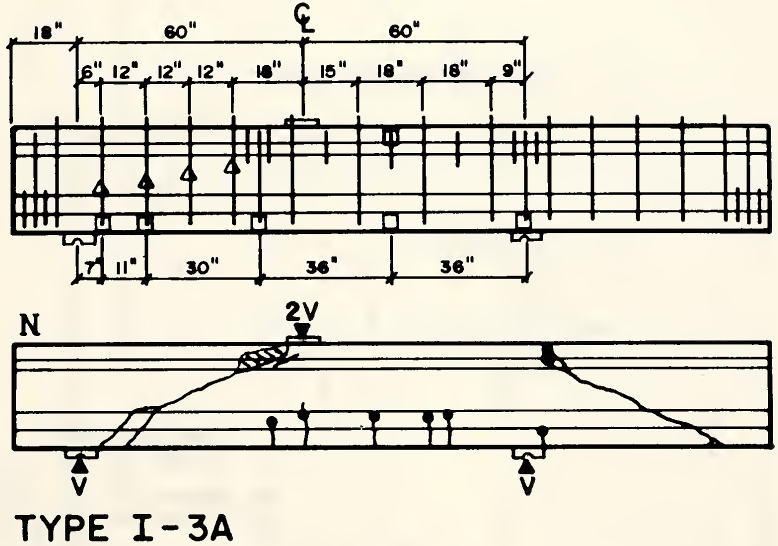

Figure 3.21 - Type I-3A Detail, Instrumentation and Failure Crack Pattern

Table 3.9 - TYPE I-3A Information

TYPE I - 3A

Geometry:

Beam Length (ft)	17
Test Span (ft)	10
Shear Span,a (ft)	5
$\frac{a}{d_p}$	2.35

Concrete:

	Transfer	Test
f'_c (psi)	5840	8810
E_c (ksi)	5620	5730
f'_r (psi)	920	-
f_{sp} (psi)	-	-

Prestressing Strand:

	Top	Bottom
Grade	270	270
A_{ps} (in^2)	0.1633	0.1633
d'_p, d_p (in)	2.00	25500
E_{ps} (ksi)	27920	27920
f_{pu} (ksi)	282.0	282.0
f_{sj} (ksi)	207.1	207.1
f_{si} (ksi)	207.6	193.3
f_{se} (ksi)	200.9	184.6
P_{e1}, P_{e2} (kips)	65.6	241.2

Mild Reinforcement:

	#5 Bar	#3 Bar
Grade	60	40
A'_s, A_v (in^2)	0.31	0.104
d', r f_y (in, psi)	2.00	80
E_s (ksi)	29020	29150
f_y (ksi)	64	46

Test Results:

FLEXURE

	ACI & AASHTO	Measured
V_{cr}	-	-
V_n	134.6	-

SHEAR

	ACI & AASHTO	Measured
V_{ci}	85.0	-
V_{cw}	101.3	98
V_s	12.2	-
V_n	97.2	113

Mode of Failure: Shear, 113 kips - Shear Tension

previous flexure cracks was observed, followed by a web shear crack in the north shear span. Approximately 50% of the strands slipped at the formation of this shear crack. As the load was increased, all strands eventually slipped until crushing of the concrete took place just north of the centerline load plate. The load versus the centerline deflection plot is shown in Figure 3.22.

3.4.4.2 Test Results of Type I-4A

Figure 3.23 shows the instrumentation detailing along with the failure crack pattern for beam Type I-4A. Table 3.10 gives the overall information for Type I-4A. A 24 inch overhang was provided for the north shear span. In this test, two web shear cracks opened; the first in the south shear span, and the second in the north shear span. No slippage was observed in the prestressing strands. Failure occurred by initial spalling of the concrete on the south edge of the load plate. This led to an explosive failure of the south shear span. The concrete removed by the failure is shown by the dashed area shown in Figure 3.23. The load versus midspan deflection curve is shown in Figure 3.24.

3.4.4.3 Test Results of Type II-1A

Figure 3.25 shows the instrumentation detail along with the failure crack pattern for beam Type II-1A. The overall general information of Type II-1A is given in Table 3.11. A 24 inch overhang was provided for the north shear span. Two web shear cracks opened, one in the south shear span and the second in the north shear span. No slippage was observed in the prestressing strands. Failure occurred by initial spalling of the top fiber concrete on the north edge of the load plate. As the load was further applied, continuing spalling occurred until the explosive failure of the top flange in the north

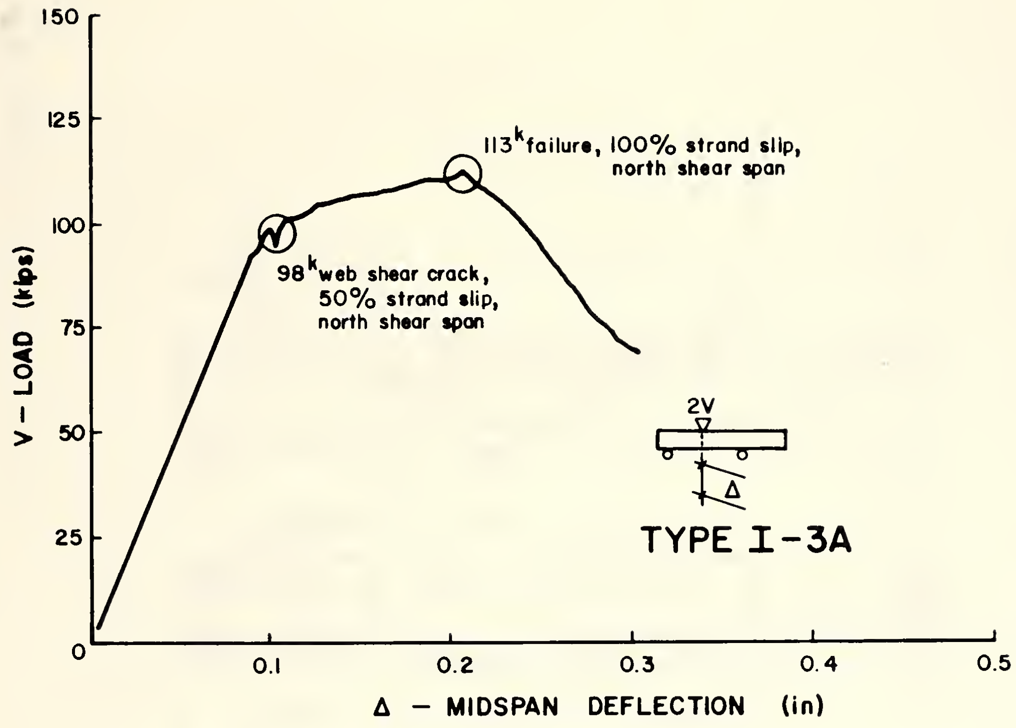

Figure 3.22 - Type I-3A Load vs. Midspan Deflection

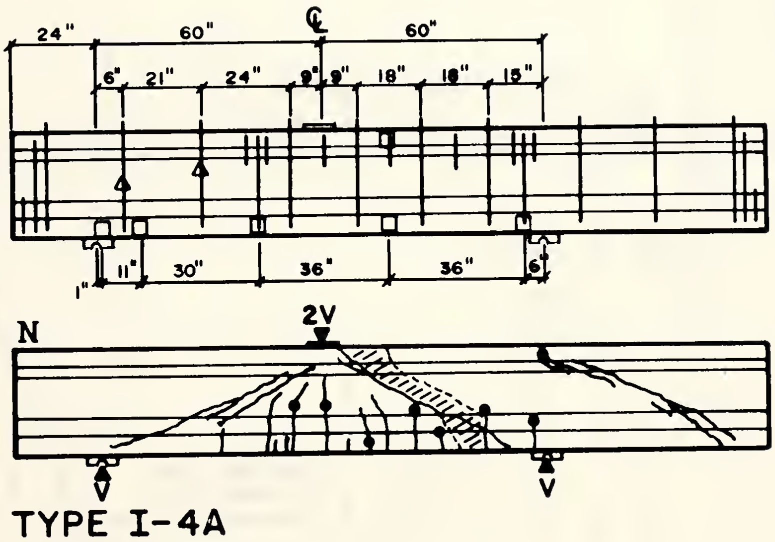

Figure 3.23 - Type I-4A Detail, Instrumentation and Failure Crack Pattern

Table 3.10 - Type I-4A Information

TYPE I - 4A

Geometry:

Beam Length (ft)	17
Test Span (ft)	10
Shear Span,a (ft)	5
$\frac{a}{d_p}$	2.35

Concrete:

	Transfer	Test
f'_c (psi)	5840	8810
E_c (ksi)	5620	5930
f'_r (psi)	920	-
f_{sp} (psi)	-	-

Prestressing Strand:

	Top	Bottom
Grade	270	270
A_{ps} (in^2)	0.1633	0.1633
d'_p, d_p (in)	2.00	26.00
E_{ps} (ksi)	27920	27920
f_{pu} (ksi)	282.0	282.0
f_{sj} (ksi)	207.1	207.1
f_{si} (ksi)	207.6	193.3
f_{se} (ksi)	199.9	187.8
P_{e1}, P_{e2} (kips)	65.3	245.4

Mild Reinforcement:

	#5 Bar	#4 Bar
Grade	60	40
A'_s, A_v (in^2)	0.31	0.19
d', r f_y (in, psi)	2.00	165
E_s (ksi)	29020	29500
f_y (ksi)	64	52

Test Results:

FLEXURE

	ACI & AASHTO	Measured
V_{cr}	-	-
V_n	134.6	161

SHEAR

	ACI & AASHTO	Measured
V_{ci}	86.2	-
V_{cw}	101.9	118 120
V_s	25.2	-
V_n	111.4	161

Mode of Failure: Shear, 161 kips - Shear Compression

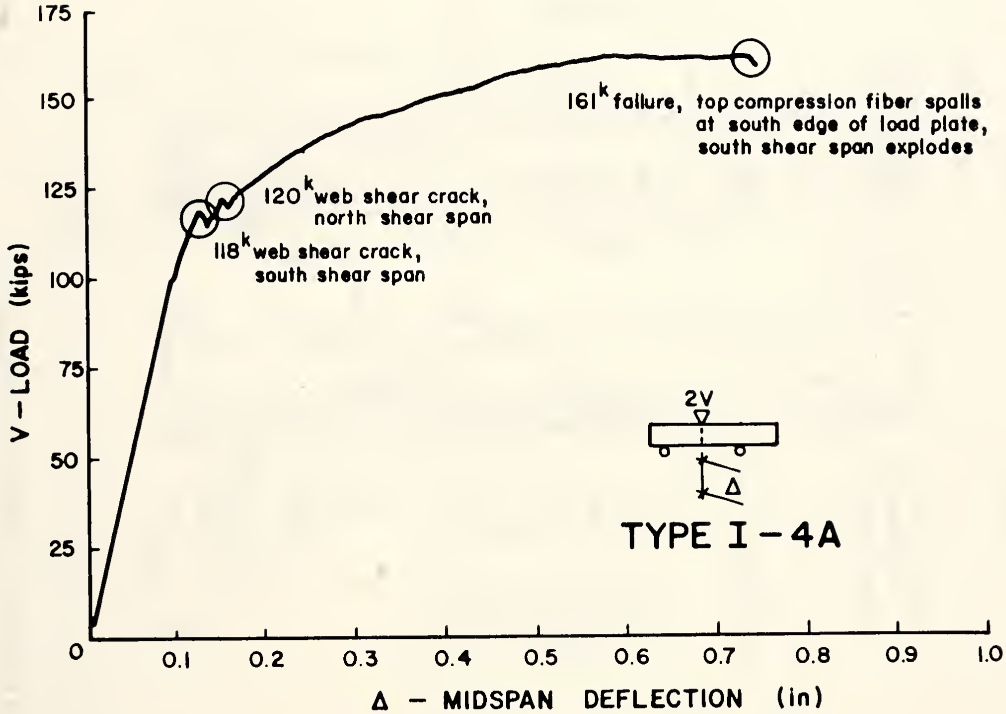

Figure 3.24 - Type I-4A Load vs. Midspan Deflection

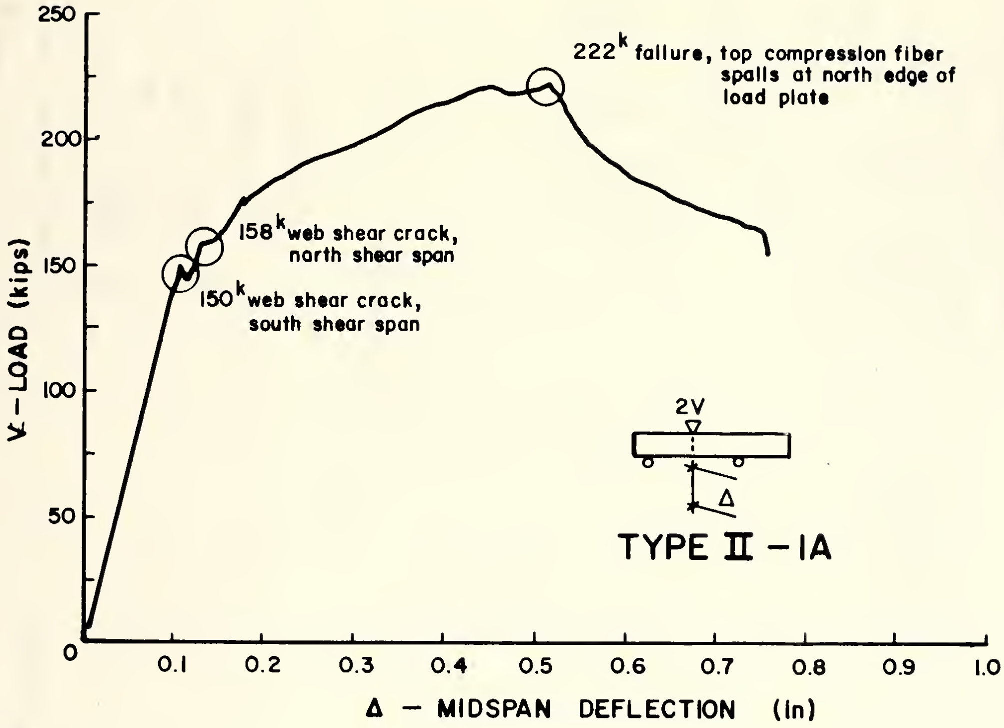

Figure 3.25 - Type II-1A Detail, Instrumentation and Failure Crack Pattern

Table 3.11 - Type II-1A Information

TYPE II - 1A

Geometry:

Beam Length (ft)	21
Test Span (ft)	12
Shear Span,a (ft)	6
$\frac{a}{d_p}$	2.16

Concrete:

	Transfer	Test
f'_c (psi)	5980	8950
E_c (ksi)	5580	5900
f'_r (psi)	920	
f_{sp} (psi)	-	-

Prestressing Strand:

	Top	Bottom
Grade	270	270
A_{ps} (in^2)	0.1633	0.1633
d'_p, d_p (in)	2.00	26.00
E_{ps} (ksi)	27920	27920
f_{pu} (ksi)	282.0	282.0
f_{sj} (ksi)	207.1	207.1
f_{si} (ksi)	207.4	193.5
f_{se} (ksi)	200.9	183.5
P_{e1}, P_{e2} (kips)	65.6	359.5

Mild Reinforcement:

	#5 Bar	#4 Bar
Grade	60	40
A'_s, A_v (in^2)	0.29	0.19
d', r f_y (in, psi)	2.00	137
E_s (ksi)	28570	29500
f_y (ksi)	62	52

Test Results:

FLEXURE

	ACI & AASHTO	Measured
V_{cr}	-	-
V_n	186.9	222

SHEAR

	ACI & AASHTO	Measured
V_{ci}	129.5	-
V_{cw}	135.3	150
		158
V_s	27.4	-
V_n	156.9	222

Mode of Failure: Shear, 222 kips - Shear Compression

shear span. The concrete removed by the failure is shown by the dashed area shown in Figure 3.25. The load versus midspan deflection plot is shown in Figure 3.26.

3.5 Analysis of Test Results

Discussion of the test results is conducted in accordance to the mode of failure. Flexural behavior is discussed first including both elastic and ultimate behavior. Finally, the shear failures are analyzed along with special topics relevant to the behavior of the test beams.

3.5.1 Flexure

The elastic behavior of prestressed I-sections is relevant to evaluate service load performance. Prior to cracking, the section behaves elastically and the response to external loadings is linear. After cracking, the load versus deflection curve becomes nonlinear as the stresses in the concrete and reinforcement exceed their elastic limits. For under-reinforced members, flexural failure occurs after initial yielding of the prestressing strand which preceeds crushing of the concrete at the extreme compression fiber.

3.5.1.1 Elastic Behavior

Deflections were measured at the midspan of each specimen and either under the point load or 12 inches from the point load towards the support. The load deflection behavior is a function of the span length, type of loading, cross section and material properties. Volume I of this study established that the current equation used to predict the modulus of elasticity of concrete is adequate for compressive strengths up to 9000 psi. Table 3.12 contains the ratio of the deflection to the point load as measured during the test and estimated by elastic theory prior to cracking of the section. The modulus

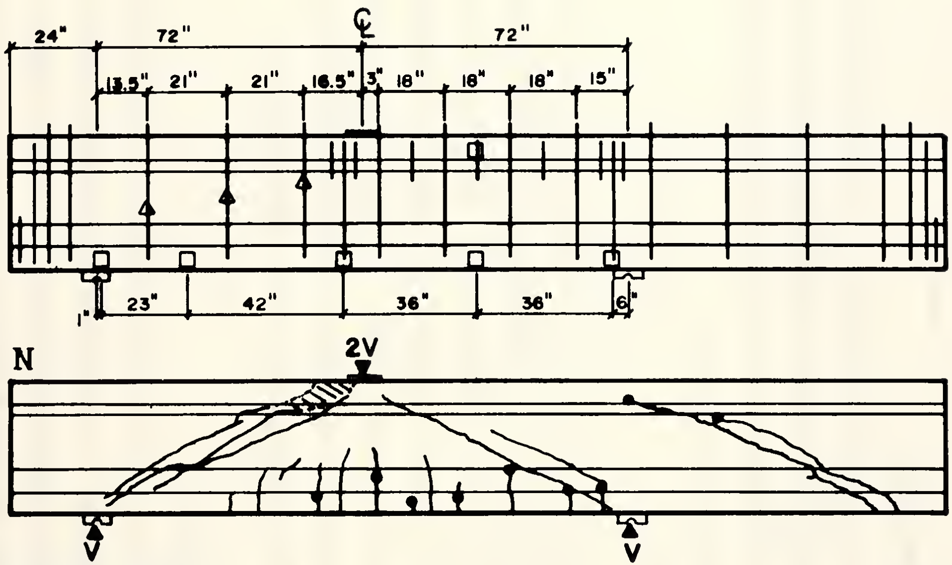

TYPE II - 1A

Figure 3.26 - Type II-1A Load vs. Midspan Deflection

Table 3.12 - Elastic Deflections

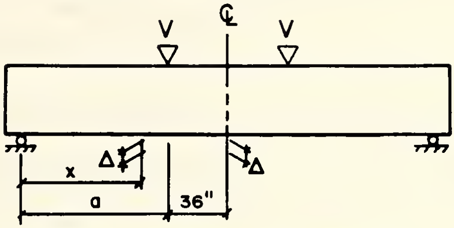

Centerline Deflection (see Appendix D)

$$\frac{\Delta}{V} = \frac{2\,a^3 + 6(36)\,a^2 + 3(36)^2\,a}{6\,E_c\,I_b}$$

Beam	a (in)	E_c (ksi)	I_b (in^4)	$\frac{\Delta}{V}$ predicted ($\frac{in}{lbs}$ x 10^{-6})	$\frac{\Delta}{V}$ test ($\frac{in}{lbs}$ x 10^{-6})	$\frac{predicted}{test}$
Type I-1	72	5200	23493	2.93	2.91	1.01
Type I-2	60	5200	23493	1.97	2.06	0.95
Type I-3	60	5220	22750	2.03	1.99	1.02
Type I-4	60	5220	22750	2.03	1.98	1.02
Type II-2	84	5430	50979	1.83	1.84	0.99
Type II-2	84	5430	50797	1.83	1.78	1.03

Quarter Point Deflection (see Appendix D)

$$\frac{\Delta}{V} = \frac{x\,(\,3\,a^2 + 6(36)\,a - x^2)}{6\,E_c\,I_b}$$

Beam	a (in)	x (in)	E_c (ksi)	I_b (in^4)	$\frac{\Delta}{V}$ predicted ($\frac{in}{lbs}$ x 10^{-6})	$\frac{\Delta}{V}$ test ($\frac{in}{lbs}$ x 10^{-6})	$\frac{predicted}{test}$
Type I-1	72	72	5200	23493	2.55	2.53	1.01
Type I-2	60	48	5200	23493	1.41	1.47	0.96
Type I-3	60	48	5220	22750	1.44	1.45	1.01
Type I-4	60	48	5220	22750	1.44	-	-
Type II-2	84	72	5430	50979	1.48	1.49	0.99
Type II-2	84	72	5430	50797	1.48	1.44	1.03

of elasticity was calculated using the AASHTO/ACI prediction equation

$$E_c = 57000 \sqrt{f'_c} \text{ (psi)}$$

This equation assumes the unit weight of the concrete, w_c, equal to 145 pcf. The moment of inertia, I_b, is based on the gross section properties. The ratio of the predicted to the measured values ranges from 0.95 to 1.03. Thus, the current method used to obtain the modulus of elasticity, and the use of the gross moment of inertia values are shown to be adequate for computation of deflections of these beams.

A comparison between the load required to produce a flexure crack and the predicted load is shown in Table 3.13. The observed to predicted ratios range from 1.10 to 1.21. The observed cracking load was difficult to measure. Each beam was white washed prior to the test to aid in the detection of any cracks. The load increment prior to the formation of the first flexure crack was 5 kips. Hence, the formation of the flexure crack could have occurred at a load 5 kips lower than observed. Another method used to determine the formation of flexure crack is based on the load versus deflection behavior. The load versus deflection behavior is elastic prior to the formation of a crack. The formation of a flexure crack results in a loss of stiffness. An increase in deflection can be seen in the load-deflection plot after the formation of the flexure crack. The load which corresponds to the loss of stiffness as determined from the load deflection graph indicates that a flexure crack occurred prior to observing the crack on the surface of the beam. However, in no case was this load less than that predicted using current established procedures, ie. AASHTO Specification (9.15). The tensile capacity of the concrete

Table 3.13 - Flexural Cracking Capacity

Beam	a (in)	f'_c (psi)	P_{e1} (ksi)	e1 (in)	P_{e2} (ksi)	e2 (in)
Type I-1	72	8340	64.4	13.49	233.8	10.51
Type I-2	60	8340	64.0	13.49	233.9	10.51
Type I-3	60	8370	65.6	13.41	241.2	10.09
Type I-4	60	8370	65.3	13.41	245.4	10.09
Type II-1	84	9090	65.6	18.17	359.5	13.16
Type II-2	84	9090	64.8	18.17	351.9	13.16

AASHTO Prediction (see Appendix C)

$$V_{cr} = \frac{1}{a}\left[S_2\left(7.5\sqrt{f'_c} + \frac{P_{e1} + P_{e2}}{A_b}\right) - \frac{w_o\, l^2}{8} + P_{e2}\, e2 - P_{e1}\, e1\right]$$

Beam	V_{cr} Observed (kips)	V_{cr} Predicted (kips)	$\frac{\text{Observed}}{\text{Predicted}}$
Type I-1	75	64.9	1.16
Type I-2	95	78.5	1.21
Type I-3	95	78.2	1.21
Type I-4	90	79.4	1.13
Type II-1	130	111.0	1.17
Type II-2	120	109.1	1.10

taken equal to 7.5 $\sqrt{f'_c}$ was shown to give conservative estimates of the cracking load of these specimens.

3.5.1.2 Ultimate Strength Behavior

AASHTO I-girders are used in composite construction. Hence, the flexural strength of the I-girder without the cast-in-place is never evaluated in design. In this study each beam was designed to fail in shear, therefore the designed nominal moment capacity was greater than the shear strength as predicted by current AASHTO equations. However, since two of the beams tested failed in flexure, a discussion of the tests is given.

Type I-1 and Type II-2 failed in flexure. Current specifications restricts the amount of flexural reinforcement to insure yielding of the prestressing strand prior to the crushing of the concrete at the extreme flexural compression fiber. This is achieved through the limitation of the reinforcement index, ω_p.

$$\omega_p \leq 0.36\ \beta_1$$

with, $\omega_p = \dfrac{A_{ps}}{b\ d_p}\ \dfrac{f_{ps}}{f'_c}$

$\beta_1 =$ 0.85 for concrete strengths f'_c up to and including 4000 psi. For strengths above 4000 psi, β_1 shall be reduced continuously at a rate of 0.05 for each 1000 psi of strength in excess of 4000 psi, but β_1 shall not be taken less than 0.65

Table 3.14 shows information relating the reinforcement index for all beams. The stress in the strand at ultimate strength, f_{ps}, was calculated using strain compatibility analysis. Table 3.15 compares the predicted stress in the strand at ultimate strength from AASHTO procedures, Column (1), to those obtained from the strain compatibility type analysis, Column (2). The two procedures

Table 3.14 - Reinforcement Index and Deflection Ductility

Beam	f'_c (psi)	f_{ps} (ksi)	A_{ps} (in^2)	b (in)	d_p (in)	ω_p	$\mu = \frac{\Delta_u}{\Delta_y}$
Type I-1	8340	258.6	1.296	12	26.00	0.129	2.09
Type I-2	8340	258.6	1.296	12	26.00	0.129	2.49
Type I-3	8370	263.1	1.306	12	25.50	0.134	
Type I-2	8370	263.2	1.306	12	25.50	0.134	
Type II-1	9090	262.2	1.960	12	33.33	0.141	
Type II-2	9090	262.2	1.960	12	33.33	0.141	1.84

$$\omega_p = \frac{A_{ps}}{b\ d_p} \frac{f_{ps}}{f'_c}$$

$$\omega_{max} = 0.36\beta_1 = 0.36(0.65) = 0.234$$

Table 3.15 - Stress in the Strand at Ultimate Strength

Beam	ρ_p	f_{pu} (ksi)	f'_c (psi)	(1) f_{ps} (ksi)	(2) f_{ps} (ksi)	$\frac{(1)}{(2)}$
Type I-1	0.0042	280	8340	260.5	258.6	1.01
Type I-2	0.0042	280	8340	260.5	258.6	1.01
Type I-3	0.0043	282	8370	261.7	263.1	0.99
Type I-4	0.0043	282	8370	261.7	263.2	0.99
Type II-1	0.0049	282	9090	260.6	262.2	0.99
Type II-2	0.0049	282	9090	260.6	262.2	0.99

Column (1) -- $f_{ps} = f_{pu} \left(1 - 0.5\ \rho_p \frac{f_{pu}}{f'_c}\right)$

Column (2) -- Strain Compatibilty Analysis

are within 1%. All beams were designed below the maximum reinforcement index as shown in Table 3.14. A common value used to measure the ductility of a flexural member is calculated by taking the deflection at ultimate strength and dividing it by the deflection of the member when the strand first yields, or the strain in the strand reaches 1%. This value is called the deflection ductility index[21], μ, and is given in Table 3.14 for beams Type I-1, I-2, and II-2. Type I-2 failed in shear, however the failure was also quite ductile.

Table 3.16 contains the predicted flexural capacity and test values for the beams Type I-1, Type I-2, and Type II-2. The stress in the prestressing strand at ultimate strength was calculated using a strain compatibility analysis. The flexural capacity predicted by AASHTO, Column (1), is much less than the actual failure load of these three beams. However, the measured stress in the prestressing strand at ultimate strength compares very well to the stress predicted by the strain compatibility analysis. The predicted load was calculated by taking nominal moment capacity and dividing it by the shear span measured from the centerline of the load application to the centerline of the support. The shear span is often taken as the distance from the centerline of the load point to the face of the support. The support plate had a width of 8 inches. Column (2) presents the results using the reduced shear span showing a much better agreement.

The current methods used to estimate the ultimate flexural capacity and predict the stress in the strand at ultimate strength are adequate for prestressed I-beams with concrete compressive strengths up to 9000 psi. Current AASHTO Specifications limit the amount of reinforcement by limiting the reinforcement index, $\omega \leq 0.3$. This limit has been shown to allow excessive amounts of reinforcement for concrete strengths in excess of 5000 psi[14]. However for this type of construction, the concrete strength of the slab will

Table 3.16 - Moment Capacities and Predictions

Beam	A_{ps} (in^2)	f_{ps} (ksi)	f'_c (psi)	d_p (in)	b (in)
Type I-1	1.296	258.6	8340	26.00	12
Type I-2	1.296	258.6	8340	26.00	12
Type II-2	1.960	262.2	9090	33.33	12

Nominal Moment Capacity, P_{AASHTO}

$$P_{AASHTO} = \frac{1}{a} \left(A_{ps} f_{ps} \left(d_p - \frac{A_{ps} f_{ps}}{2\,(0.85)\, f'_c\, b} \right) \right)$$

Beam	P_{test} (kips)	(1) a (in)	(1) P_{AASHTO} (kips)	(1) $\frac{P_{test}}{P_{AASHTO}}$	(2) a (in)	(2) P_{AASHTO} (kips)	(2) $\frac{P_{test}}{P_{AASHTO}}$
Type I-1	123	72	111.9	1.10	68	118.5	1.04
Type I-2	148	60	134.1	1.10	56	143.7	1.03
Type II-2	201	84	186.9	1.08	80	196.3	1.02

control the amount of reinforcement and not the concrete strength of the I-beam. Hence, the current limit is adequate as long as the concrete strength of the cast-in-place slab remains around 4000 psi.

3.5.2 Shear

Since the shear capacity of the composite structure (precast I beam and concrete slab deck) is mainly dependent on the prestressed I-beam, it was decided to test the beams non-composite. The following discussion includes the beams which failed in the shear mode (web crushing and shear tension). The truss model, introduced in Section 2.3.4, is used in the analysis of these beams.

3.5.2.1 Web Crushing

Type I-2 was identical to Type I-1 except that the supports were moved 12 inches towards the midspan to reduce the moment to shear ratio. In general the behavior of Type I-2 was similar to Type I-1 except for the failure mode. The stress in the strands exceeded the yield value at failure. Failure for this beam occurred when the web suddenly exploded. Figure 3.27 shows the crack pattern of the south shear span at failure along with the selected truss model to represent the distribution of internal forces at failure. The vertical tension member of the truss represents the resultant of two stirrups at yield, 39.5 kips. The failure load, 148 kips, less the contribution of the web reinforcement must be carried by the vertical component of the diagonal compression member connecting the load point and support reaction. As the load is increased, the horizontal component of the internal force in this member also increases. This horizontal force must be equilibrated by the longitudinal reinforcement to maintain equilibrium at the support. This beam had a three foot overhang which provided sufficient anchorage to the strand.

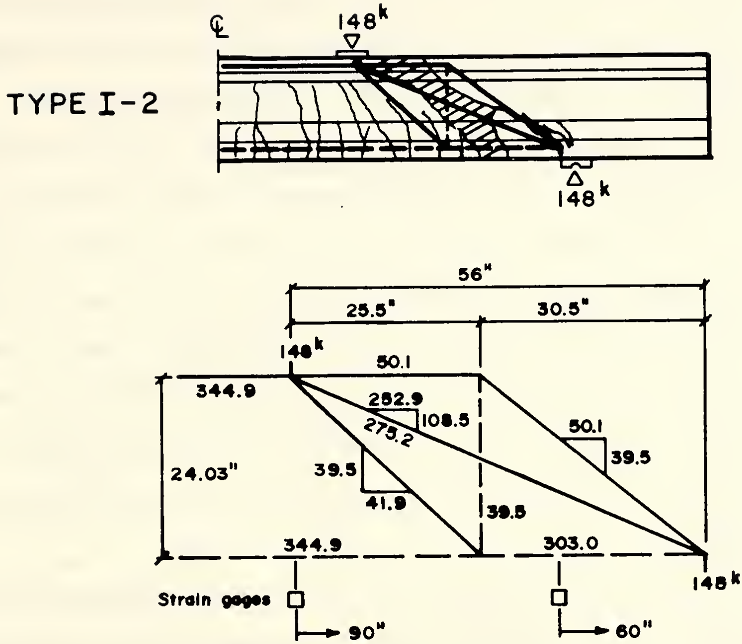

f'_{ci} = 5450 psi
f_{si} = 196.4 ksi
f_{se} = 180.5 ksi

location (in)	P_{ps} (kips)	f_{ps} (ksi)	L_t AASHTO (in)	L_t Zia (in)	L_d AASHTO (in)	L_d Zia (in)
60	315.2	243.2	30.0	22.4	61.5	61.7
96	331.2	255.6	30.0	22.4	67.7	69.4

Figure 3.27 - Type I-2 South Shear Span with Truss Model

Failure of the specimen occurred as the stress in the web exceeded the compressive strength of the concrete resulting in failure of the diagonal compression strut. Forces calculated from strain gages readings at two locations are shown in Figure 3.27. In addition, using the loads measured from strain gages the required transfer and development lengths using the AASHTO and Zia predictions are computed. For 60 inches from the end of the beam, the AASHTO method predicts a required transfer length and development length of 30.0 inches and 61.5 inches, respectively. However, the Zia equation requires 22.5 inches and 61.7 inches for the transfer and development length, respectively. The two methods predict similar development lengths; however, there is approximately an 8 inch difference in the transfer lengths. The forces calculated in the lower tension reinforcement using the truss model compares relatively well to the forces indicated by the strain gage readings.

Figures 3.28 and 3.29 show the crack patterns on the south shear span at failure along with the truss model for the beams, Type I-1 and Type II-2, which failed in flexure, respectively. The failure crack pattern was used to determine the truss model for these beams. The formation of the diagonal strut between the support and load point is most evident in Type II-2 shown in Figure 3.29. Again, a large tensile force is produced in the strand near the support due to equilibrium of the compression diagonal struts. Each beam had a two foot overhang which provided sufficient anchorage to the strand. The required development lengths from the AASHTO and Zia predictions are shown for each beam. Strain gages located 30 inches from the end of the two beams indicate an increase of stress in the strand as compared to the effective prestress force. For the two beams, the AASHTO prediction of the development length is greater than the length available; however, the Zia prediction is less than the available length. Since no slip occurred in the two beams, the

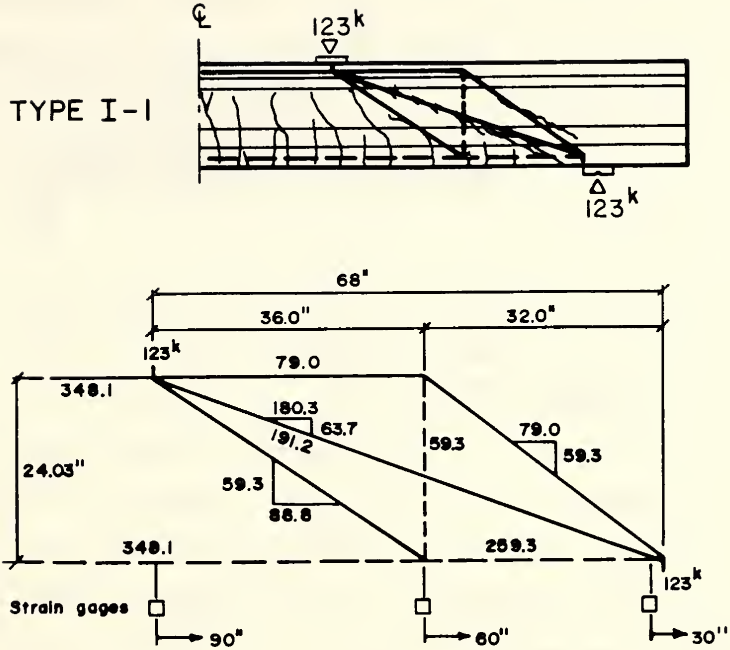

$f'_{ci} = 5450$ psi
$f_{si} = 196.4$ ksi
$f_{se} = 180.4$ ksi

location (in)	P_{ps} (kips)	f_{ps} (ksi)	L_t AASHTO (in)	L_t Zia (in)	L_d AASHTO (in)	L_d Zia (in)
30	242.4	187.0	30.0	22.4	33.4	26.6
60	296.6	228.9	30.0	22.4	54.3	52.7
96	334.2	257.9	30.0	22.4	68.8	70.9

Figure 3.28 - Type I-1 South Shear Span with Truss Model

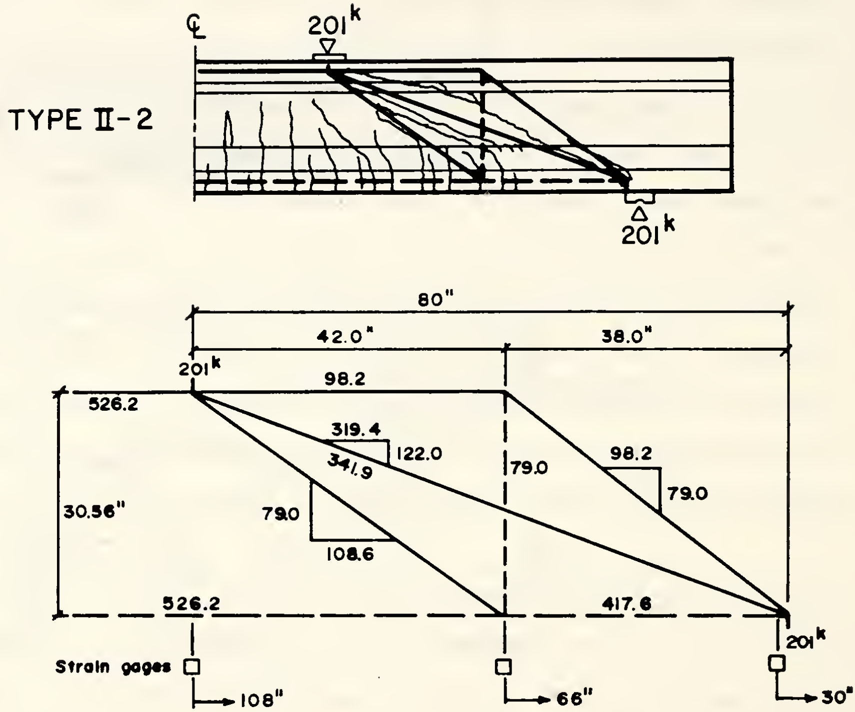

f'_{ci} = 5980 psi
f_{si} = 193.6 ksi
f_{se} = 179.6 ksi

location (in)	P_{ps} (kips)	f_{ps} (ksi)	L_t AASHTO (in)	L_t Zia (in)	L_d AASHTO (in)	L_d Zia (in)
30	361.7	184.6	29.9	24.3	32.4	27.4
66	483.9	246.9	29.9	24.3	63.6	66.3
108	506.9	258.7	29.9	24.3	69.5	73.7

Figure 3.29 - Type II-2 South Shear Span with Truss Model

Zia prediction appears to be a better prediction of the development length.

The predicted capacities using the IDOH specifications and the 1979 AASHTO Interim Specifications given in Table 3.17 are significantly less than the failure load and the prediction of the 1983 AASHTO Specifications which is equal to the web shear cracking capacity plus the web reinforcement contribution. The beams tested in this study simulated the behavior of a bridge beam near a non-continuous support. The 1979 AASHTO Interim Specifications which do not recognize the formation of web shear cracks, would under-estimate the shear capacity. The IDOH provision evaluates the shear capacity of a beam independent of the location; however, the 1983 Specifications indicate an increase in the concrete contribution as the analysis approaches the support. This phenomenon is not reflected in the IDOH or 1979 Interim Specifications, hence these provisions also under-estimate the failure load. The 1983 AASHTO Specifications attempt to predict the formation of the two types of shear crack, web and inclined flexure. For these beams tested using short shear spans with respect to the structural depth, the V_{cw} prediction controls. This prediction which is easy to apply and is an empirical approximation to the elastic solution is shown to provide the best estimate of the strength.

3.5.2.2 Shear Tension

The centerline of the support for the beams which failed in shear tension was 6 inches from the end of the beam. The web shear crack crossed the lower reinforcement and hence, the transfer length of the prestressing strand. The transfer length is the distance required to develop the prestress force at transfer. Any increase in strand stress must be transferred by the concrete in an additional length called the flexural bond length. The development length of the strand is the combination of the transfer and flexure bond lengths.

Table 3.17 - Shear Specifications versus Test Results, Type I-1, I-2 & II-2

Beam	$r\,f_y$ (psi)	b_w (in)	d (in)	h (in)	j
I-1	137	6	26.00	28.25	0.9
I-2	110	6	26.00	28.25	0.9
II-2	157	6	33.33	36.00	0.9

IDOH - $= \frac{4}{3} A_v f_y \frac{h}{s} = \frac{4}{3} r\, f_y\, b_w\, h$

AASHTO 1979 - $= 2 \frac{A_v f_y jd}{s} + 180\, b_w jd = 2\, r\, f_y\, b_w\, jd + 180\, b_w\, jd$

AASHTO 1983 - $= r\, f_y\, b_w\, d + V_{cw}$

Beam	IDOH (kips)	AASHTO 1979 (kips)	AASHTO 1983 (kips)	Test Results Load (kips)	Test Results Mode
I-1	31.0	63.7	121.3	123	Flexure
I-2	24.9	56.2	116.9	148	Web crushing
II-2	45.2	88.9	165.9	201	Flexure

The formation of the web shear crack and propagation into the transfer length destroyed the bond required to develop the prestress force leading to slip of the strand. The width of the support plate was 8 inches. The crack crossed the strand just before the face of the plate. Thus, the available transfer length was 10 inches for beams Type I-3, I-4 and II-1.

A second test was performed on these three beams to determine the length of overhang that would provide sufficient anchorage to the prestressing strand. An 18 inch overhang was used on Type I-3A. The formation of the first web shear crack produced slip in approximately 50% of the strands; however, the load which produced the web shear crack was maintained. An increase of the load eventually produced loss of bond in all of the strands leading to a shear tension failure. A 24 inch overhang was used in the second test of Type I-4A and II-1A. This length of overhang provided sufficient anchorage to the strands in these two beams.

Table 3.18 compares the actual transfer length available measured from the end of the beam to the face of the support and the required transfer length calculated by AASHTO specifications and the proposed equation of Zia and Mostafa for these six tests evaluating the shear tension mode of failure. Based on the results of these tests, the presence of the transfer length extending into the shear span could be defined as the criteria leading to a failure resulting from the formation of a web shear crack across the prestressing strand producing loss of bond. As can be seen in Table 3.18 based on the previous criteria, the AASHTO recommendations would indicate a shear tension failure for all six tests. For these tests however; the proposed equation by Zia and Mostafa would seem to give a better estimate of a shear tension failure. As in the case of beam Type I-3A where the predicted transfer length, 20.2 inches, was less than the available transfer length of 22 inches, the presence of a web shear crack did not result in immediate failure. The formation of the

Table 3.18 - Transfer Length for Beams Evaluating Shear Tension Failure

Beam	f'_{ci} (ksi)	f_{si} (ksi)	f_{se} (ksi)	L_t AASHTO (in)	Zia (in)	Transfer Length Available (in)
☞ Type I-3	5.84	193.3	184.6	30.8	20.2	10
☞ Type I-4	5.84	193.3	187.8	31.3	20.2	10
☞ Type II-1	5.98	193.5	183.5	30.6	19.7	10
☞ Type I-3A	5.84	193.3	184.6	30.8	20.2	22
Type I-4A	5.84	193.3	187.8	31.3	20.2	28
Type II-1A	5.98	193.5	183.5	30.6	19.7	28

☞ Shear Tension Failure

$$\text{AASHTO - } L_t = \frac{f_{se}}{3} d_b$$

$$\text{Zia - } L_t = 1.5 \frac{f_{si}}{f'_{ci}} d_b - 4.6$$

$$d_b = 0.5 \text{ inches}$$

web shear crack did not produce slip in all of the strands and the beam was capable of maintaining the load which produced the crack. An additional load was required to produce the full loss of bond. Hence, the test data from this study indicate that the proposed Zia and Mostafa equation seems to better predict the transfer length required to prevent shear tension failures in case that a web shear crack reached the strand. The current AASHTO recommendations are shown to be more conservative in this respect.

Table 3.19 contains the current shear predictions and the failure load for the six tests performed on Type I-3, I-4 and II-1. The 1983 AASHTO Specifications over-estimate the failure load for all of the beams failing by the mode of shear tension. In this mode of failure it is the anchorage of the strand which is the problem and not the amount of web reinforcement. Also, the different type of detailing schemes used in the lower flange near the support provided no apparent benefits to the behavior in the shear tension failures.

3.6 Summary

This chapter presented a experimental study consisting of nine tests on six AASHTO I-beams. Four Type II and two Type I AASHTO I-girders were tested using a symmetric loading system. The beams were designed to fail in shear as predicted using AASHTO Specifications. The beams were tested non-composite since the majority of the shear for a composite section is carried by the I-beam.

Elastic deformations calculated using the modulus of elasticity as predicted by the current AASHTO equation and the the gross moment of inertia gave good agreement with the actual load-deflection response.

The flexural strength of two beams, Type I-1 and II-2, was exceeded and the AASHTO predictions estimated the capacity and ultimate stress in the

Table 3.19 - Shear Specifications versus Test Results, Type I-3, I-4 & II-1

Beam	$r\,f_y$ (psi)	b_w (in)	d (in)	h (in)	j
I-3	133	6	25.50	28.0	0.9
I-4	110	6	25.50	28.0	0.9
II-1	157	6	33.33	36.0	0.9
I-3A	80	6	25.50	28.0	0.9
I-4A	165	6	25.50	28.0	0.9
II-1A	137	6	33.33	28.0	0.9

$$\text{IDOH} - \; = \frac{4}{3} A_v f_y \frac{h}{s} = \frac{4}{3} r\, f_y\, b_w\, h$$

$$\text{AASHTO 1979} - \; = 2\,\frac{A_v f_y jd}{s} + 180\, b_w jd = 2\, r\, f_y\, b_w\, jd + 180\, b_w\, jd$$

$$\text{AASHTO 1983} - \; = r\, f_y\, b_w\, d + V_{cw}$$

Beam	IDOH (kips)	AASHTO 1979 (kips)	AASHTO 1983 (kips)	Centerline of support (in)	Test Results Load (kips)	Test Results Mode
I-3	29.8	61.4	120.3	6	101	Shear Tension
I-4	24.6	55.1	117.5	6	110	Shear Tension
II-1	45.2	88.9	167.2	6	140	Shear Tension
I-3A	17.9	46.8	113.5	18	113	Shear Tension
I-4A	37.0	70.2	127.1	24	161	Shear Compression
II-1A	39.5	81.7	162.7	24	222	Shear Compression

strand for these beams very well.

The experimental program also showed that the formation of a web shear crack and its propagation across the transfer length of the lower prestressing strand can produce a premature failure due to loss of bond. This loss of bond results in the beam not being able to maintain equilibrium at the support. The formation of a web shear crack is an elastic problem occurring when the tensile strength of the concrete is exceeded. The AASHTO prediction of the formation of this crack was excellent. Although the specimens tested in this study had minimum amounts of shear reinforcement at the end regions, it is felt that the use of higher strength concrete in pretensioned beams requires an evaluation of the efficiency of the shear reinforcement in preventing this mode of failure.

The geometry, concrete strength, prestressing force, and amount of web reinforcement did not allow this study to evaluate the formation of a flexure shear crack as the failure mechanism as predicted by 1983 AASHTO Equation for V_{ci}. However, the modifications made to this equation from that first proposed by the Illinois work has made this provision quite conservative. This phenomena was also found in the University of Cornell study. This was illustrated in the beams tested where the flexure shear capacity controlled the predicted concrete contribution; however, the actual capacity of the beams was significantly greater as shown by beams Type I-1, I-2 and II-2.

Two methods to predict the transfer length of the prestressing were compared. Results indicate that the use of the proposed equation by Zia and Mostafa better predicts the transfer length of the prestressing strand for these beams.

The truss model approach provided a behavioral model on the ultimate strength of the beams under flexure and shear. The truss model gives the engineer an overall behavioral tool rather than the current section analysis

conducted for flexure and shear. The effects of web reinforcement, concrete contribution and the importance of strand anchorage and development are better illustrated by this approach.

CHAPTER 4

BRIDGE ANALYSIS EXAMPLE

4.1 General

In addition to higher strength concrete, modified I-sections have been used to obtain longer bridge spans. One characteristic of these modified I-sections is the use of a reduced web width. The reduction in dead load produced by the thinner web increases the available moment capacity resisting live loads. However, the shear design generally requires increased amounts of web reinforcement due to the reduction of the concrete contribution resulting from the thinner web. The use of Grade 60 web reinforcement compared to Grade 40 has allowed the designer to obtain the required shear capacity and at the same time maintain spacing requirements. Longer bridge spans produce high shear demands near support regions; however, the end blocks, which were once used to control stresses produced at the ends of the beams due to prestressing, have long since not been utilized in the State of Indiana. In general, the use of thinner webs, longer bridge spans, and the discontinued use of end blocks have made end regions of bridge spans critical in the shear design. A detailing problem was shown in Chapter 3 involving a premature failure of a prestressed I-girder due to the formation and propagation of a web shear crack crossing the flexural reinforcement near the non-continuous end region of a prestressed I-girder.

The end region of a bridge structure is analyzed in this chapter to further evaluate current shear design specifications. Also, the analysis of the lateral

stability of the I-section in the structure is conducted.

4.2 Bridge Information

The Granville Bridge was the structure chosen for analysis. The bridge is an eight span continuous structure spanning the Wabash River south of Lafayette, Indiana. The superstructure consists of modified Illinois Type IV prestressed I-sections and a cast-in-place slab. Precast deck panels were used in the fabrication of the deck. The cross section of the super-structure is shown Figure 4.1, consisted of five I-beams spaced laterally on 75 inch centers support the 8 inch thick, 31 foot wide, cast-in-place slab. Reinforced concrete parapets are to be placed on each side of the deck.

The modified Illinois Type IV is an Illinois Type IV with a larger top flange as shown in Figure 4.2. The Illinois Type IV on the other hand is a modified AASHTO Type IV. The web width of the Illinois Type IV is 6 inches as compared to the 8 inch web AASHTO Type IV. The weights of the Illinois Type IV and the AASHTO Type IV are 624 plf and 822 plf, respectively. This represents a 24% reduction in dead load. The top flange of the modified Illinois Type IV was increased to produce a stiffer section in the weak direction. This would aid in the handling of the I-section and especially the lateral stability. Also, the additional stiffness would aid in the control of deflections and the increased height would produce a larger internal moment arm which would be helpful in resisting flexure and shear.

4.2.1 Lateral Stability Analysis

A super-structure consisting of a cast-in-place slab and prestressed Illinois Type IV I-beams was recently constructed in the State of Indiana. The beams in the center span were 119'-6" long. Handling pick up points were placed 2 feet from each end of the beam producing a unsupported length of

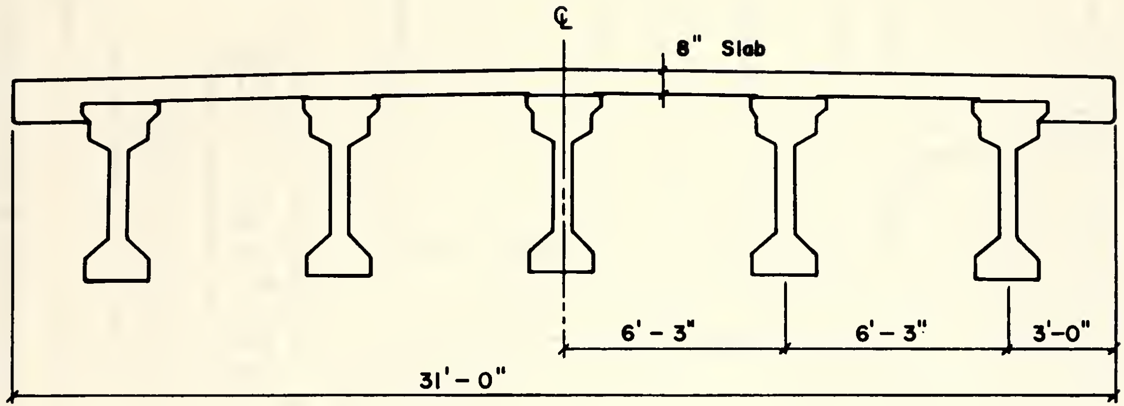

Figure 4.1 - Cross Section of Granville Bridge Superstructure

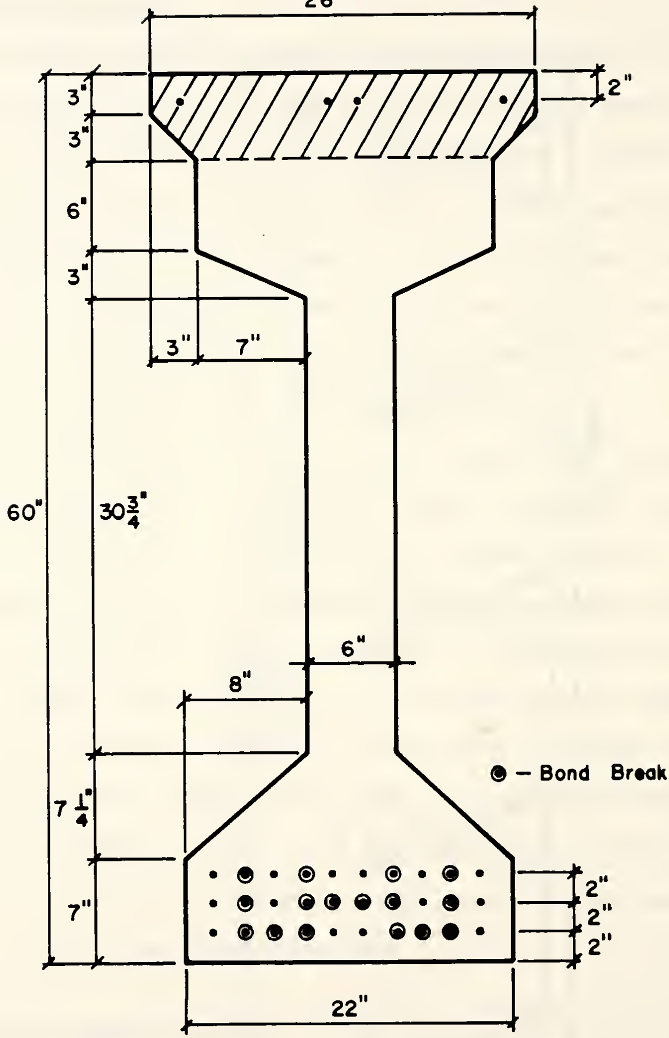

Figure 4.2 - Cross Section of Modified Illinois Type IV

115'-6". After transfer of the prestress to the I section, the fabricator attempted to move the beam from the casting bed to the storage yard. The section cleared the side forms when, the top of the beam deflected laterally. Unaware of a lateral stability problem, the fabricator provided no temporary support to the top flange and the section collapsed. The strongback shown in Figure 4.3 was fabricated for use in subsequent handling of the beams. This system proved to give the necessary lateral support to the I-section during handling and transportation. On the other hand, the interior beams of the Granville bridge are 117'-6" in length. A comparison of the lateral stability for the Illinois Type IV and modified Illinois Type IV sections is given in Table 4.1. Using the PCI Design Handbook method to evaluate the lateral stability of the Illinois Type IV, a factor of safety of 0.64 was calculated. Hence, predicting the collapse of the Illinois Type IV. The pick up points for the modified Illinois Type IV in the Granville Bridge were placed 9.5 feet from the end of each beam. Prestressing strand was placed at the top flange to control the tensile stresses produced by the overhang. The top prestressing strand, reduced unsupported length, and the additional top flange resulted in a factor of safety against lateral buckling of 1.52. The shipment of the beams was performed without the use of a strongback and no problems were encountered related to the lateral stability.

4.2.2 Shear Analysis

In this section the shear analysis of the beams in the exterior span for the Granville Bridge will be presented. Each of the three design provisions reviewed in this report is evaluated near the support region. The overall height of the section is 68 inches with 1.5 inches considered as non-structural producing a structural height of 66.5 inches. The section properties for the modified Illinois Type IV and the transformed composite section are given in

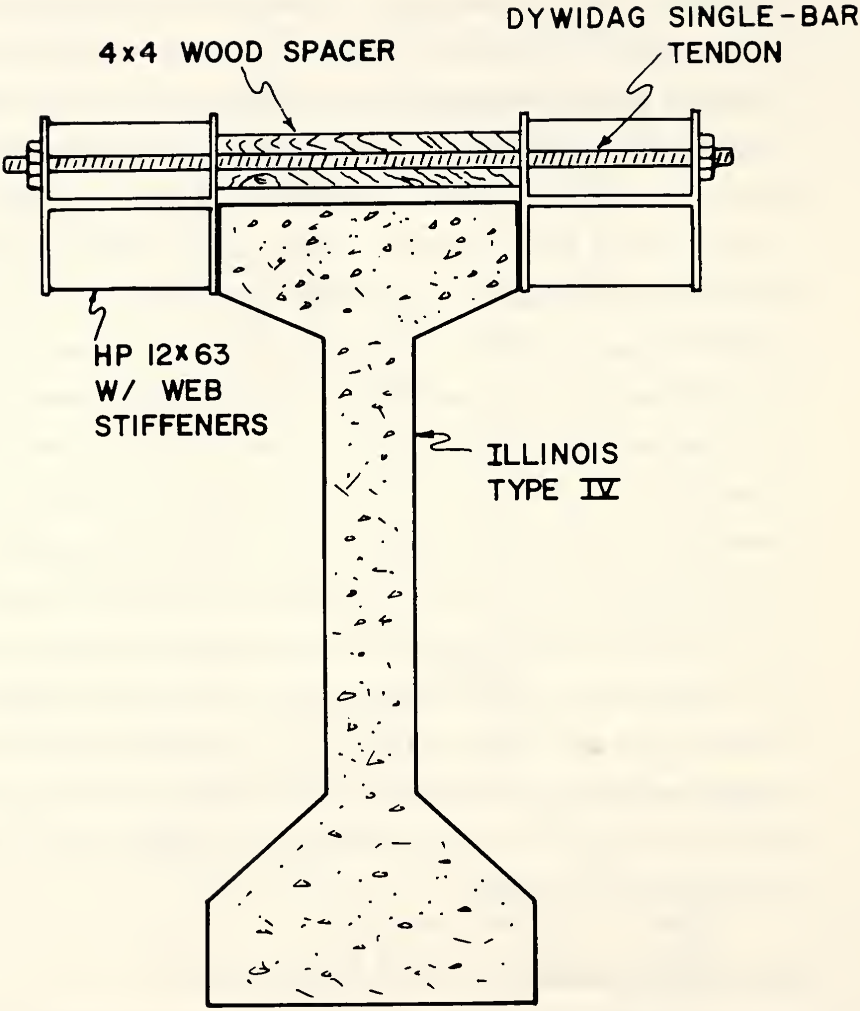

Figure 4.3 - Illinois Type IV with Strongback

Table 4.1 - Lateral Stability Evaluation

Beam	I_y (in^4)	y_t (in)	w_o (plf)	f'_{ci} (psi)	E_{ci} (ksi)
Illinois Type IV	13670	29.03	624	5000	4030
Modified Illinois Type IV	21160	28.69	777	5000	4030

$$\text{Factor of Safety} = \frac{y_t}{\beta_y}$$

$$\beta_y = \frac{5}{384}\,\frac{w_o\, l^4}{E_{ci}\, I_y}$$

$$E_{ci} = 57\,\sqrt{f'_{ci}}\ \text{(ksi)}$$

Beam	l (ft)	β_y (in)	F.S.	Comments
Illinois	119.5			total beam length
Type IV	115.5	45.4	0.64	pick up points at 2 feet from end of beam
Modified	117.5			total beam length
Illinois	113.5	34.0	0.84	pick up points at 2 feet from end of beam
Type IV	98.5	18.9	1.52	pick up points at 9.5 feet from end of beam

Table 4.2. Figure 4.4 shows the composite section. The design 28 day compressive concrete strength for the I-section, deck panel and cast-in-place slab is 6000 psi, 5000 psi and 3000 psi, respectively.

The factored and service load shear envelopes along with the 1983 AASHTO prediction of a web shear crack, V_{cw} for the first 30 feet of exterior span are shown in Figure 4.5. The shear envelopes were developed using truck and lane loads as specified by AASHTO. In addition, the elastic solution predicting a web shear crack with the concrete tensile strength equal to $4\sqrt{f'_c}$ is shown.

The critical section was taken at $\frac{h}{2}$ from the face of the support. The face of the support is located 15 inches from the end of the beam. The prestressing strand is 1/2 inch, Grade 270, Lo-Lax Special. Assuming 10% initial losses, 20% total losses, 5000 psi concrete strength at transfer, and 75% f_{pu} jacking stress, the transfer length of the strand is 27.0 inches as given by AASHTO provisions, $L_t = \frac{f_{se}}{3} d_b$, and 22.7 inches as given by the Zia and Mostafa proposed equation, $L_t = 1.5 \frac{f_{si}}{f_{ci}} d_b - 4.6$. Both transfer lengths of 27.0 and 22.7 inches are within the shear span. Figure 4.5 shows that at the critical section, the shear produced by service loads is 135 kips and the web shear capacity predicted by AASHTO is 163.2 kips producing a factor of safety of 1.20. Using the elastic solution, the web shear capacity is 193.6 kips resulting in a factor of safety of 1.43. Unlike ACI Specifications, AASHTO specifications do not allow the designer to use the elastic approach as an alternative.

At $\frac{h}{2}$ from the support face the factored shear is 239.2 kips and the web-shear cracking capacity predicted by AASHTO is 163.2 kips. At ultimate

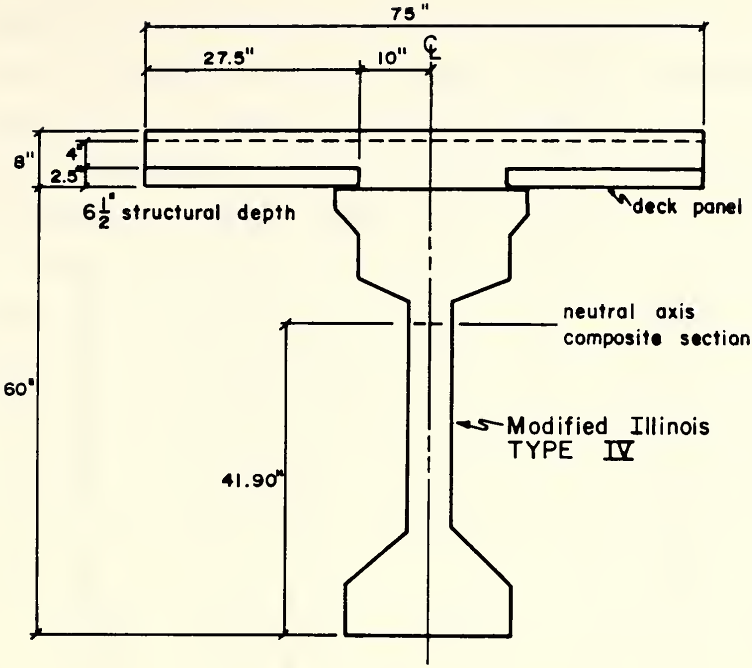

Figure 4.4 - Cross Section of Modified Illinois Type IV with Deck

Table 4.2 - Section Properties

Modified Illinois Type IV		Transformed Composite Section	
h_b (in)	60.00	h_c (in)	66.50
b_w (in)	6	b_w (in)	6
A_b (in^2)	746	A_c (in^2)	1119
I_b (in^4)	336166	I_c (in^4)	588780
c_{1b} (in)	28.69	c_{1c} (in)	24.60
c_{2b} (in)	31.31	c_{2c} (in)	41.90
S_{1b} (in^3)	11717	S_{1c} (in^3)	23934
S_{2b} (in^3)	10737	S_{2c} (in^3)	14052
Q_b (in^3)	3548	Q_c (in^3)	19362
w_b (plf)	777		

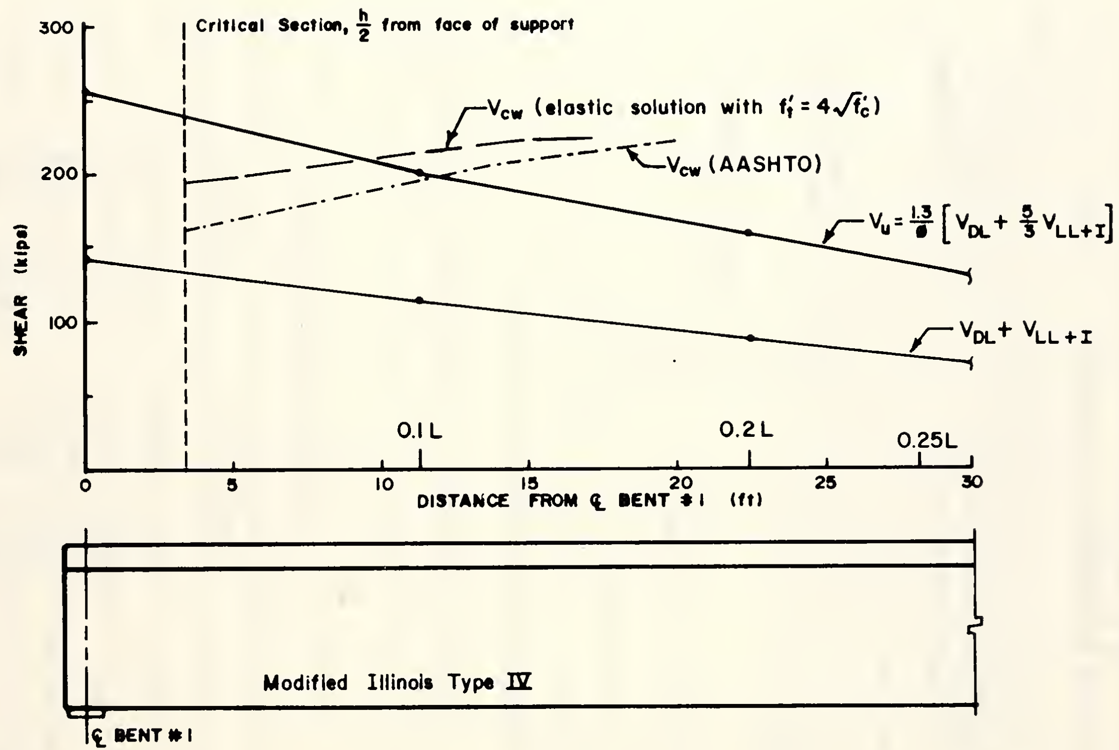

Figure 4.5 - Shear Analysis and Web Shear Crack Prediction

load level, the formation of a web shear crack will most likely occur and, with the transfer length within the shear span, the further propagation of this crack could lead to anchorage failure of the strand. Further work is needed to evaluate the efficiency of the shear reinforcement in preventing this mode of failure, in particular if higher strength concretes are being used.

Using the factored load envelope, the three design equations are evaluated for this span with the following conditions: j=0.95, d=62.5 inches, and for the web reinforcement, $A_v = 0.4\ in^2$ and $f_y = 60000$ psi. The factored shear at the critical section and the quarter point is 239.2 kips and 137.2 kips, respectively. The quarter point shear value is used in the AASHTO 1979 Interim Specifications. The required spacing shall be calculated for each design method.

IDOH

$$s_{req} = \frac{4}{3}\,\frac{A_v\ f_y\ h}{V_u} = 8.9 \text{ inches}$$

AASHTO 1979 Interim with V_u at quarter point (0.25L)

$$s_{req} = 2\,\frac{A_v\ f_y\ jd}{V_u - 180\ b_w\ jd} = 43.1 \text{ inches}$$

$$\text{1983 AASHTO with } V_{cw} \text{ at } \frac{h}{2} = 163.2 \text{ kips}$$

$$s_{req} = \frac{A_v\ f_y\ d}{V_u - V_{cw}} = 19.7 \text{ inches}$$

The required web reinforcement spacing of 43.1 inches using the AASHTO 1979 Interim Specifications and the factored shear load at the quarter point appears excessive as compared to the other two methods. For this structure and using the AASHTO 1979 Interim Specifications, the spacing of the web

reinforcement would be controlled by the tie spacing as specified by the horizontal shear strength requirements.

The IDOH specifications requires a spacing of 8.9 inches. Though the method is simple to use, it appears to be conservative near the end region as compared to the 1983 AASHTO Specifications.

4.3 Summary

The use of higher strength concrete in prestressed I beams can result in longer span lengths. The transportation and handling of these beams may become critical and a lateral stability analysis need to be conducted. The use of the PCI method to calculate the factor of safety of lateral buckling appears to be satisfactory as indicated by the two beams described. It predicted the failure of the Illinois Type IV where the use of temporary strongbacks were required to successfully handle and transport the beams. The PCI method also indicates that the modifications made to the Illinois Type IV used in the Granville bridge provided adequate lateral stiffness. These I-sections were successfully handled and transported to the bridge site.

The current IDOH specifications are easy to use and give conservative results as compared to the 1979 and 1983 AASHTO Specifications. The 1979 AASHTO Specifications, which do not recognize the formation of web shear cracks, lead to excessive spacing of reinforcement with the horizontal shear requirements generally controlling the spacing at the end regions of exterior spans. Application of the 1983 AASHTO specifications can be very difficult and cumbersome to apply especially the V_{ci} calculation. At simple supports of typical bridge structures the support centerline is usually between six and twelve inches from the end of the beam, and as a result, the transfer length of the strand extends into the shear span. Three tests conducted during this study, using this standard detailing, resulted in a premature strand

anchorage failure as a web-shear crack penetrated into the transfer length of the strand. Although the specimens tested in this study had minimum amounts of shear reinforcement at the end regions, it is felt that the use of higher strength concrete in pretensioned beams requires an evaluation of the efficiency of the shear reinforcement in preventing this mode of failure.

In general, the engineer needs to be aware of this problem. To develop the full shear capacity of the beam resisting factored loads for members with relatively thin webs, it is essential that the transfer length of the prestressing strand be protected from any additional increase in stress due to a web shear crack.

CHAPTER 5

SUMMARY, CONCLUSIONS, AND RECOMMENDATIONS

5.1 Summary

This report presented a detailed evaluation of the ultimate behavior of AASHTO I-beams with concrete strengths up to 9000 psi. The findings of this research study were used to evaluate relevant AASHTO and IDOH design specifications.

The use of high strength concrete in the fabrication of prestressed I-girders has little effect on the ultimate flexural capacity of the composite section as long as the transfer requirements remain unchanged. High strength concrete does produce benefits when evaluating stresses and deflections due to service loads.

The ultimate shear carrying capacity of the composite structure is mainly carried by the precast I-beam and it is directly affected by the increase in the concrete compressive strength. Three different methods are available to evaluate the shear strength. AASHTO Specifications present two possible alternatives. In addition, IDOH allows a third alternative for the design of the web reinforcement. The provision presented in the 1983 AASHTO specifications is the more detailed analysis procedure; however, the use of this approach in analysis and design is cumbersome and unclear for continuous structures. The approach in the AASHTO 1979 Interim Specifications is easier to apply, but it has shortcomings in the evaluation of composite sections. The IDOH Specifications, the simplest of the three methods, is a

modification of some of the earliest recommendations for prestressed concrete members.

The experimental program in this study included nine tests on six AASHTO prestressed I-beams without a cast-in-place slab, ie. non-composite. The beams were tested non-composite since the shear capacity of a composite section is mainly a function of the precast I-beam. To produce a shear failure in the beams tested, a relatively short shear span to structural depth ratio was used, and the behavior was controlled by the web shear cracking phenomena.

5.2 Conclusions

The findings of the experimental program indicated that in regard to the three procedures reviewed, the IDOH Specifications are the most conservative. The AASHTO 1979 Interim Specifications which do not recognize the formation of web shear cracks were found to under-estimate the shear capacity in regions were web shear cracks occur. The 1983 AASHTO Specifications, which predicts the formation of a web shear crack, is an empirical approximation to an elastic solution and is quite accurate in predicting the formation of web shear cracks. The 1983 AASHTO recommendations were found to give the best estimate of the overall shear strength.

A study conducted at the University of Cornell evaluated the 1983 AASHTO Shear Specifications for concrete compressive strengths up to 12000 psi. Test results indicated that these recommendations used to predict the concrete contribution representing web shear and inclined flexure cracks were conservative for this higher strength concrete. In the evaluation conducted in Chapter 2 of this report the IDOH and AASHTO 1979 Interim recommendations were also found to be conservative for these specimens.

In the experimental part of this research study, the first two beams tested had two and three foot overhangs, respectively which were used to keep the transfer length of the prestressing strand out of the shear span. This length provided sufficient anchorage to the prestressing strand which upon the formation of a web shear crack showed an increase in the stress near the support plate. However, in a typical bridge the centerline of the exterior support is between 6 and 12 inches from the end of the beam. Hence, the transfer length of the prestressing strand usually extends past the face of the support into the shear span. The stress increase in the strand upon the formation of a web shear crack in three of the beams tested with the centerline of the support plate 6 inches from the end of the beam resulted in strand slip leading to a premature failure. Although the beams tested in this study had minimum amounts of shear reinforcement at the end regions, it is felt that with the use of higher strength concretes the efficiency of the shear reinforcement to prevent this mode of failure needs to be reevaluated.

5.3 Recommendations

The following recommendations are based on the findings of this research study:

1. The use of 28 day concrete compressive strengths up to 6500 psi in the design of pretensioned I-beams for the State of Indiana can be allowed.

2. Evaluation of deflections produced by loads, which do not exceed the cracking capacity of the member, can be adequately predicted using the gross section properties and the modulus of elasticity given by current procedures.

3. The current methods used to evaluate the flexure capacity of precast composite I-sections for bridges in positive moment regions are adequate

for under-reinforced sections.

4. The use of current IDOH Shear Design Specifications for continuous bridges using pretensioned I-beams and a cast-in-place slab is adequate.

5. The transfer length of the prestressing strand must be protected from any additional increase in stress due to web shear cracks. The formation of web shear cracks is a potential problem in bridges using modified I-sections with thinner webs. In the inspection of these type of bridges, special attention should be given to the visual inspection near the end regions of exterior spans.

5.4 Future Work

Further research is needed to evaluate the efficiency of the stirrup reinforcement in preventing failures due to improper anchorage of the strand at simple supports. The behavior of composite sections in negative moment regions of high shear and flexural stresses needs further study. Further work is also needed on the effects of strand debonding on the strength of pretensioned beams. The presence of debonded strand can possibly have detrimental effects on the shear strength of pretensioned members. A design criteria is needed for the adequate debonding of strands.

REFERENCES

REFERENCES

1. Kaufman, M.K. and Ramirez, J.A., "Production and Engineering Properties of Concrete used in Precast Prestressed I-Beams for the State of Indiana," Volume I, FHWA/IN/JHRP-88/5, pp. 65.
2. ACI Committee 363, "State-of-the-art Report on High-Strength Concrete," (ACI 363R-84), ACI Journal, Proceedings Vol. 81, No. 4, July-August, 1984, pp. 364-411.
3. IDOH, "Standard Specifications for Highway Bridges,"
4. AASHTO,"Standard Specifications for Highway Bridges," Thirteenth Edition, 1983, 394 pp.
5. Jobse, H.J., "Applications of High Strength Concrete For Highways Bridges," PCI Journal, Vol. 29, No. 3, May/June 1984, pp. 44-73.
6. Shah, S.P., Ahmad, S.H., "Structural Properties of High Strength Concrete and its Implications for Precast Prestressed Concrete," PCI Journal, Vol. 30, No. 6, November/December 1985, pp. 92-119.
7. Zia, Paul, "Structural Design with High Strength Concrete," Report No. PZIA-77-01, Civil Engineering Department, North Carolina State University, Raleigh, Mar. 1977, 65 pp.
8. Nilson, Arthur, H., "Design Implications of Current Research on High-Strength Concrete," ACI Special Publication-87, pp. 85-118.
9. Whitney, Charles S., and Cohen, Edward, "Guide for Ultimate Strength Design of Reinforced Concrete," ACI Journal, Proceedings Vol. 53, No. 5, Nov. 1956, pp. 445-475.
10. Lin, T.Y., "Design of Prestressed Concrete Structures," First Edition, Second Printing, John Wiley & Sons, Inc., 1956, pp. 192-207.
11. ACI Committee 318, "Building Code Requirements for Reinforced Concrete (ACI 318-56)," American Concrete Institute, Detroit, MI, 1956, pp. 913-986.
12. AASHTO,"1979 Interim Standard Specifications for Highway Bridges," 1979.
13. ACI-ASCE Joint Committee 323, "Tentative Recommendations for Prestressed Concrete," Journal of the American Concrete Institute, Vol. 54, January, 1958.
14. ACI Committee 318, "Building Code Requirements for Reinforced Concrete (ACI 318-83)," American Concrete Institute, Detroit, MI, 1983, 111 pp.

15. ACI Committee 318, "Commentary on the Building Code Requirements for Reinforced Concrete (ACI 318-83)," American Concrete Institute, Detroit, Michigan, 1983, 155 pp.

16. MacGregor, J.G., Sozen, M.A., and Seiss, C.P., "Investigation of Prestressed Reinforced Concrete For Highway Bridges, Part IV: Strength in Shear of Beams with Web Reinforcement," Report No. 14 of The Investigation of Prestressed Reinforced Concrete for Highway Bridges, Project I HR-10, University of Illinois, August 1965.

17. Elzanaty, Ashraf H., Nilson, Arthur H. and Slate, Floyd, O., "Shear Capacity of Prestressed Concrete Beams Using High-Strength Concrete," ACI Journal, Proceedings Vol. 83, No. 3, May-June 1986, pp. 359-368.

18. Elzanaty, Ashraf H., Nilson, Arthur H. and Slate, Floyd, O., "Shear-Critical High-Strength Concrete Beams," Research Report No. 85-1, Department of Structural Engineering, Cornell University, Ithaca, Feb. 1985, 216 pp.

19. Zia, Paul and Mostafa, T.; "Development Length of Prestressing Strands," PCI Journal, Vol. 22, No. 5, September/October 1977, pp. 54-65.

20. Prestressed Concrete Institute, "PCI Design Handbook, Precast and Prestressed Concrete," Third Edition, Chicago, Illinois, 1985.

21. Pastor, J.A.; Nilson, A.H.; and Slate, F.O., "Behavior of High Strength Concrete Beams," Research Report No. 84-3, Department of Structural Engineering, Cornell University, Ithaca, Feb. 1984, pp. 311.

APPENDICES

APPENDIX A

Stress Strain Curves for Reinforcement

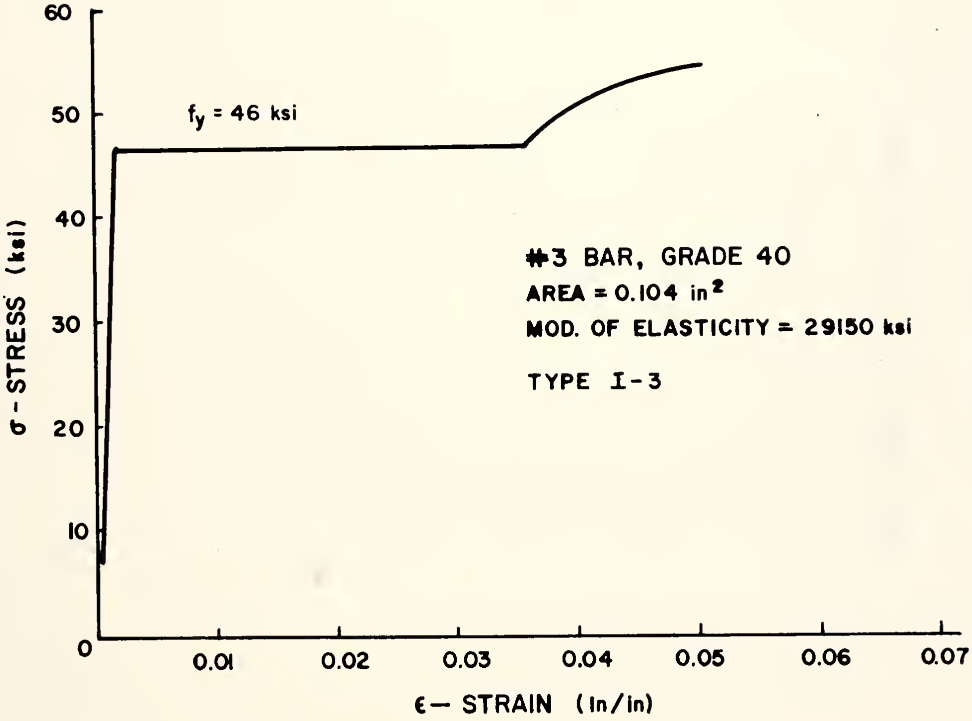

Figure A.1 - Stress vs. Strain, #3 Bar

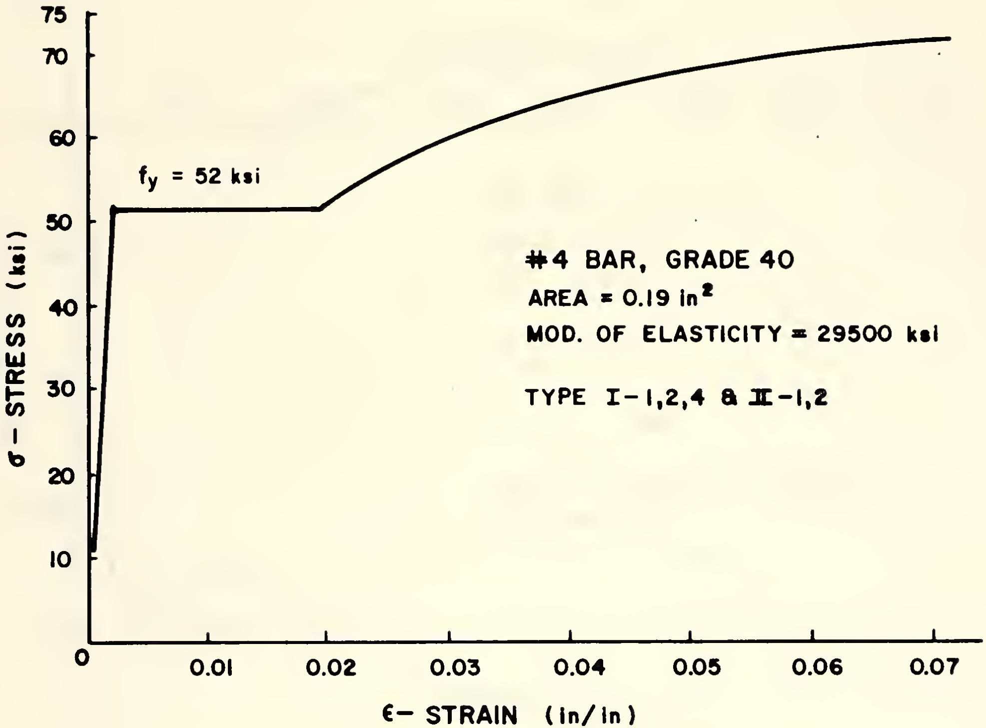

Figure A.2 - Stress vs. Strain, #4 Bar

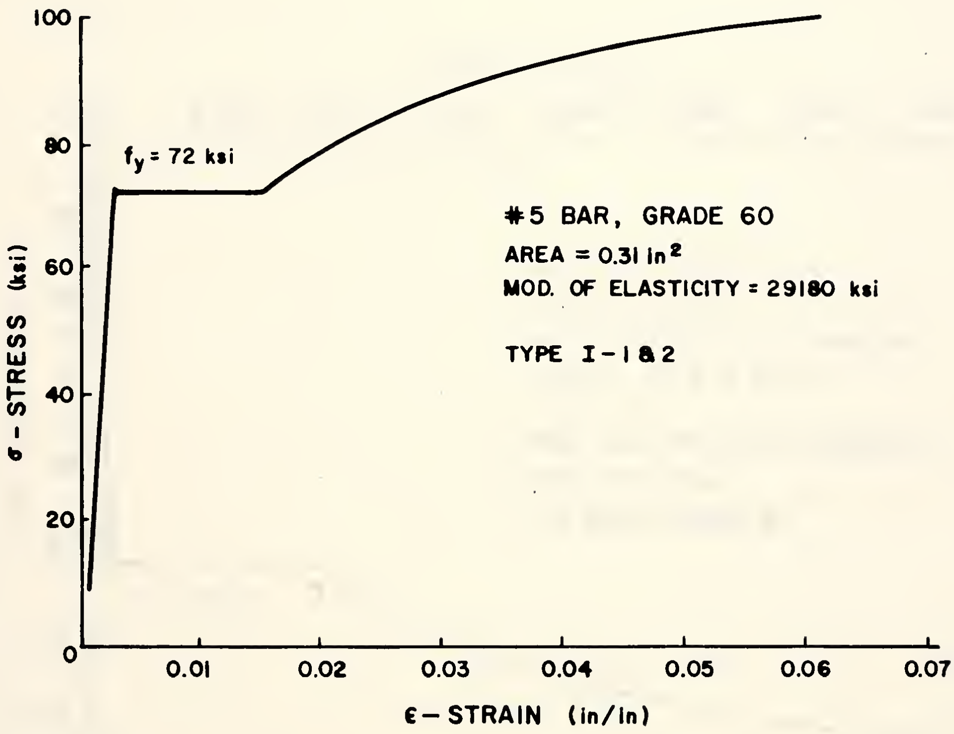

Figure A.3 - Stress vs. Strain, #5 Bar, Type I-1 & 2

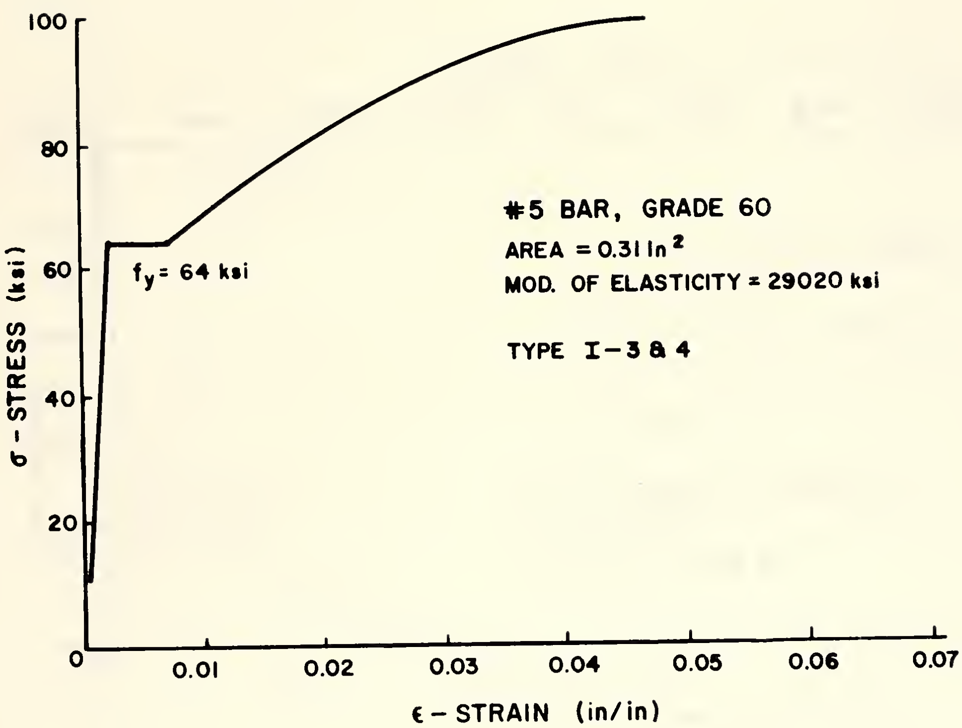

Figure A.4 - Stress vs. Strain, #5 Bar, Type I-3 & 4

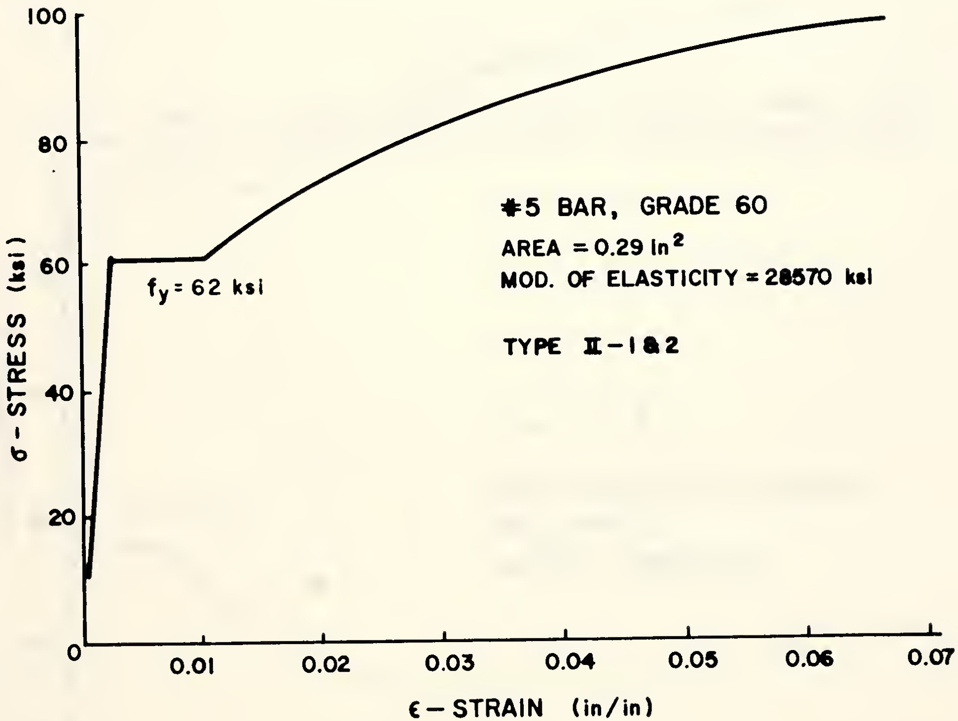

Figure A.5 - Stress vs. Strain, #5 Bar, Type II-1 & 2

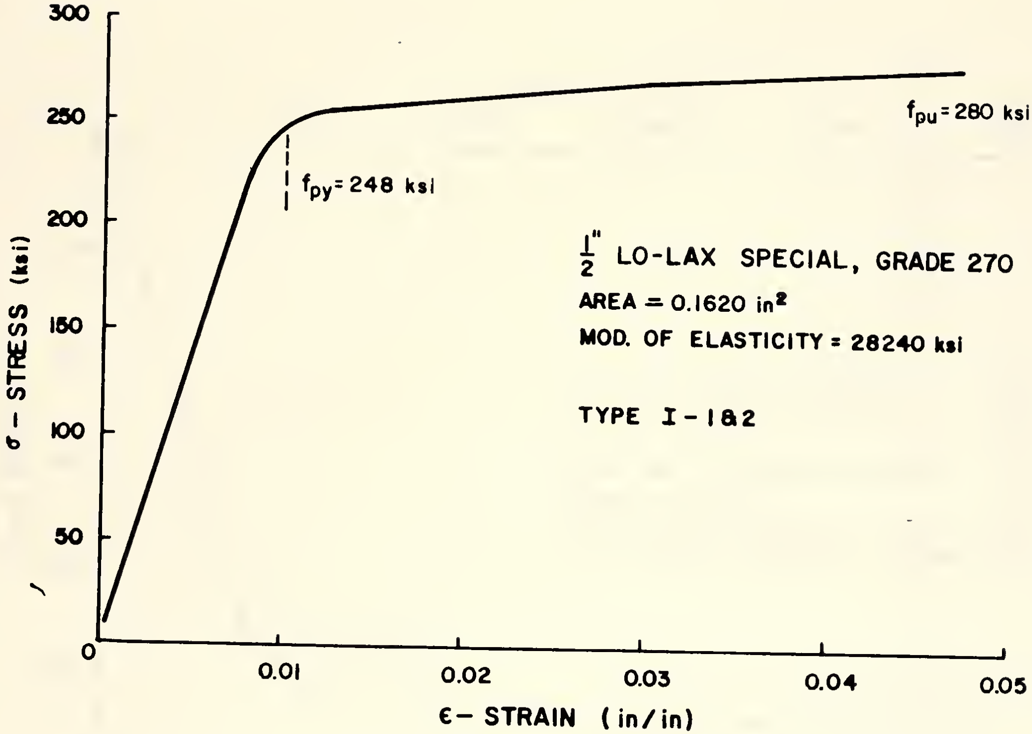

Figure A.6 - Stress vs. Strain, Prestressing Strand, Type I-1 & 2

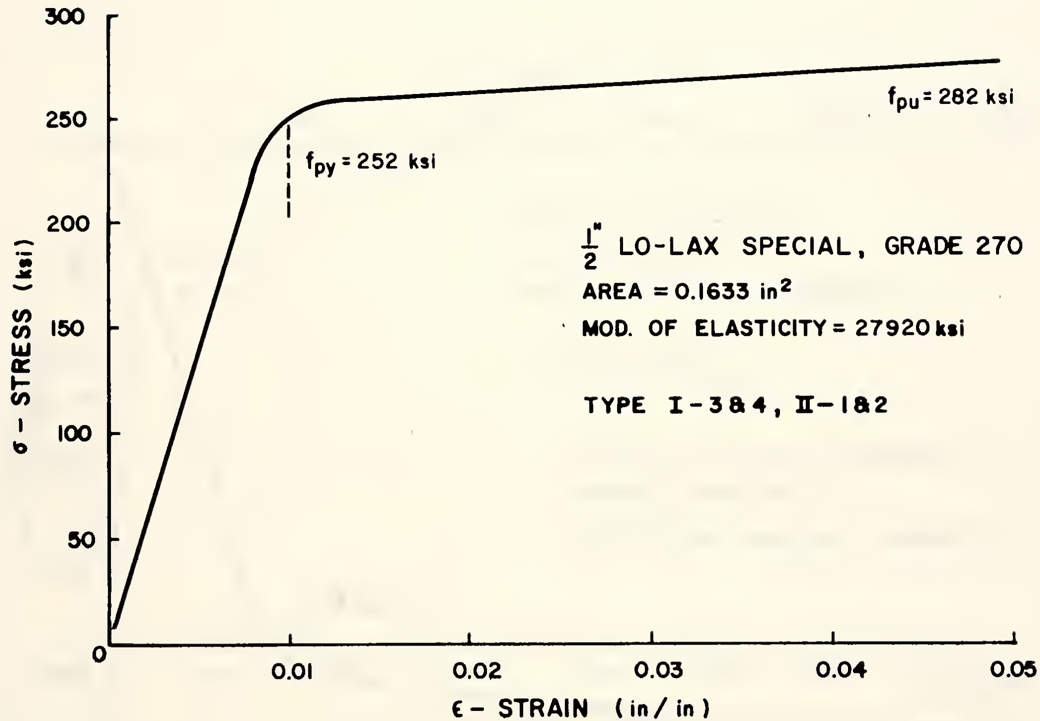

Figure A.7 - Stress vs. Strain, Prestressing Strand, Type I-3 & 4, Type II-1 & 2

APPENDIX B

Elastic Solution Predicting a Web Shear Crack for a Composite Section

Elastic Solution Predicting a Web Shear Crack for a Composite Section

Assumptions: unshored construction

centroid of composite section remains within the web

tensile strength of the concrete = f_t'

distance between the centroids of the I-beam and the composite section = Δ_y

Figure B.1 contains a detail which is used in the following discussion. Determine the compressive stress in the concrete at the centroid of the composite section due to both prestress and moments resisted by precast member acting alone.

$$f_{pc} = + \frac{P_{e2}}{A_b} - \frac{P_{e2}\ e2\ \Delta_y}{I_b} + \frac{M_d\ \Delta_y}{I_b}$$

The shear stress at the centroid of the composite section shall be calculated using the formula, $\tau = \dfrac{V\,Q}{I\,t}$

$$\tau = \frac{V_d\ Q_b}{I_b\ b_w} + \frac{V_l\ Q_c}{I_c\ b_w}$$

From Mohr's circle,

$$\tau = f_t' \sqrt{1 + \frac{f_{pc}}{f_t'}}$$

Substituting for τ,

$$\frac{V_d\ Q_b}{I_b\ b_w} + \frac{V_l\ Q_c}{I_c\ b_w} = f_t' \sqrt{1 + \frac{f_{pc}}{f_t'}}$$

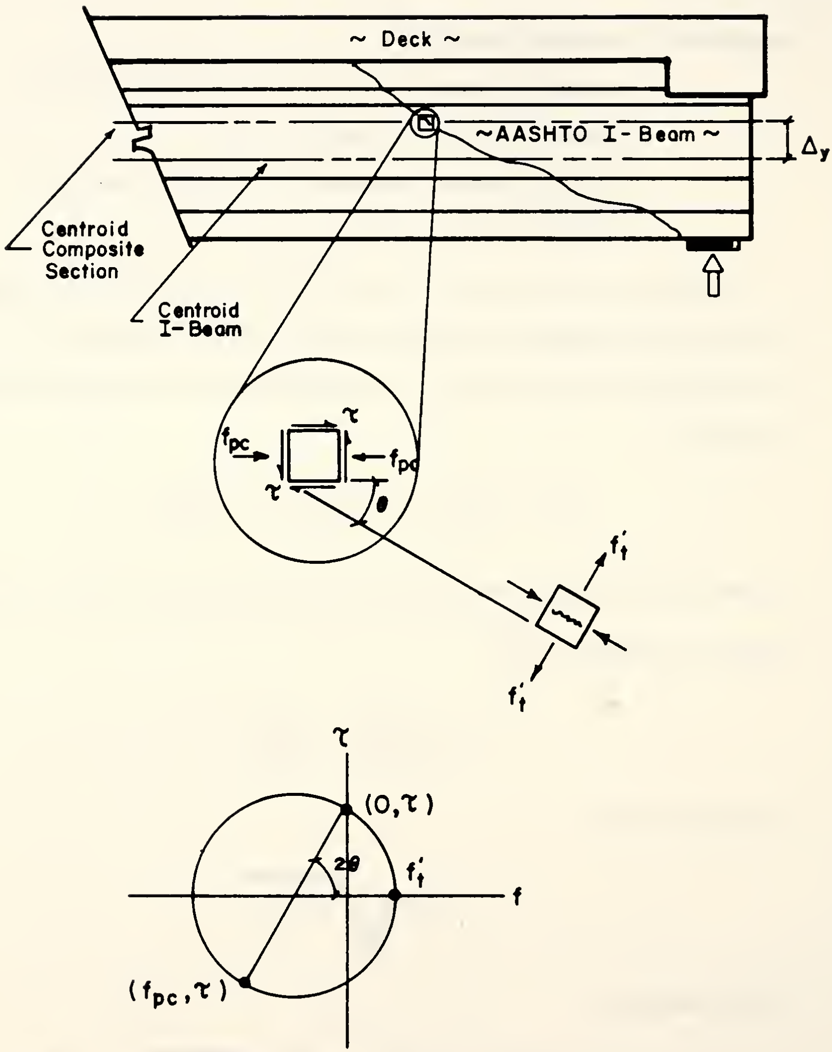

Figure B.1 - Elastic Solution for Web Shear Crack, Composite Section

Let the load required to produce a web shear crack be equal to the sum of the live and dead load,

$$V_{cw} = V_d + V_l$$

Combining the last two equations, solving for V_{cw} and simplifying,

$$V_{cw} = \frac{I_c\ b_w}{Q_c}\left(f_t'\sqrt{1 + \frac{f_{pc}}{f_t'}} - V_d\ \frac{Q_b}{I_b\ b_w}\right) + V_d$$

APPENDIX C

Shear Load Required to Produce Flexure and Shear Capacities

Shear Load Required to Produce a Flexure Crack at Midspan

Assumptions: tensile strength of the concrete $= 7.5\sqrt{f'_c}$

moment at midspan due to dead load, $M_o = \dfrac{w_o\, l^2}{8}$

the moment, M, is equal to the shear load, V, multiplied by the shear span, a.

Determine the external shear load to produce a flexure crack at midspan taking into account the effects of the prestress force and dead load. Solving for the tensile strength of the concrete:

$$7.5\sqrt{f'_c} = -\frac{P_{e1} + P_{e2}}{A_b} + \frac{P_{e1}\, e1}{S_2} - \frac{P_{e2}\, e2}{S_2} + \frac{M_o}{S_2} + \frac{V_{cr}\, a}{S_2}$$

Solving for the external load, V_{cr} and simplifying,

$$V_{cr} = \frac{1}{a}\left[S_2\left(7.5\sqrt{f'_c} + \frac{P_{e1} + P_{e2}}{A_b}\right) - \frac{w_o l^2}{8} + P_{e2}\, e2 - P_{e1}\, e1\right]$$

Shear Load Equivalent to the Nominal Flexure Capacity

Take the nominal flexure capacity predicted by AASHTO and divide this by the shear span.

$$V_n = \frac{1}{a}\left[A_{ps}\, f_{ps}\left(d_p - \frac{A_{ps}\, f_{ps}}{2\,(0.85)\, f'_c\, b}\right)\right]$$

Shear Load Producing an Inclined Flexure Shear Crack

Assumptions: tensile strength of the concrete $= 6\sqrt{f'_c}$

moment at point load due to dead load, $M_o = \frac{w_o\, a}{2}(1 - a)$

shear at point load due to dead load, $V_d = w_o(\frac{1}{2} - a)$

The AASHTO Equation predicting a flexure shear crack is:

$$V_{ci} = 0.6\sqrt{f'_c}\, b_w\, d_p + V_d + \frac{V\, M_{cr}}{M_{max}}$$

The cracking moment at the point load taking into account dead load and effects of the prestress force is;

$$M_{cr} = S_2\left(6\sqrt{f'_c} + \frac{P_{e1} + P_{e2}}{A_b}\right) - \frac{w_o\, a}{2}(1 - a) + P_{e2}\, e_2 - P_{e1}\, e_1$$

Substituting the $\frac{M}{V}$ ratio and the dead load shear,

$$V_{ci} = 0.6\sqrt{f'_c}\, b_w\, d_p + w_o(\frac{1}{2} - a) + \frac{M_{cr}}{a}$$

Shear Load Producing a Web Shear Crack

The compressive stress, f_{pc}, at the centroid resulting from the effective prestress force is;

$$f_{pc} = \frac{P_{e1} + P_{e2}}{A_b}$$

The shear load producing a web shear crack is;

$$V_{cw} = (\ 3.5\sqrt{f'_c} + 0.3\ f_{pc}\ )\ b_w\ d_p$$

APPENDIX D

Elastic Deflections

Elastic Deflections at Centerline and Quarter Point

Assumptions: use the conjugate beam method shown in Figure D.1 to calculate deflections

Load the span with the $\frac{M}{EI}$ diagram and determine the reactions:

$$\text{Reaction} = \frac{V\,a}{E\,I}\left(\frac{a}{2} + 36\right)$$

Determine the centerline defection by summing moments about centerline;

$$\Delta = \frac{Va}{EI}\left(\frac{a}{2}+36\right)(a+36) - \frac{Va}{EI}\left(\frac{a}{2}\right)\left(36+\frac{a}{3}\right) - \frac{Va}{EI}\left(\frac{b^2}{2}\right)$$

Solving for the ratio $\frac{\Delta}{V}$ and simplifying;

Centerline Deflection

$$\frac{\Delta}{V} = \frac{2\,a^3 + 6(36)\,a^2 + 3(36)^2\,a}{6\,E\,I}$$

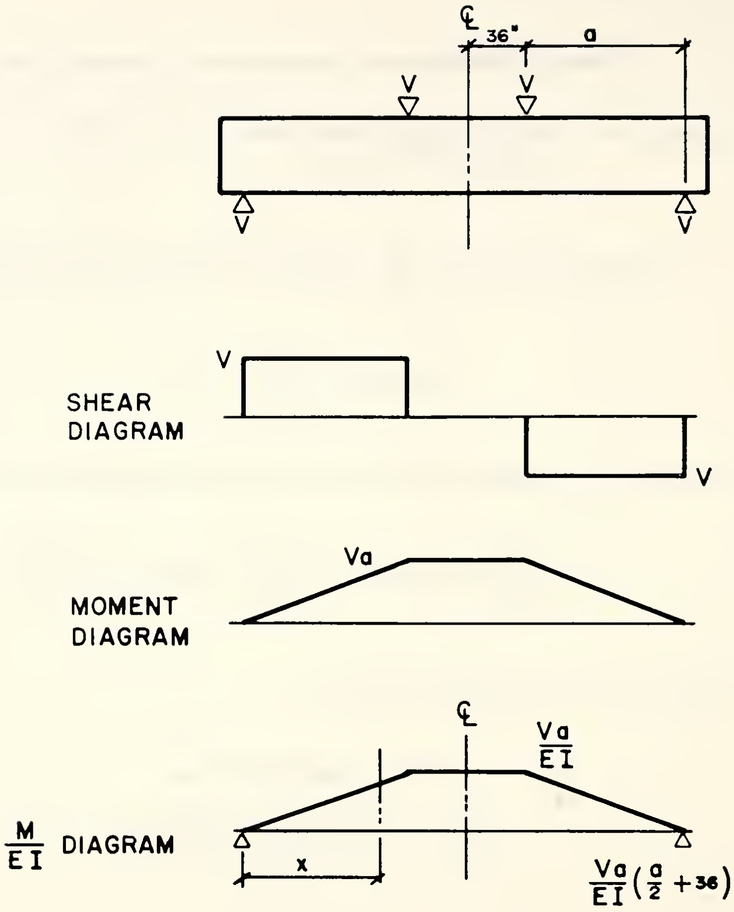

Figure D.1 - Deflections Using Conjugate Beam Method

Determine the deflection at a distance x measured from the centerline of the support by summing moments about the point of interest;

$$\Delta = \frac{Va}{EI}\left(\frac{a}{2}+36\right)(x) - \frac{Vx}{EI}\left(\frac{x^2}{6}\right)$$

Solving for the ratio $\frac{\Delta}{V}$ and simplifying,

Quarter Point Deflection

$$\frac{\Delta}{V} = \frac{x\,(\,3\,a^2 + 6(36)\,a - x^2)}{6\,E\,I}$$

ACKNOWLEDGEMENTS

Appreciation is extended to Ms. Erin Flanigan, undergraduate and to Mr. Kenneth Pensinger, graduate research assistant for their contribution during the laboratory studies conducted in this project. We also wish to express our gratitude to W.R. Yoder and all of the personnel of Hydro-Conduit, Lafayette, Indiana. The valuable contributions of Messrs. Steve Hull, Frank Derthick, and Scott Herrin, IDOH, and Mr. Paul Hoffman, FHWA representative. are also recognized. Our deepest gratitude goes to Prof. Harold L. Michael, Director, JHRP, Purdue University, for his assistance and thoughtful guidance.

COVER DESIGN BY ALDO GIORGINI